# WETTABILITY ANALYSIS ON THE MERAMEC FORMATION USING SURFACTANT ASSISTED IMBIBITION (MARATHON OIL COMPANY)

A Thesis

by

BRIAN WOODY WU

Submitted to the Office of Graduate and Professional Studies of
Texas A&M University
in partial fulfillment of the requirements for the degree of

MASTER OF SCIENCE

| | |
|---|---|
| Chair of Committee, | David S. Schechter |
| Committee Members, | Hadi Nasrabadi |
| | Maria Barrufet |
| Head of Department, | Jeff Spath |

August 2019

Major Subject: Petroleum Engineering

ABSTRACT

Enhanced Oil Recovery (EOR) has been a popular topic as of lately with numerous field cases showing a higher recovery is achievable with the addition of certain chemical additives. This EOR refers to any method of trying to increase the volume of hydrocarbons that are produced by injecting chemicals to improve flow conditions for hydrocarbon production. Though this process is usually thought of as taking place after the completions operation is finished, surfactant addition to slickwater during hydraulic fracturing has been proven in many cases to increase the recovery factor when compared with slickwater/gel alone. Surfactants are now commonly used in all the major plays across the United States as operators are seeing higher recovery factors in comparison to wells on the same pad pumping only slickwater. This phenomenon can be described as the beginning phase of the EOR process that happens at the completions stage. Previous studies such as Alvarez et al. (2014) have shown the effectiveness of surfactant addition during hydraulic fracturing in tight liquid-rich carbonate and shale reservoirs, and its ability to shift the native wettability from oil-wet to water-wet. Other studies such as (SPE 189829) have shown that surfactants can assist flowback operations by decreasing pressure drop across the wellbore, reducing formation damage. All of this is only achievable through the application of the correct surfactant and concentration based on scientific experiments. Many different companies develop surfactant chemicals specifically tailored for oilfield application and choosing the correct type starts with proper classification. Surfactants are amphiphilic, meaning they have a polar head group and a hydrophobic tail. A common method of classifying

surfactants is according to the polar head group; these include cationic, anionic, and nonionic. Once the type of surfactant is chosen, the proper concentration is found through experimentation that favors the spontaneous imbibition of any residual oil, the process by which a wetting fluid, such as fracture fluid, is drawn into a porous medium by capillary action. It is also known that the addition of surfactants may not shift the native wettability, especially in native water-wet reservoirs, both of these topics are discussed in more detail in the Methodology section. These experiments and theories have been thoroughly tested on the Bakken, Eagle Ford, Wolfcamp, and Marcellus rocks by our laboratory, but have yet to be tried on the Meramec shale to this date.

This study focuses on the data and materials taken from the Meramec formation in Kingfisher County, Oklahoma, more specifically the Rosemary 1-14H well. At the time of this project, there is little available information regarding the STACK Meramec, but production in this area is on the rise and getting notice amongst E&P companies looking to capitalize in a low market. The purpose of this study is to evaluate a change in contact angle (CA) and interfacial tension (IFT) that leads to wettability alteration, and the effect that certain types of surfactants have on these fluid properties. IFT and CA variation are measured in the presence of different types of surfactants at reservoir temperature and used in conjunction with spontaneous imbibition experiments to prove that wettability alteration is possible and could in some cases favor production.

# DEDICATION

All of this work would not have been possible without the full support of my two loving parents, Dr. Ding Zhu and Dr. Dan Hill. Their guidance and wisdom along my journey through graduate school is the only reason I had the courage to pursue a Master's degree in petroleum engineering.

ACKNOWLEDGEMENTS

I would also like to express my sincerest gratitude to my advisor, Dr. David S. Schechter, for giving me the chance to prove myself and grow as a person. Thank you also to my research group for the help and support.

I would like to thank the facility employees that help keep our building clean and organized, especially John Maldonado and Joevan Beladi

Final thanks to the undergraduate workers.

Thanks, and gig em'!

## CONTRIBUTORS AND FUNDING SOURCES

Marathon Oil Company

Dr. David S. Schechter

Dr. Hadi Nasrabadi

Dr. Maria Barrufet

This research project was made possible by Marathon Oil Company, for partnering with the Department of Petroleum Engineering at Texas A&M University.

This work was supported by a dissertation committee consisting of Professor David S. Schechter (advisor), Dr. Hadi Nasrabadi (committee member), Dr. Maria Barrufet (committee member) and Dr. Jeff Spath of the Department of Petroleum Engineering.

The water data analyzed for Section 2.2.3 was provided by David Burnett of the Department of Petroleum Engineering. The experiments were initially setup by students of our research group and then developed for this research project.

All other work conducted for the dissertation was completed by the student independently.

## NOMENCLATURE

| | |
|---|---|
| $S_{oi}$ | Initial Oil Saturation |
| C&F | Centrifuging & Filtering |
| $\Theta_w$ | Wetting angle |
| CA | Contact Angle |
| IFT | Interfacial Tension |
| ZP | Zeta Potential |
| SI | Spontaneous Imbibition |
| mD | Milllidarcy |
| μm | Micrometer |
| mN/m | Millinewtons/Meter |
| TDS | Total Dissolved Solids |
| TOC | Total Organic Content |
| PPM | Parts Per Million |
| K | Kelvin |
| SEM | Scanning Electron Microscope |
| CMC | Critical Micelle Concentration |
| bbl | Barrels |
| lbs. | Pounds |
| SPF | Shots Per Foot |
| HU | Hounsfield Units |
| g/cc | grams/cubic centimeter |

TABLE OF CONTENTS

LIST OF FIGURES

LIST OF TABLES

# 1. INTRODUCTION

## 1.1 Research Background and Objective Overview

The goal of this project is to provide insight about the flow behavior and wetting properties in the presence of surfactant chemicals in the Meramec formation for Marathon Oil Company (MRO), who currently has operations all across the SCOOP/STACK region. This is done through wettability lab experiments using the data and materials provided by MRO from the Rosemary 1-14H, a horizontal hydraulically fractured well. Wettability is a term used to describe the tendency of one fluid to spread onto a solid surface in the presence of another immiscible fluid [40]. The information will then be used to capitalize on operations in the future through a deeper understanding of current practices. The STACK is still in the early stages of development so there is a scarce amount of literature on the behavior of this particular area. With that being said, it is on the rise to become one of the most prolific producing formations in the United States. The data and materials presented in this paper all pertain to the Rosemary 1-14H. More information on the completion and operations design will be provided in Section 2.2.1.

Addition of surfactants to slickwater during the hydraulic fracturing process has been verified by both laboratory and field experiments to affect the total amount of recoverable hydrocarbons and the recovery rate by altering wettability and interfacial tension. The degree of this affect, and whether it is positive or negative, depends mostly on formation properties and the type of surfactant used. A better understanding of this chemical interaction involves the amalgamation of lab experiments and possibly

reservoir simulation due to the complexity of hydraulic fracturing and production from a wellbore. One argument that many researchers agree upon is that spontaneous imbibition is the main driving force of fracture fluids into the rock matrix, meaning it is a critical issue when trying to understand reservoir wettability (Mattax and Kyte 1962). This imbibition process occurs post-frac, when the well is shut-in and the fracture fluids are allowed to soak into the matrix before the well is put on production.

There is still much research to be done on spontaneous imbibition and what factors govern it, but much focus today is geared towards studying capillary pressure, pore scale distribution, and permeability. Some believe that this phenomenon occurs when the surfactant causes a reduction in interfacial tension of the oil/water contact allowing any residual oil left to flow out of the matrix (Olafuyi et al. 2007). This theory has been proven for conventional cores but does not always hold true in lower permeability rocks where the pore size distribution is on the nanoscale. In order for the imbibition process to take place at maximum efficiency, the reservoir must be in a water-wet system so that the injected fluid can imbibe into the matrix and replace the non-wetting hydrocarbons. Surfactant addition to fracture fluids will decrease the affinity that oil has to the rock matrix, causing the residual oil to become non-wetting (Gupta and Mohanty 2011). A methodological approach must be taken when choosing the type of surfactant and its loading by conducting lab experiments to ensure the most optimal conditions for imbibition to occur. The effect is confirmed and captured in our lab using 4 separate types of experiments while analyzing the results as a collective. These 4 experiments being contact angle (CA), interfacial tension (IFT), zeta potential (ZP), and

spontaneous imbibition (SI) in no particular order. The procedures and methods for each experiment will be explained in further detail in the Methodology section. Contact angle measurements are a method of characterizing reservoir wettability by analyzing the drop shape of oil displaced from a syringe and adhering on a rock surface. A special HD camera is used to record the interaction between the oil and rock chip. The captive bubble method is used for this research and a more detailed explanation will be provided in Section 2.2.5 regarding the reasoning behind the procedures taken. Interfacial tension between a liquid-liquid interface is measured using the same experimental setup as contact angle with the reverse pendant drop method. A syringe is placed in a solution containing surfactant and a drop of oil is displaced until the oil bubble releases from the needle. This method of measuring IFT is static and drop size dependent, but a dynamic method can also be used to show IFT dependence on temperature with time. Spontaneous imbibition is analyzed using an Amott Cell where a small core plug is submerged in a surfactant solution at reservoir temperature. CT scans are taken to show the displacing fluid enter the rock matrix and forcing the residual oil out. The cores are soaked for over 200 days on average in a vacuum of crude oil from the Rosemary 1-14H to ensure initial wettability is restored. Imbibition has shown to correlate the most with surfactant performance in the field and will be discussed in more detail. Zeta potential is measured using Phase Analysis Light Scattering (PALS) technique using a rock-powder made from the core samples. This is a measure of particle stability or electrophoretic mobility in a solution, which is believed to tie into wettability. The surface charges of the particles in the colloidal dispersion depend on the acidic or basic strength of the

surface groups as well as the pH of the solution. This means that colloids with a high value of zeta potential, positive or negative, are electrically stabilized while low zeta potential is believed to coagulate. The behavior of the colloid does not necessarily represent the wettability of a reservoir, so more discussion on this will be provided in the zeta potential section.

### 1.1.1 The Role of Surfactants

Surfactants are ubiquitous compounds that we do not think about on a daily basis, even though they are found in many ordinary household product cleaners like detergents and shampoo. Meriam Webster defines it as a "compound that lowers the surface tension between two liquids, and may also act as a detergent, emulsifier, wetting agent, or foaming agent", more commonly known as soap. Surfactants, short for surface active agent, are applicable to many areas of petroleum exploration and production such as drilling, acidizing, and transportation (Bhardwaj et al.). The concept of applying these household cleaners in order to enhance the production of a well was introduced in the early 1900's, research during this time was focused mainly on the creation of synthetic surfactants. It wasn't until the mid-1980's when the benefits of alkali and surfactants combined were discovered, this led to tremendous amounts of research on designing surfactants specifically for enhanced oil recovery (EOR) (Negin et al. 2016). The development of surfactants requires an understanding of the conditions in which the surfactant must perform since most reservoirs today pose as unfamiliar and harsh environments, variables such as salinity and temperature must be taken into account.

Surfactants can be divided according to the electrical charge on the hydrophilic, or water-loving end of the molecule. This can be anionic when the charge is negative, cationic when the charge is positive, or nonionic when no charge is present. Cationic surfactants are not popular in the oilfield and were not used in this study. Common components found in anionic surfactants include sodium, ammonium, magnesium, and sulfonate. Nonionic surfactants usually contain ethoxylates, alkoxylates, and cocamide. Nonionic surfactants also have proven in the past to have good solvency, high tolerance for hard brine, and high chemical stability (Raney, 1991). The surfactants tested in this project are presented in the Appendix beginning on page 90 along with their composition.

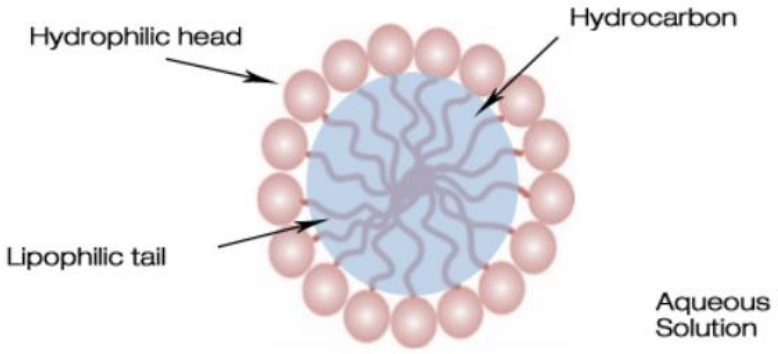


Figure 1: Surfactant molecules encapsulating a hydrocarbon molecule. Reprinted from en.wikipedia.org

Surfactants exhibit both a cloud point temperature and a Krafft point temperature. Beyond the cloud point temperature and the solution will become cloudy or turbid, this could pose as an issue when trying to measure contact angle and IFT since both require a clear picture (Bhardwaj et al.). Temperatures above the cloud point will cause the formation of densely packed micelle groups as well, also known as aggregates. An illustration of an aggregate is provided in Figure 1. The Krafft point temperature is the temperature needed for the initiation of critical micelle concentration (CMC), or the minimum temperature needed for surfactants to precipitate into aggregates. Below the Krafft point temperature and the solution will precipitate, causing the surfactant to drop out of the aqueous solution. Extremely high temperatures can also have an adverse effect on the concentration of the solution and is thought to affect anionic surfactants more than cationic and nonionic surfactants. The diagram presented on the following page labeled Figure 2 is provided by the USGS and depicts a survey done in 2015 of over 300,000 different wells and what types of chemical additives were being used since 1945. As can be seen in the black dashed line, a large spike in the use of surfactants occurred around the year 2010. This rise in surfactant usage resulted from both a scientific and economic advancement that occurred right after the boom in unconventional hydraulic fracturing technology. Operating companies had to find a way to maximize efficiency and minimize expenses in order to profit from wells during such a depressed market. Surfactants have proven in previous field trials to increase the recovery rate when compared with wells that use only slickwater. Companies consistently report changes in recovery factors ranging from 0%-60%, the large

variability is mainly due to proper surfactant type and concentration as well as the formation it is being applied to. Surfactants have been traditionally used for surfactant-polymer flooding operations as a tertiary recover method. Some of the most attractive EOR targets in the past have been west Texas unconventional carbonate reservoirs. The attempt to decrease surface tension using surfactants has long been the goal for engineers to enhance production in sandstone reservoirs, however, the same methodology doesn't always hold true for tight carbonate reservoirs. One more thing to note is the principals applied to surfactant flooding do not completely represent the spontaneous imbibition process used in this study, one example would be the one-dimensional flow front of a flooding operation versus the All Faces Open (AFO) technique used for imbibition.

Concerns with the recent fracing boom has led many people to believe that the chemicals used in the fracture fluid can contaminate ground and surface water supplies, making it harmful for consumer use. There have been multiple studies refuting this claim, one in particular led by Colorado University-Boulder in 2015 on analyzing fracture fluids in different regions of the United States showed that many of the chemicals found in the fluid samples taken from groundwater were also found in common products that are being washed down drains in every home. The chemicals also comprise of such a small percentage of the fracture fluid that they pose no significant threat to the environment. The study concluded that with safe and consistent engineering practices, fracing with chemical additives such as surfactants has a minimal effect on the environment and absolutely no negative effect on the groundwater. Scientific

developments in the field of hydraulic fracturing are being developed constantly to help reduce the environmental footprint this operation has.

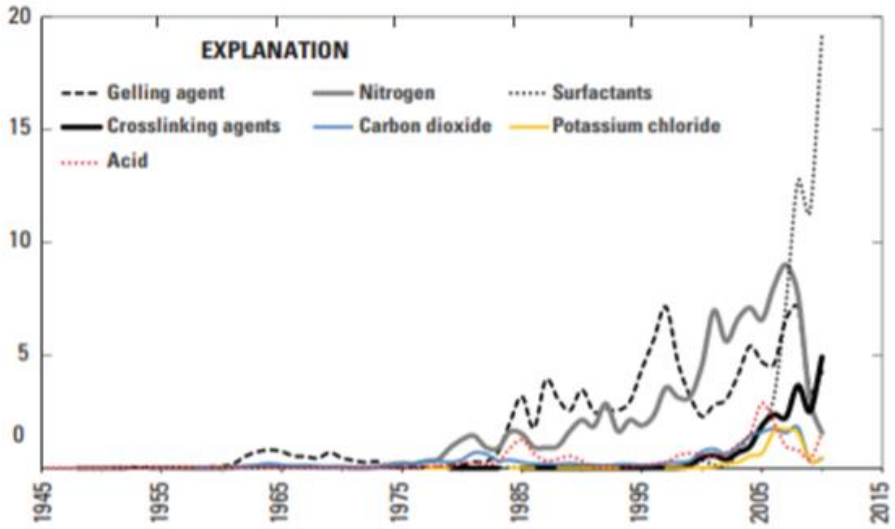


Figure 2: Fluid record of 330,000 wells shows spike in use of surfactants around 2010. Reprinted from USGS

# 2. METHODOLOGY/LITERATURE REVIEW

## 2.1 The STACK (Meramec Formation)

Defining the STACK, or Sooner Trend Anadarko basin in Canadian and Kingfisher counties, is significant since it references a geographical area rather than a specific formation in this context. The play consists of the Meramec and Woodford shales in Canadian, and Kingfisher counties, the “C” and “K” in STACK. Some companies will define the STACK as any layer including and between the Meramec and Woodford formations. The STACK region and the Meramec formation have been attracting lots of attention in recent years with companies buying up all the acreage in the midst of one of the worst downturns in history. It currently poses as one of the most active horizontal plays in North America that is still in the early stages of development. Figure 3 on the next page is a graph representing the growing rig count in the STACK since 2013 to 2015, this increase in drilling rigs occurred during the recent downturn. In 2015, the STACK became the second most active play in the lower 48 states just behind the Permian Basin in terms of active drilling (Yee et al. 2017). This is due to the immense lateral expanse and vertical extent that the STACK region presents, along with the already developed infrastructure necessary for transportation and storage needs. Oil production in Oklahoma skyrocketed from 2011-2014 by 74% according to the U.S. Energy Information Administration. The stacking of formations poses as an opportunity for E&P companies looking to target strata at multiple depths, allowing more exploitation of hydrocarbons while using the same surface footprint. This revival in Oklahoma’s energy market is largely driven by the emerging new resource plays that

encompass both conventional and unconventional formations all across the state. The main counties that the STACK entails are all located within Oklahoma, the Canadian, Kingfisher, and Blaine counties. Companies are specifically targeting the Oswego, Meramec, Osage, and Woodford formations.

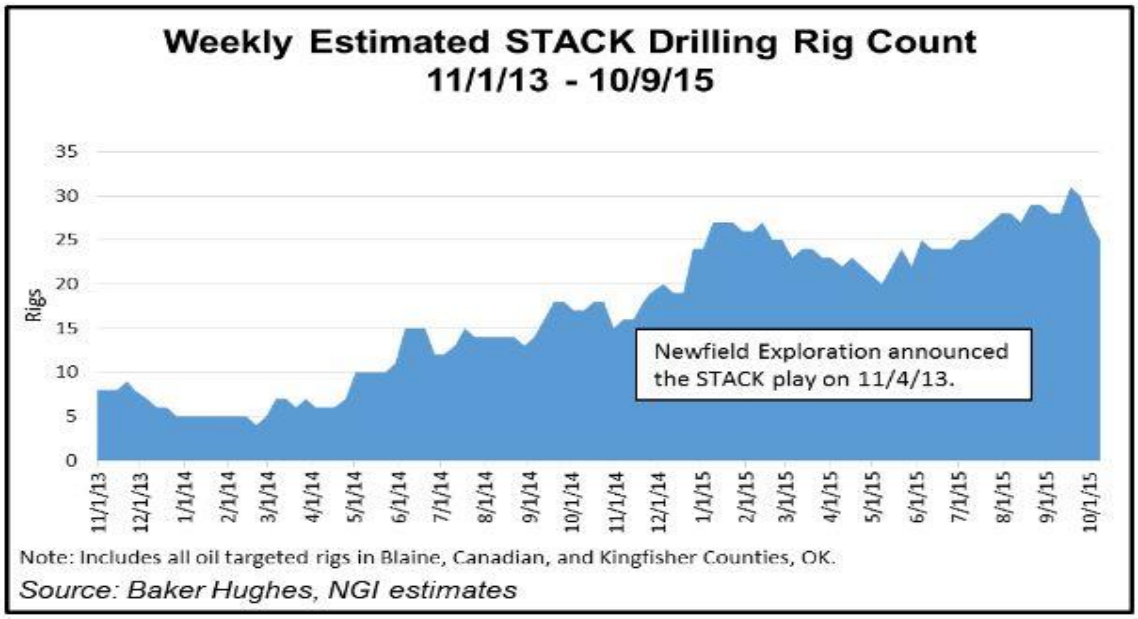


Figure 3: Estimate of drilling rigs in the STACK from 2013 to 2015. Figure courtesy of Baker Hughes and NGI estimates.

| System | Zone | Group | Formation |
|---|---|---|---|
| PENNSYLVANIAN | Missourian | Hoxbar | |
| | Des Moinesian | | Oswego |
| | Atokan | | |
| | Morrowan | Morrow | |
| | | Springer | |
| MISSISSIPPIAN | Chesterian | Chester | |
| | Meramecian | Meramec | |
| | Osagean | Osage | |
| | Kiderhookian | | Woodford |
| DEVONIAN | Upper-Middle | | |
| | Lower | | Hunton |
| SILURIAN | | | |

Figure 4: Anadarko Basin Stratigraphy.

### 2.1.1 Well Information

This research project uses data and materials taken from the Rosemary 1-14H (API 3507324902) located in Kingfisher County, Oklahoma in the Watonga-Chickasha TR field. The Rosemary 1-14H is a 14,000' hydraulically fractured toe-up horizontal well initially designed to target the Meramec Lime formation in the STACK region of Oklahoma. The 4,294' of usable lateral contains 15 stages using the plug and perf completion method with an average cluster spacing of 75' and an average of 212' from the top perforation to the bottom perforation. This well was put on production on July 12, 2014 and has produced on a daily average 40% oil, 50% natural gas, and 10% water to date. The perforation schedule was designed at 6 SPF with 7 shots each stage using 60-degree phasing, a detailed chart is provided in the Appendix showing the perforation schedule and well trajectory labeled Figure 1. The well was completed using standard 5 ½ inch 23# casing joints. The average injection rate of this well was 55-65 BPM at 6,500 psi. The pump schedule consisted of 15 stages, stage 1 contained 5000 gallons of 15% HCl, 280,000 gallons of fracture fluid, and a total of 220,000 lbs. of sand. 61,000 bbl of this fluid was 25# crosslinker gel and the rest was slickwater. The next 14 stages used 2,500 gallons of 15% HCl per stage with a total of 350,000 gallons of fracture fluid per stage and 340,000 lbs. of sand, each subsequent stage contained 30% more crosslinker gel than stage 1. The proppant pumped was mixture of 40/70 and 20/40 White and finished with a sweep of 20/40 Oil Plus proppant.

### 2.1.2 Formation Properties

The Meramec formation is a Mississippian-aged limestone which sits on top of the Woodford shale source rock, much of the formation is interbedded with shale and silt streaks. The formation reaches up to 500 feet thick in some areas and the overlying Chester Shale acts as a top seal to mitigate hydrocarbon migration and over-pressuring (USGS). Thermal maturity trends westward towards the deeper part of the basin and transitions from dry gas all the way to normally pressured oil moving in an eastward direction. The average reservoir temperature of the formation is 195 °F. Initial findings indicate that this area of the Meramec formation is a native neutral/intermediate-wet system. This is quantified by both contact angle experiments done on multiple rock samples which show the average wetting angle ranging from 50°-75° (Reed and Healy 1984) and imbibition experiments which show recovery is possible with only water. More on these findings will be discussed in Section 2.2.4 and 2.2.6. The lateral of the Rosemary 1-14H originally targeted the Meramec lime formation and XRD logs show strong heterogeneity and relatively high clay content throughout the interval of interest. The composition of the clay consists mostly of illite, smectite, and mica with some trace amounts of kaolinite and chlorite. XRD data was provided for each plug used in the imbibition and contact angle experiments. Permeability and porosity values for the side-wall plugs, which were provided by MRO on behalf of Core Lab, show a range of values from .0001 mD - .202 mD and 1% - 7% respectively. Two charts are given on the next page that plot the porosity vs. permeability for the core plugs used in the experiment. There is a relatively strong correlation between the two metrics as shown in the graphs, a

Pearson correlation of .65 was calculated for the permeability of air and .68 for the Klinkenberg permeability. A facies diagram labeled Figure 6 is provided on the following page courtesy of Chemostrat to give a visual representation on the mineral composition of the Rosemary 1-14H. The diagram assumes a true 3 component system and the minerals shown are in equilibrium over a range of pressure and temperature. Each colored dot on the chart represents a core sample taken from the well and its location on the chart corresponds to the mineral composition. The corresponding color-coded legend for the diagram that contains all the mineralogy's present in the Rosemary 1-14H can be found in the Appendix labeled Figure 6.

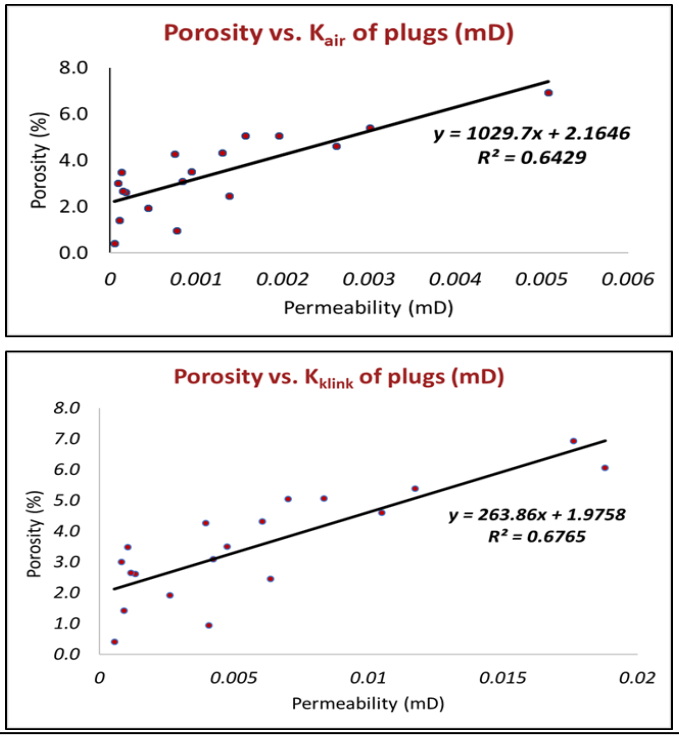


Figure 5: Chart showing porosity vs. permeability for core plugs in inventory.

The dominate mineralogy as seen from the facies diagram below is siliceous mudstone that contains >50% quartz/feldspar and <10% carbonates and the next most dominate mineralogy is silica dominate mudstone that comprises of >80% quartz/feldspar and no detectable carbonates.

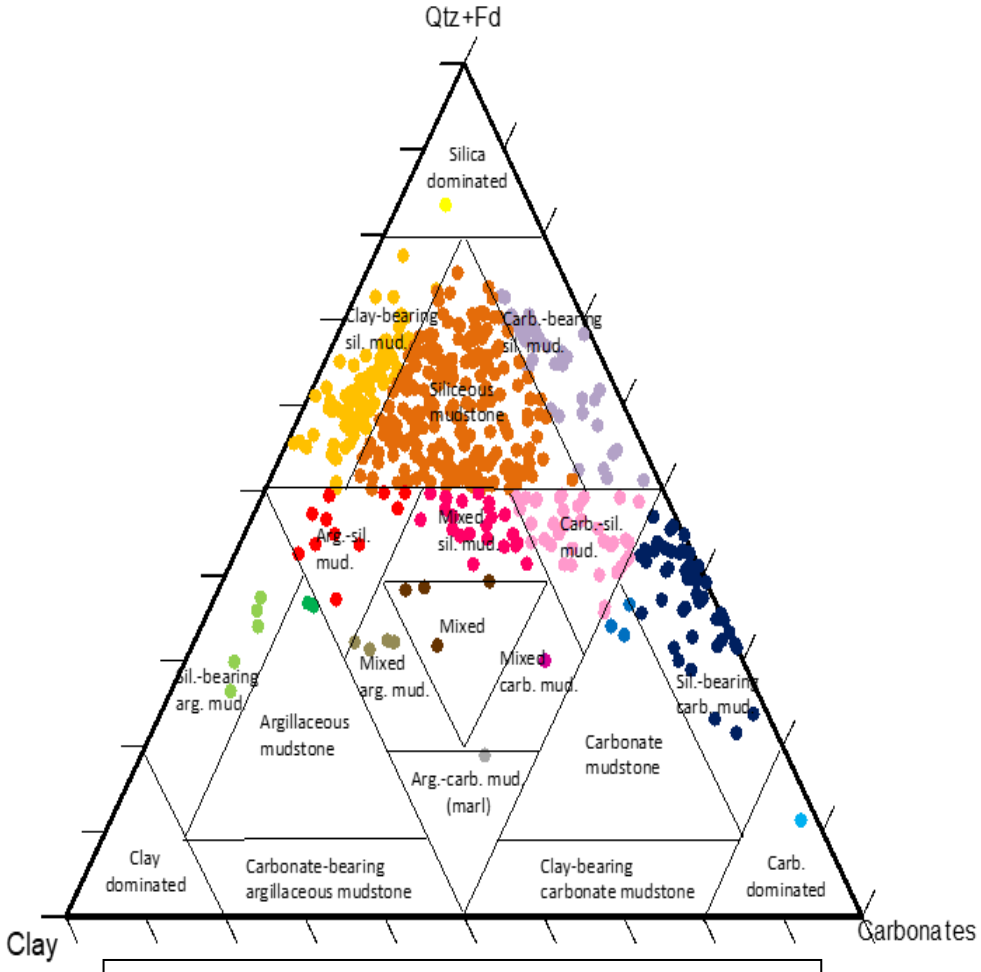


Figure 6: Facies diagram for Rosemary 1-14H showing lithology differences.

### 2.1.3 Data and Materials

The data and materials used for this research project were taken from the Rosemary 1-14H well located in Kingfisher County, OK. This includes the oil, core plugs, PVT data, and any information regarding the geology or design of the well. The depth interval of the plugs is 9478'-9890' TVD with a total of 53 plugs of various condition and length. This research project did not require the use of all the plugs that were provided. The inventory of plugs used for imbibition experiments along with their respective properties is located in the Appendix as Table A. The plugs that contained petrophysical information were chosen for spontaneous imbibition experiments while plugs that showed visible damage were used for contact angle and zeta potential since both these require that the plug be broken into small chips. Changes in composition with depth can be seen when visually inspecting the plugs, a pilot log of the Rosemary 1-14H is provided in the Appendix labeled Figure 3 for broader look of the XRD of the well. A few of the plugs were assigned permeability values above 0.1 mD which is significantly higher than the rest of the plugs. An in-house porosity test was also conducted to verify the information on the core plug samples and to test the possibility of a gas injection study. More on this will be included in the Methodology section.

All of the surfactants used in these experiments have been labeled with a number followed by a letter of the alphabet with the exception of one surfactant labeled "Surf X". The number represents a specific company and the letter represents a specific type of surfactant. For examples 6-A, 6-C, 6-D, and 6-E all come from the same company but have might have different amounts of certain components. The SDS for 6-A, 6-C, and 6-

D are the same and the physical properties do not change with the replacement or removal of the components. 6-E has a separate SDS that is also provided in the Appendix. The flash points for surfactants 6-A, 6-C, and 6-D are in a range of 96-103 °F and the pH levels ranged from 4-9, while 6-E has a much higher flash point, greater than 214 °F. Surfactants 2-A, 2-A (#4), and 2-B were also tested for imbibition and contact angle at various loadings. 2-A is a combination of two different surfactants labeled #3 and #4, each at a 1 gpt loading. 2-A (#4) is only the #4 surfactant at 1 gpt loading. These surfactants showed the most promise in that they had the best alteration of wetting angle and compatibility in hard brines at high temperatures. A total of 6 surfactants were tested in this project and were chosen based on availability and the potential for compatibility in the Meramec.

### 2.2 Laboratory Experiments

In order to quantify the wettability of the Meramec formation, lab-scale experiments using surfactants and the Rosemary 1-14H data and materials are conducted using core samples. Lab scale analysis can provide a detailed insight on the intrinsic behaviors of a formation where simulation cannot. This project will describe and analyze the results of four different lab experiments and is supplemented with additional information from MRO. The four aforementioned experiments being contact angle, interfacial tension, zeta potential, and spontaneous imbibition. All of these are conducted with and without surfactants that were previously mentioned at different concentrations to test whether surfactants can alter the wettability of fractured wells to favor imbibition

in the Meramec. The first procedure was to try and establish the native wettability of the Meramec shale formation at reservoir conditions. This is done by running contact angle tests on multiple rock chips in distilled water alone, investigating all lithologies is important due to the extreme heterogeneity in the Meramec and the effects this can have on wettability alteration. Contact angle experimentation have shown in the past to correlate strongly with spontaneous imbibition, especially in conventional formations (Schechter et al., Saputra et al.). Higher value wetting angles are believed to cause worse recovery factors due to the stronger adhesion that oil has for the rock and the decrease in capillary pressure. Surfactants can be used in both experiments and the change in wettability can be measured by recovery factor and rate comparison during imbibition experiments. Initial CA experiments done in the lab showed that the Meramec shale is in fact a weakly water-wet system, meaning the average wetting angle fell between 50°- 75 °F. These results were determined by using both a synthetic brine comparable to field conditions and distilled water at 175 °F. Three separate rock samples were chosen based on lithology from XRD data in the initial experiments and reproducibility of results was confirmed by running 15-20 tests per rock chip. A more detailed insight into these results will be provided in the contact angle Section 2.2.5. After the initial wettability is determined using contact angle experiments, surfactants are added into the experiments to test whether they benefit, hinder, or have no effect on oil production. Initial IFT measurements of the Rosemary 1-14H oil is also tested to show the change when surfactants are introduced. This was done using both crude oil and C&F oil. Imbibition experiments can be used to estimate oil production when upscaled to the field scale

using simulation, but the lab-scale experiment also provides valuable information. Production information from the core plugs such as recovery factor, recovery rate, and $S_{oi}$ are just a few examples of metrics that can be calculated during imbibition experiments. Imbibition testing is also supplemented with timely CT scans to show the change in the CT number of the cores while imbibition takes place. Scanning the core plugs with a CT scanner also allows for a visual representation of the imbibition process as well, the aqueous solution has a higher CT number compared with the oil due to the differences in density. As the aqueous solution imbibes into the core plug and replaces the trapped hydrocarbons, the CT number of the core plug will increase. This means the non-wetting fluid is being expelled from the rock matrix as the aqueous solution is filling the pore spaces. The initial hypothesis was that a nanoscale pore size paired with the water-wet nature of the Meramec formation would not be a viable candidate for surfactant enhanced recovery. This later proved to be wrong, but only when the proper surfactant and loading was chosen for imbibition experiments. More on these results will be discussed in Section 2.2.6.

### 2.2.1 Material Preparation

Material preparation for these set of experiments is a critical step to ensure that the results are both reliable and reproducible. Any amount of contamination or procedural difference during the testing or preparation stages can lead to erroneous results. The two main components being tested for these set of experiments are crude oil and core plugs. Both the crude oil and the core plugs underwent a specific preparation

phase before the experiments started. The crude oil that was received was centrifuged and filtered to eradicate the oil of any foreign material and produced water. More detail on the methodology used for the C&F process can be found in the next section. For contact angle, small rock chips approximately 0.5" x 0.5" must be made out of core plug samples, which are then aged in crude oil. Surface roughness is not considered but the chips must have a relatively flat surface to allow for testing. For spontaneous imbibition, core plugs are selected based on size and available petrophysical properties. The plugs are first aged in crude oil in a vacuum at reservoir temperature. The aging time for core plugs can be determined with CT scans to ensure the original saturation is restored, for this study the aging lasted from 100-200 days. The petrophysical information can be used to calculate the $S_{oi}$ and is compared with the measured $S_{oi}$ that was calculated using the difference in weight before and after aging and the porosity. The zeta potential analysis requires the use of a rock powder that is finer than 300 microns in diameter, which is measured using a number 52 sieve. This entire process is explained in more detail in Section 2.2.7.

The depth interval that is being investigated shows strong heterogeneity, with XRD and petrophysical data varying from predominantly carbonate, mixed (quartz & carbonate), to predominately quartz. XRD pie charts have been generated for each plug used in CA experiments to show the relative clay content as well as the composition. CA laboratory experiments were initially conducted on three different samples based on lithology, the XRD for these samples are shown in Table 1 on the next page. Quartz and calcite weight percent for each sample is boxed in maroon and shows the difference

between compositions of each plug. These plugs were chosen to ensure that any lithology that could be encountered in the Rosemary 1-14H is taken into consideration during experimentation. The most prominent types of clay present in the core samples are illite, smectite, mica, and chlorite with trace amounts of kaolinite.

XRD Data for samples being tested

| Plug Name | 227H | 129H | Core 6 |
|---|---|---|---|
| Depth (feet) | 9890.95 | 9695.55 | N/A |
| Mineral | wt % | wt % | wt % |
| Quartz | 17.3 | 36.4 | 53.6 |
| Plagioclase | 3.1 | 8.6 | 15.3 |
| Calcite | 74.1 | 28.0 | 13.58 |
| Dolomite & Fe-Dolomite | 1.4 | 3.4 | <1.0 |
| Total Clay | 3.1 | 19.1 | 13.4 |

Table 1: XRD data for three different plug samples being used for CA and ZP.

### 2.2.2 Oil Information

The original oil provided to our laboratory was crude oil taken from the Rosemary 1-14H. The oil arrived in 5-gallon barrels that had visible amounts of produced water and solid particles, it is a relatively light oil with an API gravity of 43.5 at 60 °F according to a multi-stage separator test provided by MRO. After conducting preliminary CA experiments with the crude oil, it was observed that the produced water and the other materials in the crude oil were causing ambiguity in the results. In order to

separate the produced water, the oil was poured out of the barrel into a beaker and allowed to sit for over 24 hours before being slowly poured into a new beaker, leaving most of the water behind. Afterwards, the now separated oil was transferred to a centrifuge where the solid particles were removed. This device uses centrifugal force to separate fluids of different densities by rotating the oil around a fixed axis at 4500 RPM. The centrifuge process took 4-5 hours to remove as much of the foreign material and any leftover water from the separation process. Once the oil was transferred from the centrifuge tube to a new beaker, it was filtered through a 0.2 μm PTFE filter. This filtering process was slow and due to the strict timeline, the oil was only filtered once. Filtering the oil further increased the IFT by another 4% compared with just the centrifuged oil. After the C&F process was complete, the oil density and viscosity decreased by over 20% and both were recalculated in the lab for experimental purposes. An example of this C&F process can be found in the Appendix labeled Figure 11 showing the filtering process as well as the solids removed after the centrifuging. This was done using an Anton-Parr DMA$^{TM}$ 4100M, which calculates the density of fluids at both low and high temperatures. It could also be visibly seen through our HD camera that any foreign material in the oil was removed from the C&F process. The interfacial tension of the oil increased by 50% after the C&F process. An example of the oil before and after the C&F process is provided in Figure 7 on the next page. The density recorded by Core Lab in their fluid analysis of the Rosemary 1-14H crude oil is 0.552 g/cm$^3$ at 194 °F and the density of the C&F oil is 0.590 g/cm$^3$ at 194 °F. A table of the reservoir fluid summary showing the composition of the Rosemary 1-14H oil is provided in the

Appendix labeled Table B. There is a considerable amount of methane in the crude oil, around 60%, as is expected with a light oil but the composition will change slightly after the C&F process is complete.

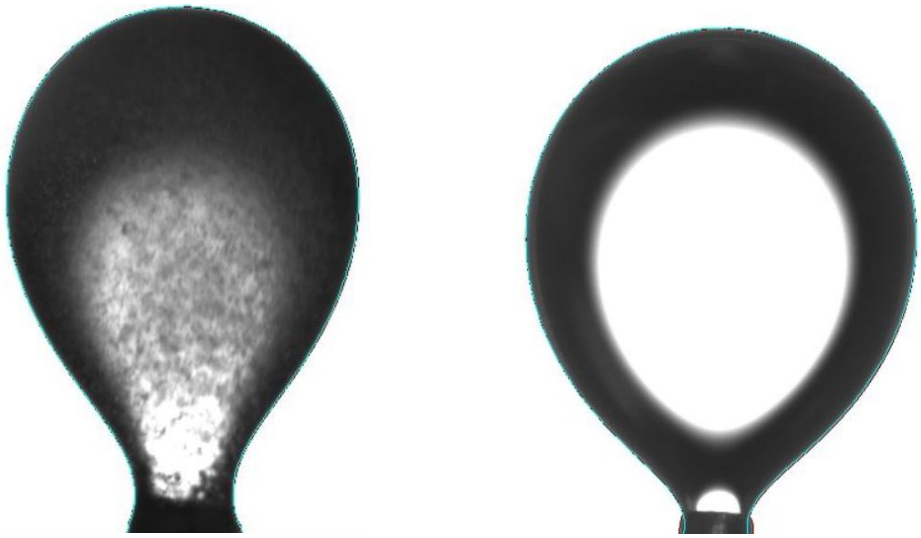

Crude Oil C&F Oil

Figure 7: Comparison of oil before and after the C&F cleaning process.

2.2.3 Core Plug/Water Information

The produced water from the Rosemary 1-14H was analyzed in our research labs at Texas A&M for alkalinity, pH, hardness, and TOC. The produced water is relatively neutral with a pH of 7.32. The concentration of sulfate and $H_2S$ are 18 and 25 ppm

respectively. The TOC concentration is 976 ppm and the TDS concentration is 4100 ppm. TOC values at this depth are relatively high (0.98%), and SEM data shows that the Meramec-D contains intergranular pores with solid organic materials, much of this rock is clay-bearing siliceous mudstone. Generally speaking the TOC should decrease the imbibed volume of oil and water into the matrix, the explanation being the reduction in effective permeability due to the plugging of the pore network by pyrobitumen, a solid amorphous organic material. An example of this organic material plugging the pore network is shown in the Appendix labeled Figure 2. This theory was tested but the results were not conclusive, TOC values were only given for less than 1/3 of the plugs. It is difficult to directly test this concept using the experiments presented in this paper due to the lack of data for all plugs tested and the difference in petrophysical properties between the core plugs. The interval of plugs being investigated is 9490'-9590', this is within the target lateral zone of the Rosemary 1-14H. The plugs chosen for experimental use were done so based on available petrophysical data, condition, and size. It is important during the imbibition experiment that the plugs being used are all the same dimensions so that scaling $S_{oi}$ to bulk volume will remain consistent, more on this will be discussed in Section 2.2.6. A picture of all the plugs provided for this project is shown on the next page and labeled as Figure 8. These side-wall plugs were provided by MRO on behalf of Core Lab. There were 4 broken core plugs, which were used to make powder samples for ZP testing and rock chips for contact angle. All the plugs went through the initial inspection and preparation stage. This involves running all the plugs through our CT machine to learn more about the density and possible bedding planes,

weighing each plug, and determining the possibility of gas injection if permeability and porosity allow for it. These plugs fall in the category of "unconventional" in that the average permeability is less than .1 mD and the average porosity is around 5%, though one of the core plug samples showed possible signs of being in the conventional category with a permeability value of 0.2 mD with a porosity of 6%.

Figure 8: Photograph of core plugs provided by Marathon Oil Company.

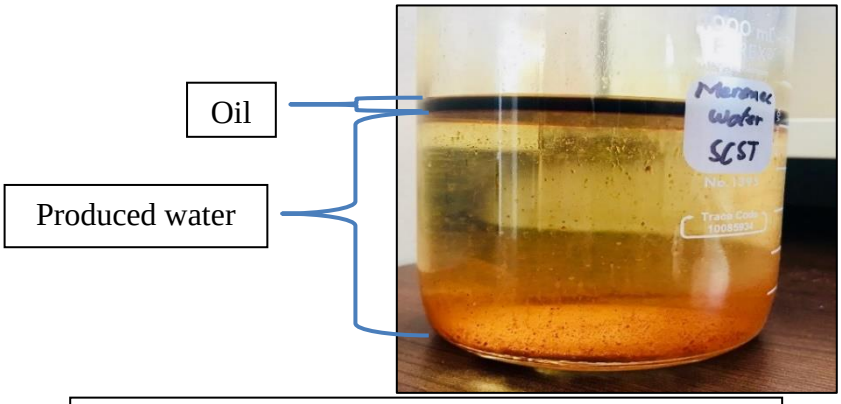


Figure 9: Produced water from the Rosemary 1-14H.

### 2.2.4 Contact Angle

Wetting forces and the contact angles that form are present in many aspects of life such as rain drops beading up on the surface of a car. The preference of oil-water wetting has a large contribution in the performance of enhance oil recovery techniques. Wettability is the preference of a solid to be in contact with one fluid over another, through a balance of surface and interfacial forces. Contact Angle (CA) experiments have been proven in previous studies to have a strong correlation with spontaneous imbibition when using the Captive Bubble method as presented by Alvarez et al. (2014, 2015), Teklu et al. (2015), Anderson (b, 1986). This is when a controlled drop of oil, less than .3 μL in volume, is displaced from a gastight syringe onto a rock chip submerged in an aqueous solution at reservoir temperature. The contact angle is the angle of intersection of the interface between the aqueous solution and oil at a solid rock surface. The aqueous solution can either be water or water mixed with a chemical additive. This method of experimentation gives a direct measurement of wettability by analyzing the contact angle created by a non-wetting phase relative to the wetting phase, in our case oil and water.

The angle created will be referred to as the wetting angle, $\Theta_w$, in the remainder of the paper. The basic ideology is that oil is either a non-wetting or wetting fluid, depending on the rock type and oil type. This wetting can be directly measured from the solid surface through the aqueous phase. The larger the surface area the oil drop covers, the larger the wetting angle is and vice versa. The area of rock in contact with the oil drop can be changed by introducing a surfactant, which should alter the interfacial

tension (IFT) between the liquid-liquid interface leading to a reduction in contact area. An OCA Pro dataphysics drop shape analyzer is used to record, capture, and calculate the contact angle of the oil drop. This particular machine has an integrated HD camera that films the entire process and built in analytical software that can perform the calculations based on the drop volume and density relative to the aqueous phase. It also has a built-in temperature probe to monitor the temperature of the fluid during the experiment.

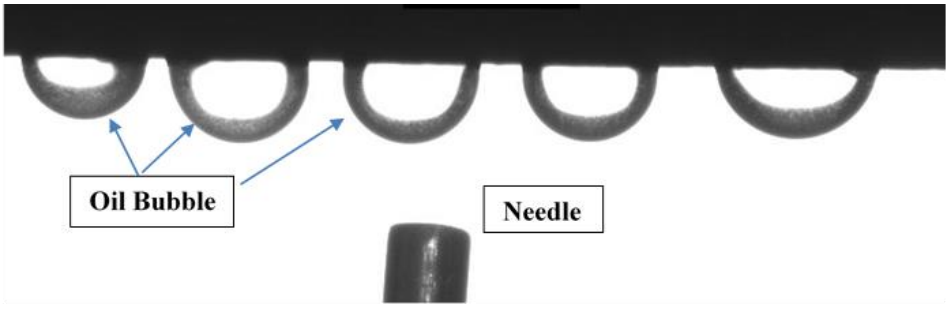


Figure 10: Picture of oil bubbles forming on a rock chip during contact angle experiments.

| Contact Angle Range | Wettability |
|---|---|
| 0°-75° | Water-Wet |
| 75°-115° | Intermediate-Wet |
| 115°-180° | Oil-Wet |

Table 2: Wettability categorization by contact angle range from (Reed and Healy 1984.)

The CA experiment process begins by cutting small square rock chips from larger plugs or blocks, no bigger than 0.5” x 0.5” in size; The cut chips were not polished in order to represent the reservoir as closely as possible so surface roughness is not investigated in this study. Before the experiment can take place, the chip is placed in a clean vial and submerged in crude oil taken from the same well to age and restore the initial wettability, this aging last anywhere from 3-5 weeks at a minimum and happens in a vacuum oven at reservoir temperature. A picture of this oven is provided in the Appendix and labeled Figure 13. If testing with a surfactant, the solution is allowed to agitate for 10 minutes at 350 RPM prior to testing. Before any experiments begin, all the required materials must be thoroughly cleaned such as the syringe and cuvette. Once this is done and the required materials are dried, the glass cuvette is placed on the CA machine, filled with the surfactant solution, and allowed to reach a specific set temperature. A rock chip is then carefully placed on a platform inside the cuvette using a pair of long-nose pliers. A more detailed step-by-step procedure is provided on page 35 and lists the entire contact angle process from start to finish.

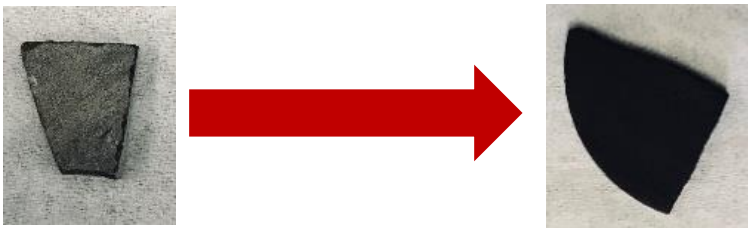

Figure 11: Comparison of rock chip before and after aging process in crude oil.

The above figure is a side-by-side comparison of a core plug rock chip sample before and after being saturated in oil for 4 weeks. You can see from the pictures that the original wettability of the chip is restored after the aging process by the color change that takes place. Each of these chips is wiped down in a rigorous and repeatable manner using KIMTECH wipes to remove any oil residue from the surface before testing begins. Consistency during this step is crucial and must be done using the same technique for all CA measurements. Preliminary contact angle measurements were taken using the crude oil from Rosemary 1-14H which contained visible particulates along with produced water. Using rock chips taken from Core 6, crude oil, and distilled water at 170 °F to mimic reservoir conditions, the inference was that the native wettability is a weakly water-wet system, with some measurements falling in the oil-wet category. For this particular experiment, there was a large variation in contact angle measurements and the impurities in the oil were thought to be the cause. Floating sand/dirt particles along with water in the crude oil could be seen through the HD camera on the contact angle device and caused a standard deviation of +/- 15°. Though this set of experiments did not give a firm consensus on the native wettability of the formation due to the erraticism of results, it showed us that surface charges from particles in the oil are a major factor for contact angle experiments and can cause discrepancies.

The largest hindrance of the contact angle experimentation and analysis, particularly the Captive Bubble method, is consistent reproduction of results. The Captive Bubble method is relatively laborious and complacency during any step will lead to erroneous results. Having a definite pre-experimental procedure and material

preparation is necessary and much care must be taken during the beginning stages to avoid any contamination or outside factors. The syringe, needle, and cuvette are sterilized and cleaned before every experiment to avoid cross-contamination from prior usage. Every chip that is used goes through the exact same preparation before being place in the surfactant solution. After removing the chips from the oven, both sides of the chip are wiped 10-12 times with a KIMTECH wipes to remove any residual oil. Each chip is used for 10-15 measurements before another chip from the same vial replaces it. The quality and composition of the oil being used is also important to note. Initial contact angle measurements for this project used crude oil that contained solid particulates along with produced water. This crude oil resulted in a wide range of contact angle values, with a standard deviation of +/-15°, when compared with using centrifuged & filtered oil. The cleaning and filtering process removed most of the produced water and solids, lowering the density, and resulted in more stable contact angle measurements. This centrifuged & filtered oil, or C&F oil, is used for reporting the following results in this study.

The native wettability of the Meramec using C&F oil was established by testing contact angle values in distilled water on 5 different core plug samples of varying lithological composition. 3-4 rock chips from the same core plug were tested and after 10-15 measurements were taken from each rock chip, the average was taken for all the rock chips and the wetting angle value calculated turned out to be 63°. This native wettability includes over 120 different contact angle measurements. Once the native wettability of the Meramec was established using only distilled water, the addition of

surfactants was tested. 6 different surfactants were selected for use in CA experiments for this study to test the possibility of wettability alteration, they were chosen based on the likelihood of compatibility and availability. A comparison of contact angles in distilled water only along and with 4 out of 6 chosen surfactants is presented in Figures 12 and 13 respectively.

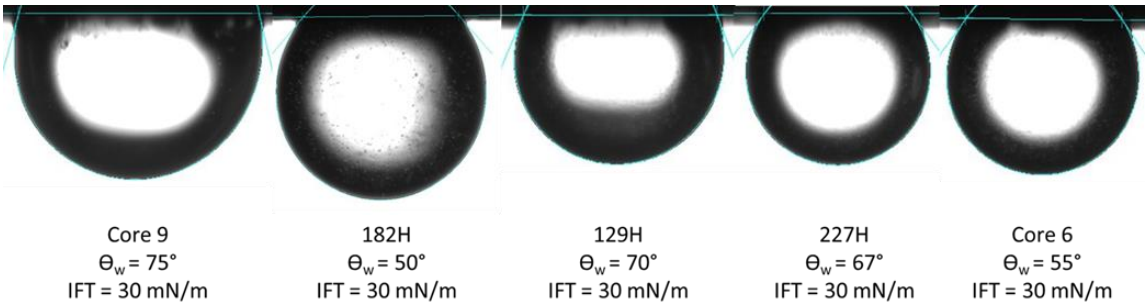


Figure 12: Average contact angle for 5 rock samples tested in distilled water. 15-20 measurements taken for each rock sample and the average is shown. Average native wetting angle is 63°.

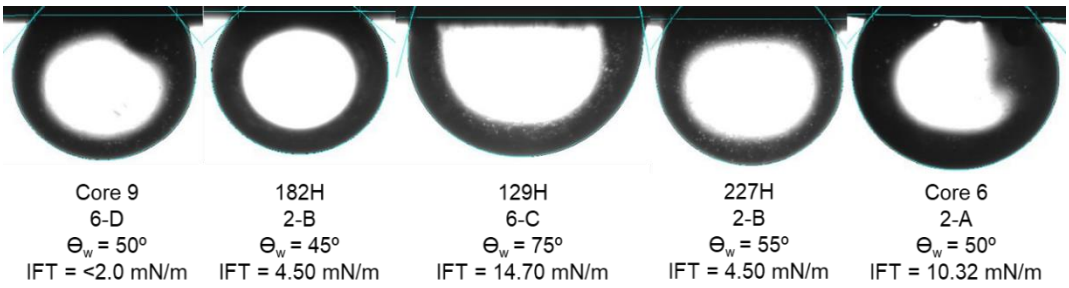


Figure 13: Average contact angle for 5 rock samples tested in various surfactants. 15-20 measurements taken for each rock sample and the average is shown. Average wetting angle with these surfactants is 55°.

As can be seen in the previously mentioned figures, the addition of surfactants did in fact alter the wettability, even though the alteration was minor and the native wettability is already water-wet. It must also be considered that the average wetting angle with surfactants shown in Figure 14 includes 4 out of 6 surfactants that were tested, not only the best performing surfactant. The standard deviation of the measurements shown in Figures 12 and 13 ranged from 5° to 12° depending upon which surfactant and rock chip was being used. For all the distilled water tests shown in Figure 12, the standard deviation equaled to 9° while the standard deviation for all the surfactant tests shown in Figure 13 equaled to 11°.

Surfactants 2-A and 2-B at 1 gpt were chosen first and tested on samples 129H, 227H, 182H and Core 6, these are both nonionic surfactants. XRD pie charts for these samples showing the difference in lithology are presented in the Appendix on page 94 as Figure 8. Each rock sample was used for 10-15 measurements and the average measurement is used to define the wettability of the respective rock chip. Surfactant 2-A at a 1 gpt loading did not drastically decrease the wetting angle when compared with distilled water or the synthetic brine. The average wetting angle with 2-A at 1 gpt when including all the measurements and rock chips used is $\Theta_w = 55°$, with the best performing rock chip being from Core 6. Surfactant 2-B performed the best overall out of all the surfactants tested and decreased the wetting angle by an average of 17%, meaning the average wettability with 2-B at 1 gpt across all the rock chips would hypothetically be $\Theta_w = 52°$. When increasing the loading to 2 gpt for surfactant 2-B, the average wetting angle across all the rock chips is still $\Theta_w = 52°$, meaning there was no

change in wettability when compared with 1 gpt. The difference in IFT values between 2-A and 2-B is over 50% and while most literature says that lower IFT surfactant will perform better, this is not the case in the Meramec. Surfactant 2-A (#4) was tested at 1 gpt as well, the results did not differ too much from 2-A but there is a reduction of 4% in the average wetting angle.

Surfactants 6-A, 6-C, 6-D, and 6-E were then tested at 1 gpt on all the rock samples previously mentioned. 6-C at a 1 gpt loading did not alter the wettability compared with distilled water alone, but when increased to a 2 gpt loading, decreased the average wetting angle compared with distilled water to $\Theta_w = 58°$, or an 8% reduction. This specific surfactant performed the best when tested on sample 129H, which contains the highest amount of clay compared with the other rock samples tested. The average wetting angle using 6-C at 2 gpt for sample 129H is $\Theta_w = 54°$ or a 14% reduction. Both surfactants 6-A and 6-E did not alter the wettability at 1 gpt and 2 gpt loadings. These two were thoroughly tested to ensure the results were accurate and repeatable. Surfactant 6-D is the ultra-low IFT surfactant with an IFT value < 1 mN/m, and performed the best at 1 gpt loading out of these set of surfactants. When tested at 1 gpt, the average wetting angle across all rock chips tested decreased by 13% when compared with distilled water alone, giving an average $\Theta_w = 55°$. Out of the 6 surfactants tested, both 2-A and 2-B at 1 gpt loading gave the best results in terms of wettability alteration for contact angle experiments, showing the most promise for spontaneous imbibition.

| Core Plug Sample | 2-A | 2-A (#4) | 2-B | 6-A | 6-C | 6-D | 6-E | Surf X |
|---|---|---|---|---|---|---|---|---|
| Core 6 | 50° | - | 51° | 63° | 61° | 53° | 66° | 69° |
| Core 9 | 52° | 51 | 54° | 64° | 63° | 54° | 69° | 74° |
| 129H | 59° | 57° | 55° | 70° | 75° | 52° | 75° | 77° |
| 182H | 57° | 55° | 51° | 64° | 65° | 56° | 71° | 73° |
| 227H | 53° | 53° | 54° | 63° | 62° | 52° | 70° | 79° |

Table 3: Summary of contact angle ($\Theta_w$) results for all rock samples and surfactants tested at 1 gpt.

Previous studies such as Sharma et al. (2013) and Reed et al. (1984) have shown that low salinity brine will favor contact angle experiments compared with high salinity and can increase the recovery in many carbonate-dominate reservoirs. To test this theory, a synthetic brine was developed to the specifications of the produced water from the Rosemary 1-14H. Five types of salts were added to distilled water based on a TDS report of the produced water and tested on samples 129H, Core 6, and 227H. The brine is mainly composed of sodium chloride, which accounts for 2/3 of the total ion concentration. Produced water from the Rosemary 1-14H was analyzed during this time for hardness and TOC from an in-house test, a more detailed report of these findings can be found in the Appendix as Figure 15. The synthetic brine was allowed to agitate and heated up for 10 minutes to ensure full miscibility before the start of the experiment. When tested with the Captive Bubble method, the results actually showed that the addition of salts either decreased or had no effect on the wetting angle of the oil,

meaning either a shift towards a more water-wet state or no significant change in wettability. A set of pictures comparing the average contact angle for the synthetic brine and distilled water is shown on the next page in Table 4. For sample 129H, which is the mixed lithology sample containing 20% clay, the wetting angle decreased by almost 30% when introducing salt, causing an even more water-wet system. The same occurred when synthetic brine was tested on rock chips taken from Core 6. Sample 227H is the calcite dominate sample with no clay content and the addition of salt had little to no effect on the contact angle. The experiments done on Core 6 and 129H show that the addition of salt ions have a dramatic decrease in the wetting angle when most current literature says the opposite happens in shale reservoirs.

| *Sample* | *Distilled Water* | *Synthetic Brine* | *Lithology* |
|---|---|---|---|
| ***227H*** | 67° | 70° | Calcite |
| ***129H*** | 74° | 50° | Mixed |
| ***Core 6*** | 64° | 43° | Carbonate |

Table 4: Comparison of distilled water and synthetic brine wetting angles for 3 different rock samples. Average wetting angle is shown for 15 measurements. Standard Deviation = 9°-13°.

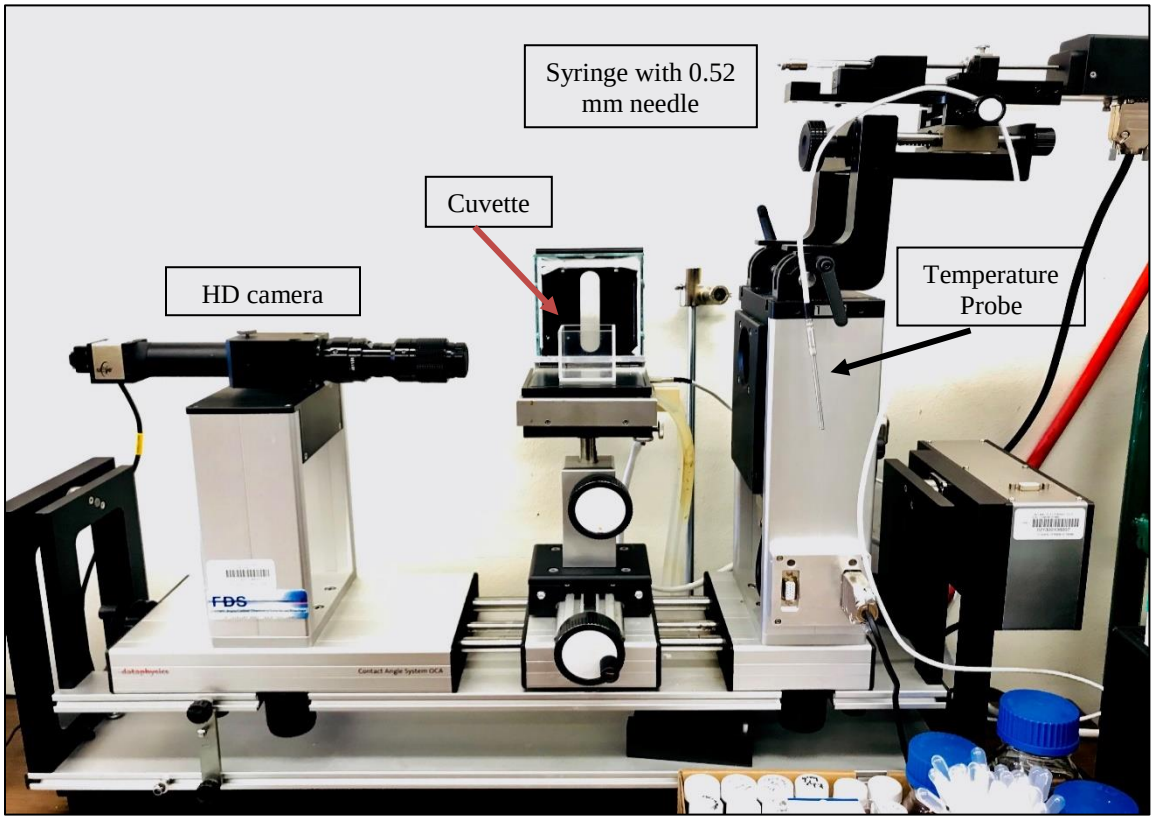


Figure 14: Picture of FDS OCA device used for IFT/CA experiments.

**Contact Angle Experimental Setup/Procedure**

1. Rock chips from core samples are made by slicing the core samples into thin sections that are flat on at least one side. Dimensions of the chip samples are around 0.5” x 0.5” and 0.5 centimeters in thickness.
2. Rock chips are then placed in a glass vial, crude oil is added the vial enough to fully cover the rock chips, and vials are placed in an oven to age at reservoir temperature See Figure 13 in Appendix.
3. The aging process last at least 4 weeks long before testing can begin.

4. Before starting contact angle measurements, a single chip is removed from the glass vial and cleaned using KIMTECH wipes to remove any crude oil from the surface of the rock chip.
5. Rock chip is then placed in surfactant solution that has been heated to reservoir temperature and contact angle measurements can be taken as shown below. Pictures, video, and calculations are taken with the OCA dataphysics machine and can saved in a file.
6. This method does not move the syringe needle to the left or right to release the oil bubble once the oil bubble comes in contact with the rock. The syringe is moved directly downward once the oil comes in contact with the rock. It is important to note how the oil bubble is formed because of the vast amounts of contact angle measuring methods that are used in our industry.
    a. The following images on pages 36-38 are not labeled as Figures and are provided as supplementary information for the reader.

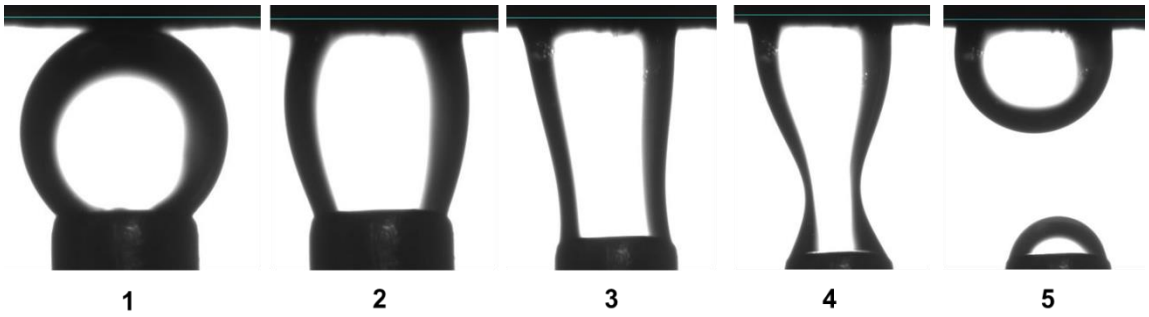


Example of contact angle measurement process in a 5-step illustration showing the release of the oil drop onto a rock chip surface.


Pictures of plug 38H imbibing in surfactant 2-A (#3+#4) at 1 gpt. Oil bubbles cover the entire plug surface but are small in diameter.

---

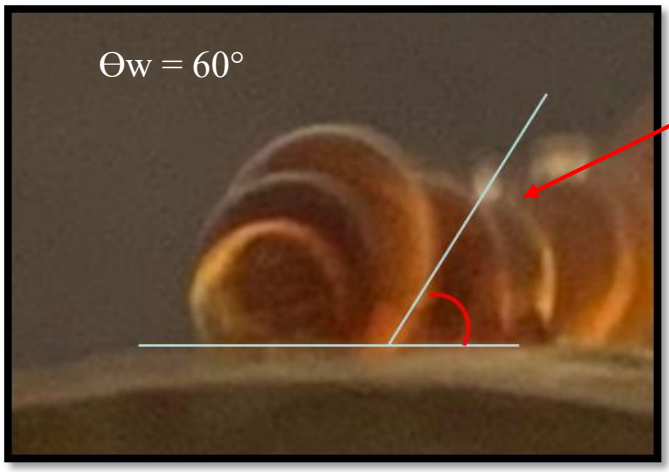



Core 41H during imbibition process showing the water-wet nature of the oil bubbles on the surface of the core. This is 50 hours into imbibition with surfactant 2-A (#4) at 1 gpt loading.

Close-up of plug 41H testing in 2-A (#4 only) during imbibition. Showing that oil bubbles are in a water-wet state after 50 hours of imbibition. This agrees with the contact angle measurements taken using this surfactant that also resulted in a water-wet state.

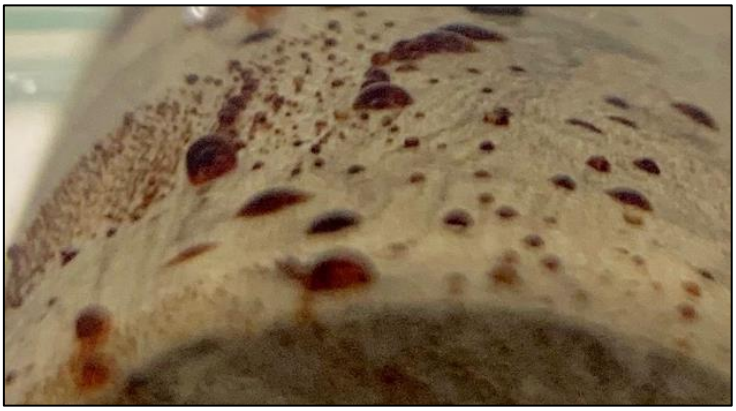

Close-up of plug 50H imbibing in only distilled water at 170 °F. The contact angles forming on the surface of the core plug look to be in a intermediate-wet to oil-wet state, which agrees with the initial contact angle measurements taken using the crude oil in distilled water.

Deglint et al. (2017) presented a contact angle studying using SEM technology to compare micro contact angles to macro contact angles. The macro-scale oil bubbles were displaced using the sessile drop method and the micro-scale bubbles with an environmental field emission scanning electron microscope (E-FESEM). The results indicated that there is a significant difference in these two metrics, micro contact angles depend much more on grain composition than macro contact angles such as the ones used in this study. The varying clay content of the seems to affect the wettability of the rock sample. Each sample was tested 5 different times, each with 10-15 measurements, to compare the average CA across different lithology. The results indicate that clay content and main composition of the rock, quartz or calcite, dictate the wettability. Conventional belief is that carbonate rocks are naturally water-wet, hydrophobic, and thus have the most favorable native wettability. The opposite is said for calcite dominate samples. The results presented in this study confirm this belief, Core 6 tested the best for both contact angle experiments and had over 75% quartz content with a relatively medium clay content compared with the other two samples.

### 2.2.5 Interfacial Tension

Interfacial tension (IFT) is the tendency of an interface to become spherical to decrease its surface energy to as little as possible, these could be liquid-liquid, liquid-solid, or solid-air. This term is usually denoted by the symbol σ and is measured by force per unit length. The SI unit is millinewton per meter (mN/m) which is equivalent to the

popular cgs unit, dynes per centimeter (dynes/cm). IFT plays an important role in the investigation of emulsification, which are heterogeneous systems consisting of at least one immiscible liquid dispersed in another in the form of droplets. Once these two immiscible liquids are in contact, they will maintain as small an interface as possible. If this aqueous system is agitated or shaken, small spherical droplets will form, as the liquids will maintain as small a surface area as possible and the IFT will be maintained between the two liquids. When a surface-active agent, or surfactant, is introduced, it's molecules will orient between the two interfaces with the polar ends in the polar phase and the non-polar ends in the non-polar phase, lowering the overall IFT of the solution and resulting in miscibility. This IFT reduction will produce smaller droplets while reducing the tendency of droplets to flow together when mixing, termed coalescence. The interfacial tension between oil and water is of critical importance when investigating whether surfactants will enhance or inhibit oil production. There are multiple methods of calculating IFT and each has different applications, techniques, and required equipment. A study conducted by Drelich et al. (2002) explains the five most popular methods currently used in the oil and gas industry. They are listed below in no specific order.

1. Microbalance (Wilhelmy plate, Du Nouya ring)
2. Capillary Pressure (maximum bubble pressure, growing drop)
3. Capillary-Gravity Force Analysis (capillary rise, drop volume)
4. Gravity-Distorted Drops (pendant drop, sessile drop)
5. Reinforced Distortion of Drop (spinning drop, micropipette)

The OCA machine used in these experiments can calculate IFT using either the pendant drop or sessile drop method. These methods are popular amongst research scientists because the analysis is done using an HD camera and does not require any other instrumentation besides a gastight syringe. IFT is calculated using an image analysis software that analyzes the drop shape dimensions, then a numerical solution is used to calculate the IFT.

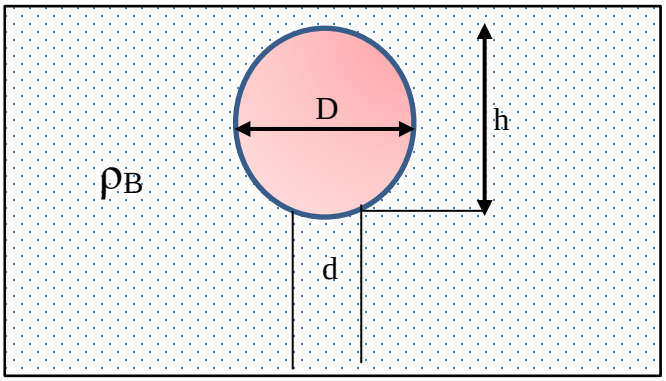


Figure 15: Reverse pendant drop, used for IFT measurements. D is the equatorial diameter, h is the height of the drop, and d is the diameter of the syringe.

The IFT is the relation between the free energy *F* cause by an interface with an area *A* between two phases:

$$\gamma = \left(\frac{\delta F}{\delta A}\right)_{T,V,n} \quad \text{.....Eq. 1}$$

The dimensions of $\gamma$ is $MT^{-2}$ or $N/m^2$ (force/length). The IFT value is then calculated using the following equation:

$$\gamma\ (IFT) = \frac{\Delta\rho g D^2}{H} \text{……. Eq. 2}$$

Where $\Delta\rho$ is the difference in density, $g$ is the gravity constant, $D$ is the drop diameter and $H$ is the shape dependent parameter. The shape dependent parameter (*H*) corresponds to the value of a shape factor that is proportional to $d/D$. The experiment begins by making sure all the required equipment is cleaned. This includes the gastight syringe, the needle, and the cuvette that contains the solution. The syringe is then filled with C&F Meramec oil and the needle is placed in the solution that is at reservoir temperature. Figure 12 in the Appendix shows an example of this experimental setup. Okasha et al. (2014) did a study on the effect of temperature and pressure on IFT and contact angle measurements. It is known that increasing temperature decreases the IFT between oil and water. They also concluded that increasing pressure does not seem to have a large effect on IFT or contact angle, but 6x increase in pressure lead to a slight decrease in wetting angle of 7%. Temperature has shown to affect the IFT and critical micelle concentration of surfactants, this affect is reported to be more severe in anionic surfactants. Surfactants also have a cloud point as previously mentioned, or temperature at which phase separation begins to occur. This leads to a decrease in the concentration of chemicals as the temperature of the surfactant solution increases. Mirchi et al. (2014) proved that temperature has the larger impact on IFT compared with pressure by measuring the IFT over time at various pressures and temperatures. The surface energy

of materials plays a large contribution during the imbibition process, when capillary pressure forces the non-wetting phase out of the pore spaces. Centrifuging the crude oil resulted in a change in the surface energy due to various cations being removed, this change in fluid properties caused the IFT values, when measured in distilled water, to almost double when compared with using the crude oil. It is believed that decreasing the IFT causes the two phases, oil and water, to interfere less with each other thereby shifting the relative permeability curve upwards. Wettability and the heterogeneity of the reservoir are also known to have a significant effect on the shape of the relative permeability curves. The Dykstra-Parsons method is used to establish how heterogenous this area of the Meramec formation is and the work can be found in the Appendix labeled Figure 33. The shift from a negative to a positive capillary pressure is caused by the change in wettability in the presence of surfactants. According to the Young-Laplace equation stated on page 46, the surface tension and contact angle ($\Theta_w$) both positively affect the capillary pressure, both of these values can be directly measured using the same experimental setup previously shown in Figure 14. Several references that are cited, such as Mirchi et al., Okasha et al., suggest a high surface tension value is favored during the production process when hydrocarbons are flowing out of the pore spaces. The opposite is favored during the soaking process when completing the well, when a low IFT value will allow the fluid to penetrate the pore spaces at a faster rate. All this takes into consideration that capillary pressure is the driving force for the imbibition process. Results from the first round of imbibition using Core 9 shows early signs that this belief may be true. An ultra-low IFT surfactant was compared with distilled water in

the same conditions and resulted in an overall lower recovery factor and recovery rate during imbibition. The surfactant consistently gave IFT values <1 mN/m using the reverse Pendant Drop Method, a more accurate analysis could be taken using the Spinning Drop Method, but for our purposes this is unnecessary as we are looking at the data from a broader, more qualitative standpoint. A higher positive capillary pressure should push more hydrocarbons from the pore spaces, but this does not seem to be the case when dealing with the nanopores that are present in the Meramec. Small pore sizes, or confined spaces, will also results in a larger capillary pressure as can be seen in the Young-Laplace equation. Literature, such as Teklu et al. and Akkutlu et al., suggest that at ultralow pore sizes, the interaction between the hydrocarbon molecules, and the pore wall will change the properties of the bulk fluid such as IFT, density, and viscosity. The conclusion is that with increased confinement, the IFT of the pore fluid will decrease. This brings the question as to how valid the Young-Laplace capillary pressure equation is in unconventional formations such as the Meramec where the pore sizes can be significantly smaller. Below is a comparison between oil drops that shows the IFT value of the C&F and crude oil from the Rosemary 1-14H. Both of these measurements were taken 10-15 times and the average value is given below next to each picture. The difference between the IFT values as well as the purity of the oil can be seen between the two types of oil due to the cleaning and filtering process.

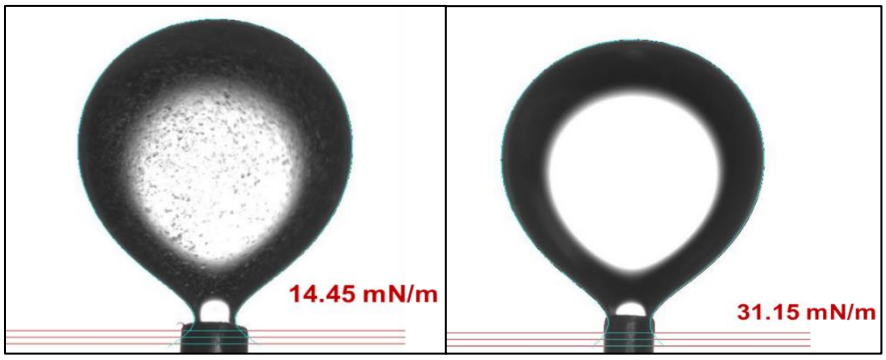


Figure 16: IFT comparison between crude oil (left) and C&F oil (right) from Rosemary 1-14H. 50% increase in IFT after the C&F process.

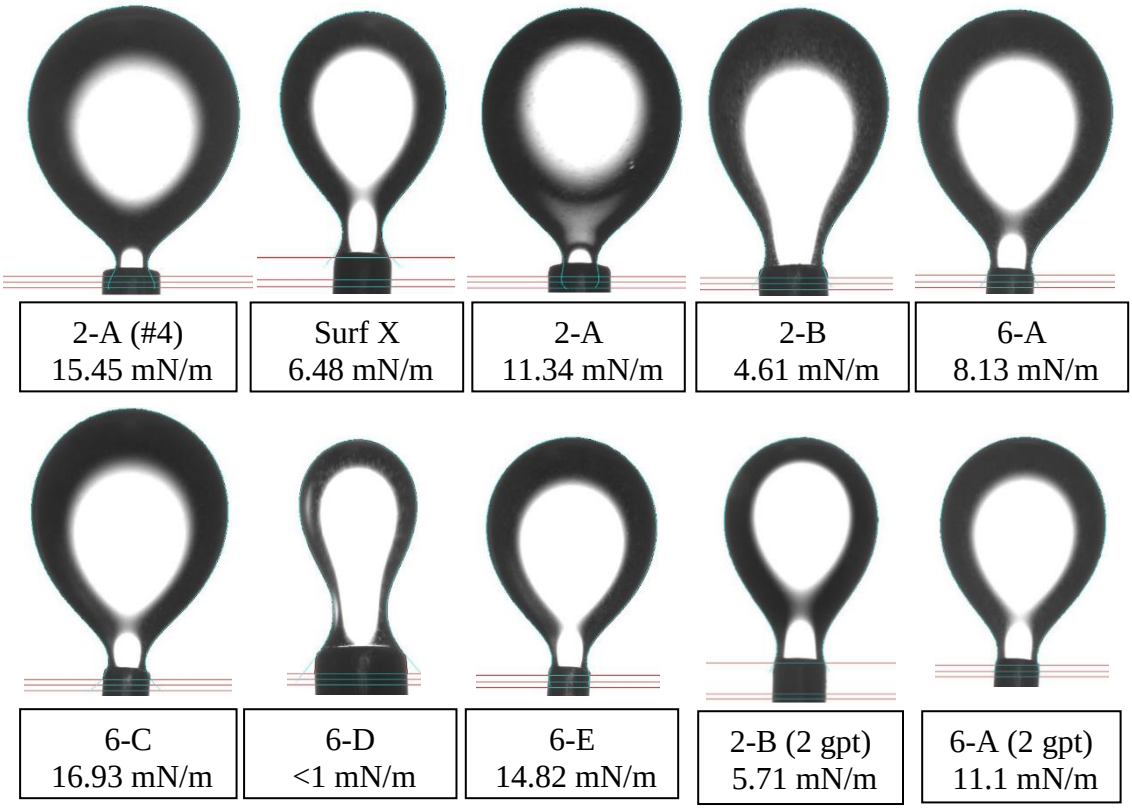


Figure 17: IFT of all the surfactants used in this project. Results on rows 1 and 2 were done at 1 gpt while 3rd row was done at 2 gpt with aqueous temperature at 170 °F.

**IFT Experimental Setup/Procedure**

1. Clean the syringe, needle, and cuvette before starting the experiment. If using a surfactant solution, allow agitation for 10 minutes.
2. Once the solution is ready, pour into the cuvette and place temperature probe in the solution.
3. Set OCA device to desired temperature and allow it to heat up.
4. Once solution is at temperature, lower the syringe into the solution.
5. Displace 0.05-0.1 μL of oil at a time, depending on type of surfactant, until oil bubble is displaced from syringe, record the process.
6. Set the density of the oil relative to the temperature, OCA software will calculate the IFT value.
7. A pictorial example of the experimental setup is provided in the Appendix labeled Figure 12.

### 2.2.6 Spontaneous Imbibition

Imbibition with the assistance of a surfactant additive in fractured reservoirs has been studied for 50+ years in the oil and gas industry. The physical process that governs the spontaneous imbibition of a non-wetting fluid into the matrix depends largely on pore size distribution, capillary forces and formation properties, especially in heterogenous unconventional formations. Oil production from fractured reservoirs can occur by spontaneous water imbibition alone, but the addition of surfactants to lower IFT or alter wettability will further enhance this process (Chen et al. 2000). Similar studies such as Alvarez et al. (2017) and Saputra et al. (2018) done on core samples taken from the Bakken, Eagle Ford, Wolfcamp, and Marcellus formations have shown

the potential of improved recovery when the optimal surfactant is mixed with the fracture fluid. These formations tend to be initially oil-wet, by having an average wetting angle greater than 90°, making them viable candidates for surfactant testing. Before the experiment begins, multiple factors must be considered when investigating the effects that surfactant additives could have on the chemical interactions in the formation. Surfactants will typically show an indifferent effect during spontaneous imbibition when the core sample is already a native water-wet system coupled with a nanoscale pore distribution. If this is the case, a reduction in IFT only poses as an inhibitor during imbibition due to the decrease in capillary pressure without any change in the wetting angle, $\Theta_w$ (Lohne et al. 2012). This is all mathematically represented by the Young-Laplace equation, which states that capillary pressure is a function of IFT and the angle that forms between the capillary wall and the fluid. This equation was first developed by Thomas Young in his 1805 paper *An Essay on the Cohesion of Fluids.* In a sufficiently narrow capillary tube with radius *r*, the liquid surface will be a portion of the spherical surface and is related by $R = \frac{r}{\cos(\theta)}$. This assumption has its limitations and raises questions when the wetting angle is equal to 90°, making the capillary pressure zero. If capillary pressure is not present in the pore space but is thought to be the main driving force, production of oil should not take place. The Young-Laplace equation is stated below labeled Equation 3 along with a graphic representation of the capillary tube experiment, where capillary pressure ($P_c$) is related to IFT ($\sigma$), the wetting angle ($\Theta_w$) and the pore radius ($r$):

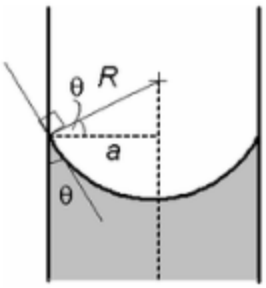


$$P_C = \frac{2\sigma\cos(\theta)}{r}$$.....Eq. 3

The purpose of the SI experiments presented in this paper is to investigate the effects that wettability alteration and petrophysical properties have on recovery rate and recovery factor in the Meramec formation. The experiment begins by selecting core plugs of similar dimensions, this step is critical when calculating recovery factor as the differences in dimensions will affect the final results. If the results are to be upscaled to a field level for simulation purposes, scaling the results to the core properties using dimensionless time $t_D$ is necessary (Mattax and Kyte 1962). When analyzing the recovery results using this method, the various conditions and rock properties are taken into account. Scaling the recovery factor results to include the differences in rock properties was first presented by (Mattax and Kyte 1962) to try and overlay the results into one generalized curve. This is done by calculating the dimensionless time variable, which includes properties such as porosity, permeability, and characteristic length. This dimensionless variable can be used as an approximation for recovery factor when the rock properties are different, which will minimize the amount of laboratory work needed. This procedure does not come without its limitations and is based on the Leverett J-function where multiple assumptions about the conditions of imbibition were

made. One example being the absence of pore size distribution, which plays a major role in the production of hydrocarbons in unconventionals. The scaling model introduced by Mattax and Kyte is presented below:

$$t_D = t\sqrt{\frac{k}{\varphi}}\frac{\sigma}{\mu_w L^2} \text{.....Eq. 4}$$

Where $t$ is the time in hours and $L$ is the characteristic dimension of the core sample. After the proper cores are chosen, they are placed in a via and filled with crude oil from the same well, the vial is then placed in a vacuum oven at reservoir temperature to begin aging the cores. This aging process is time consuming and full saturation depends on the properties of the plug. If time is a constraint, a soaking method where the oil is injected into the core can be used instead. This is done by placing up to 10 core plugs in a large pressurized chamber, usually up to 10,000 psi, while oil is circulated through the core plugs. The soaking method was not used for this study. Once the aging is complete, the plug is carefully cleaned with a KIMTECH wipes to remove any residual oil on the outer surface and weighed again to measure the change in mass, it is then scanned once more to confirm full saturation took place. The Spade Amott cell was used to house the core plug samples in the surfactant solution, Figure 17 in the Appendix shows examples of two types of Amott cells that were used for these SI experiments. This glass apparatus has a graduated cylinder that is used to measure the amount of oil produced from the core. Oil production measurements are taken every 2-6 hours for the first 48 hours and then every 12-24 hours for the rest of the experiment. Pictures and CT scans are taken at every stage of the process for documentation, these CT images are

processed using ImageJ software. The CT number, or computed tomography number, can be described as a unit of measurement that reflects the X-ray attenuation coefficient in a single image voxel. This value that is measured in Hounsfield unites (HU) is dependent upon a variety of factors such as the CT scanner model, tube voltage, and reconstruction algorithm. CT imaging provides another means of analyzing imbibition results, since the CT number should increase as aqueous solution imbibes into the core. A Toshiba Aquilion TSX-101A CT unit is used in this study. After the plug is scanned, the CT number of the plug can be determined through an in-house MATLAB code and then converted to a density value by using the equation presented in Massicano et al. (2009). It converts the CT number to density by the following equation:

$$\rho = 1.017 + \frac{0.592 * CT\#}{1000} \text{.....Eq. 5}$$

The CT number of a core plug is calculated by averaging the CT numbers of each voxel, or image. A graph can then be produced showing the change in CT number over time and a comparison can be made with the recovery factor curve. Since the aqueous solution is far denser than the oil trapped in the pore spaces, the CT number should steadily increase as time continues and the aqueous phase imbibes into the core. The main driving force of imbibition can be calculated by determining the inverse Bond Number $N_B^{-1}$ of each individual core plug. Shechter et al. (1994) discussed the application of the inverse Bond Number to determine the main driving force of imbibition. This is defined by Eq. 6 below:

$$N_B^{-1} = C \frac{\sigma \sqrt{\frac{\emptyset}{k}}}{\Delta \rho g h} \text{..... Eq. 6}$$

Where $C$ is a constant dependent on the capillary tube model, in this case we use 0.4 taken from Zhou et al. (1989), and $h$ is the height of the medium. A large inverse Bond numbers means that capillary forces dominate while a small inverse Bond number means gravity forces dominate. If the wetting properties are known, Schechter et al. (1994) concluded that capillary forces are dominate for $N_B^{-1}$>5 and gravity forces are dominate for $N_B^{-1}$<1. If the value falls between 0.2 and 5, both capillary and gravity forces can be active in the displacement of the non-wetting fluid. $N_B^{-1}$ was calculated for the core plugs previously mentioned in this paper and are presented in the table below. As can be seen in the table below, most of the plugs exhibit gravity as the dominate force with the exception of 56H.

| *Core plug sample* | $N_B^{-1}$ | *Dominate Driving Force* |
|---|---|---|
| 38H | 0.11 | Gravity |
| 41H | 0.075 | Gravity |
| 50H | 0.15 | Gravity |
| 56H | 0.24 | Capillary&Gravity |
| 71H | 0.11 | Gravity |
| 77H | 0.105 | Gravity |
| 86H | 0.07 | Gravity |
| 95H | 0.061 | Gravity |
| 105H | 0.11 | Gravity |

Table 5: Inverse Bond Number calculated for core plug samples that underwent imbibition experiments, equation used is presented in Schechter et al. (1994).

Preliminary SI tests were first conducted on 5 core plug samples taken from a large block core labeled “9”. Core 9 did not originally come in the box with the rest of the plugs but is still from the Rosemary 1-14H. The plugs were all cut to the same dimensions, 3” x 1.5”, and aged in the Rosemary 1-14H crude oil. The aging process for this set of plugs lasted 200 days in a vacuum oven to ensure maximum wettability was restored. Core 9-1 was chosen to test in only distilled water while 9-2, 9-3, 9-4, and 9-6 were tested in various surfactants at 1 gpt loading. Core 9-5 was broken when trying to cut it from the core block so it was used to make rock chips for contact angle and powder for zeta potential. The surfactants chosen for these experiments are all water soluble and a mix of anionic, nonionic, nonionic/anionic. The viscosity of the surfactant solution after 15 minutes of mixing did not vary significantly from that of distilled water. A viscometer test was conducted to confirm this assumption. A table is provided in the Appendix labeled Table D that summarizes the experiments done using Cores’ 9-# along with the specific surfactant and loading used. This set of imbibition experiments ran for 500 hours, but after 100 hours the recovery rate starts to level off and production slows down. The IFT of Core 9-1, which is distilled water only, is similar to the IFT of Core 9-4 even though a surfactant was added, but Core 9-4 showed a higher recovery rate and recovery factor. Core 9-6 used an ultralow IFT surfactant solution of <1 mN/m and had the worst performance in terms of recovery factor and rate. The results of 9-6 agree with the earlier statement that reducing the IFT of the aqueous solution will hinder recovery in an already water-wet system. The surfactants used in this round of imbibition consisted of 5-20% by volume alcohol mixed with a “proprietary blend” at a classified

concentration and CAS number. Surfactant 6-C is a nonionic and anionic mix that contains 5-20% isopropanol with the rest being proprietary. Surfactant 6-D contains 3 proprietary components at 1-5% by volume along with ethylene glycol, 1,2,3-propanetriol, and sodium chloride. A table listing the surfactant composition is given in the Appendix and includes all the known information pertaining to the surfactants used for these experiments beginning on page 90. Recovery factor for each core can be both calculated and measured if the information is available. Core 9 did not have any available petrophysical information so effective pore volume ($S_{oi}$) was measured for this set SI experiments. This was done by assuming an effective porosity for all the plugs and calculating the effective pore volume by weighing the core before and after the aging process, then dividing that value by the density of the saturated fluid. The next set of the plugs used for SI experiments had supplementary information given by Core Lab such as dimensions, porosity, and permeability.

The second round of imbibition used eight core plugs that were originally provided by Core Lab. These plugs are all 1" in diameter and had slight differences in lengths with an average of 2.5". The aging process for this set of cores lasted 150 days in a vacuum oven to allow full saturation restoration. A figure in the Appendix labeled Figure 5 shows the correlation between the $S_{oi}$ measured after the aging process and the porosity value for each plug provided by Core lab for the previously mentioned core plugs. Table C in the Appendix lists the core plugs used for imbibition and the chemical additive that each core plug was tested in along with the IFT and final recovery factor. Surfactant 2-A consists of two different surfactants at 1 gpt each, these are labeled "Type

3" and "Type 4". The mixing of these two surfactants is done at the discretion of the chemical company that developed them. These sets of experiments were allowed to imbibe for 250 hours even though production of oil ceases or slows at 100 hours as previously mentioned. Cores plugs 50H, 56H, and 77H were chosen to test in only distilled water at reservoir temperature. Sample 77H performed the best in terms of final recovery factor, but also had the highest porosity value compared with 56H and 77H. Both core plugs 50H and 77H are shown in Figure 18 after 22 hours of imbibition and the oil bubbles forming on the surface of the core seem to be in an oil-wet state, which is contrary to the contact angle experiments taken in distilled water presented in Section 2.2.5. The oil bubbles on core plug 77H also appear to be in a more water-wet state compared with 50H. Core 38H, tested in surfactant 2-A, performed the best out of all the imbibition experiments with a recovery factor of 35% after 250 hours of imbibition. This core also had the highest porosity of 7.0%, this is 27% greater compared with the next highest porosity core, 77H. Core 105H, which was tested in "Surf X" at 1 gpt had the lowest recovery factor of 10.5%, this surfactant did not perform as well in contact angle experiments so these results were expected. Sample 105H also had a relatively low porosity and permeability compared with the other cores. A graph of recovery factor versus porosity is given in the Appendix labeled Figure 18 and shows the strong correlation between the two metrics. This graph brings into question the effectiveness of surfactants on the Meramec formation. Sample 38H might have performed the best, but it also has the highest porosity value and $S_{oi}$. The only method of confirming this phenomenon would be to test the same exact core in the same conditions with distilled

water alone. Graphs showing the recovery factor versus time are available in the Appendix for all the experiments mentioned in this section.

Figure 18: Pictures of core 50H and 77H at 24 hours imbibing in distilled water.

| *Sample* | *Test Type* | *Hours in Imbibition* | *IFT (mN/m)* | *RF (%)* |
|---|---|---|---|---|
| ***38H*** | 2-A 1 gpt | 250 | 12.2 | 35% |
| ***50H*** | Distilled Water | 250 | 31 | 18.8% |
| ***56H*** | Distilled Water | 250 | 31 | 19.3% |
| ***71H*** | 6-A 2 gpt | 250 | 10.1 | 15.8% |
| ***77H*** | Distilled Water | 250 | 31 | 25.3% |
| ***86H*** | 2-B 2 gpt | 250 | 6.2 | 24.2% |
| ***95H*** | 6-C 2 gpt | 250 | 6.5 | 21% |
| ***105H*** | Surf X 1 gpt | 250 | 7.3 | 10.5% |

Table 6: Imbibition summary showing final recovery factor for each core plug after 250 hours of imbibition.

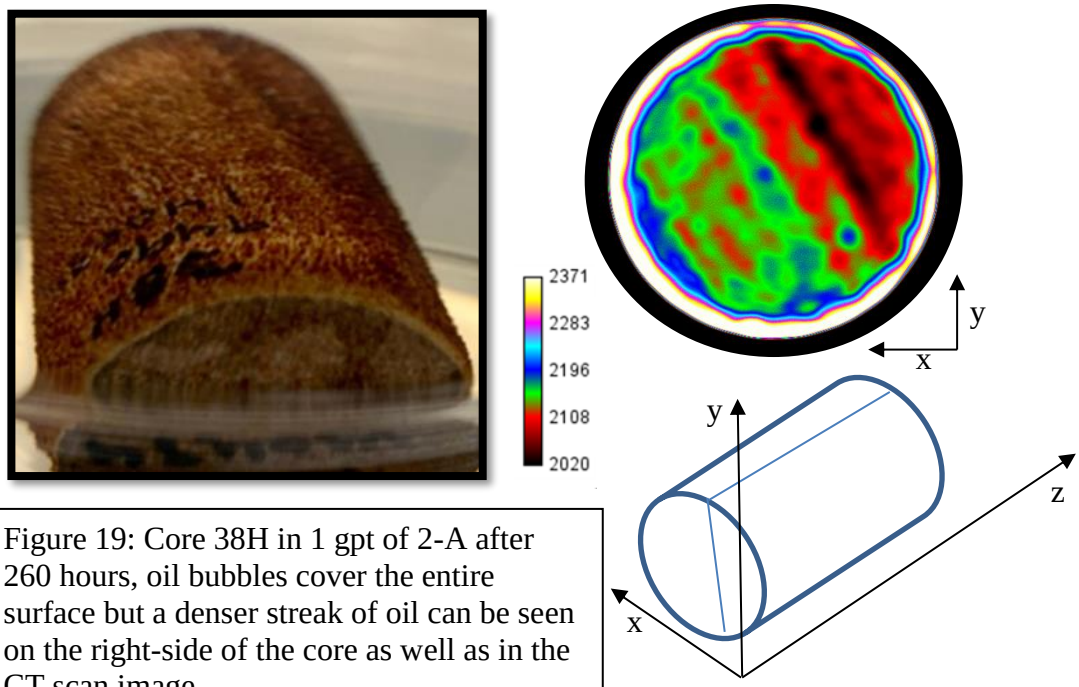


Figure 19: Core 38H in 1 gpt of 2-A after 260 hours, oil bubbles cover the entire surface but a denser streak of oil can be seen on the right-side of the core as well as in the CT scan image.

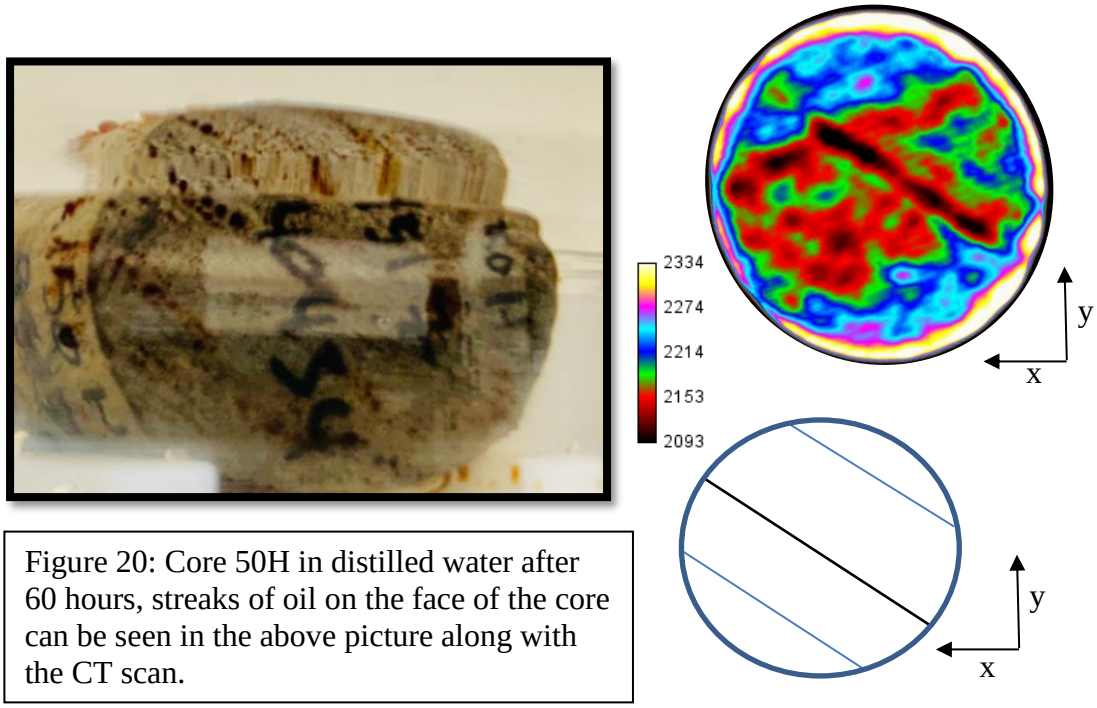


Figure 20: Core 50H in distilled water after 60 hours, streaks of oil on the face of the core can be seen in the above picture along with the CT scan.

**Spontaneous Imbibition Experimental Setup/Procedure**

1. Plugs are chosen based on dimensions and available petrophysical data. They are first scanned in our CT machine as dry core and then placed in a closed vial filled with crude oil.
2. Plugs are aged in crude oil inside a vacuum oven set at reservoir temperature for 3-5 months to ensure wettability restoration.
3. After aging is complete, the plug is removed from the vial and the oil on the face of the core is gently wiped off using a KIMTECH wipes. It is then weighed to measure the change in mass after aging and scanned again. If testing with surfactant, allow solution to mix for 15-20 minutes at 500 rpm before filling Amott Cell.
4. The plug is placed in the Amott Cell and the cell is filled with the surfactant solution. Careful not to fill the cell to the top as the water level will rise when the temperature starts to increase.
5. The Amott Cell is placed inside an oven at reservoir temperature and the imbibition process begins. Cells are scanned every 4-6 hours for the first few days, then every 10-12 hours thereafter until the experiment is complete.
6. It is important to scan the cell as quickly as possible to ensure minimal temperature changes as CT number is heavily dependent on temperature.
7. Pictures are taken of the core at every scan. Produced oil is measured using the linear graduation marks, 1 dash is 0.05 mL.
8. The information is then plotted to show recovery factor over time.

The contact angle and distribution of the oil droplets on the surface of the core plug during SI can be used as secondary information by taking a close-up picture of the core plug and comparing those to the CA values from the OCA device. Close-up pictures of the core plug were taken at different times during imbibition and are provided in the

Appendix starting on page 117. It can be seen that the concentration of the oil droplets is not evenly distributed and seems to form along natural fractures. This means production is taking place in the lower density/higher porosity areas of the core. This can be confirmed by looking at the CT images of the core on the Z-X and Z-Y plane. Examples of these planar CT images are shown in the Appendix starting with Figure 19. By looking at these images, it becomes apparent that if natural fractures or bedding planes are present in the core plugs, they are accountable for the majority of oil production during SI. This also agrees with the graph in the Appendix showing the $S_{oi}$ versus porosity.

### 2.2.7 Zeta Potential

Zeta Potential (ZP) measurements is the fourth metric used in this line of experiments. Research in this area focuses mostly on the magnitude of the measurement, recorded in millivolts, which should to correlate with wettability results. Nanoparticles or colloidal particles exhibit a surface charge when they are in suspension. When an electric field is present, particles will move due to the interaction between the applied field and the charged particle. This motion, both velocity and direction, is a function of the charge, electric field strength, and suspending medium. This particle velocity is proportional to the electrical potential of the particle at the shear plane, or the zeta potential as shown in Figure 21. There is ongoing discourse on the topic of zeta potential, and specifically its relation, if there is any at all, to wettability. Zeta potential is indirectly measured in our lab via Phase Analysis Light Scattering (PALS), which

determines the electrophoretic mobility of charged, colloidal suspensions. This electrophoretic mobility increases for more highly charged solutes and for solutes of smaller size as can be inferred from the equation below.

$$u_{ep} = \frac{q}{6\pi\eta r} \text{..... Eq. 7}$$

Where $u_{ep}$ is the electrophoretic mobility, q is the solute's charge, η is the buffer viscosity, and $r$ is the solute's radius. The Brookhaven ZetaPALS machine can use the measured data to then calculate the zeta potential of the colloidal system. A PALS experiment is similar to the conventional laser Doppler electrophoresis method, but differs in that it measures the phase change $\frac{d\varphi}{dt}$ of the sample interfering beam with the reference beam, which is supposed to be proportional to the change in position of the particles (Sharp et al. 1985). This can then be translated to the respective mV. This measurement is taken using an open dip-in electrode that is submerged in < 400μL of solution. Zeta Potential is understood to be an indicator of the stability of a colloidal dispersion that is being measured. This colloidal dispersion has different variations such as emulsion, suspension (our experiments), and association colloids. There are also many kinds of instability in which colloidal dispersions can be subject to. If particles stick to the surrounding surface, it is referred to as deposition. Particles can also stick to each other (aggregation, coagulation, or flocculation, as well as separate (sedimentation). Addition of surfactants can, in some cases, counteract these mechanisms by imposing a strong electrostatic repulsion, this repulsion can be parameterized by the zeta potential value. In some other cases, the electrostatic interactions can be unfavorable and

destabilize the dispersion. This can happen when some elements in the fluid system carry a strong polarized charge (David Grier, NYU). Previous studies on the effects of zeta potential on wettability have resulted in conflicting conclusions that do not always explain the entire picture. The first being that the magnitude of the zeta potential is a direct measurement of the degree of electrostatic repulsion between adjacent particles also in the dispersion (Blinks et al. 2000). Furthermore, it is stated that a high magnitude of zeta potential corresponds with the particles in solution being stable and resisting aggregation.

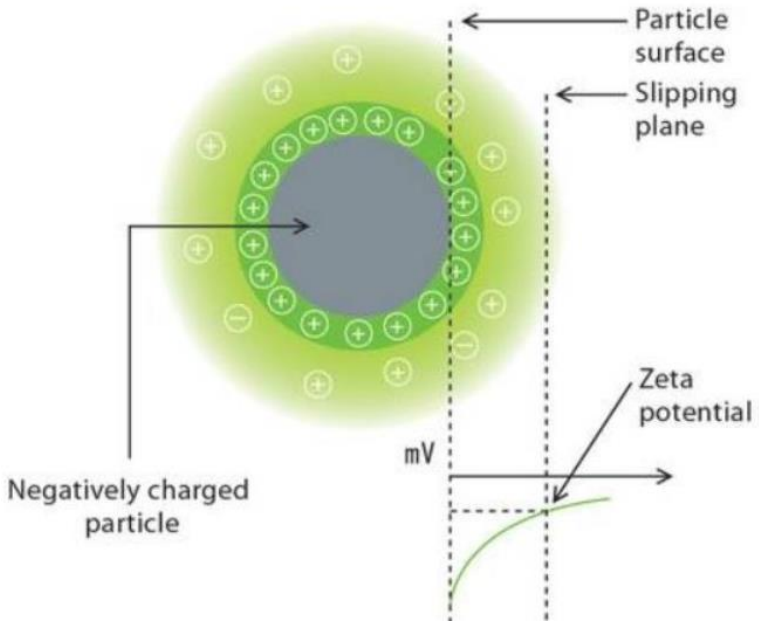


Figure 21: Diagram of a charged particle in a surfactant solution. Reprinted from Instruments (2011).

A solution that has a low magnitude of zeta potential will in turn cause flocculation, which is when the particles start to adhere to each other due to the attractive forces exceeding the repulsion. Surfactants are believed to help this by preventing the flocculation and therefore preventing permeability damage, which is supposed to help with loss of proppant bed permeability (Palla et al. 2014). The pH of the solution is also known to have a correlation with the zeta potential value. At a static concentration, the magnitude of zeta potential increases as the pH of the solution increases. This means that a more basic solution is favorable and will cause more particle stability. This was tested and proved by Nasr-El-Din et al. (2015) with an analogous experimental setup (SPE-173763). The method presented in this study involves crushing up the rock samples to a fine powder. A brick and mortar method are used for this crushing process and afterwards the powder is sieved using a size 45 sieve, or 350 μm.

Zeta potential experiments performed on the Bakken, Eagle Ford, Wolfcamp, and Permian rock samples by Alvarez et al., Hoxha et al., and Nasr-El-Din et al. show that the average value of these formation in distilled water alone is ~ -20 mV. The belief is that most rocks with a large magnitude of zeta potential values exhibit water-wet behavior while oil-wet rocks tend to have a lesser magnitude of zeta potential value (SPE-180097). This claim does not hold true when including the Meramec formation which is already in a water-wet state, but has the same zeta potential values as formations that are oil-wet (SPE 187176). When testing zeta potential with surfactants, the value only has intrinsic meaning within the surfactant being tested. Zeta potential experiments were performed on rock samples 129H, 227H, and Core 6 using the same

surfactants as the contact angle and SI experiments. Bar graphs are given in the Appendix labeled Figure 31 that show the average zeta potential value taken for each surfactant. Surfactants 2-A and 2-B exhibit the largest negative average zeta potential value when tested at 1 gpt on the samples previously mentioned. This means that 2-A and 2-B prevent the flocculation of particles the most compared with the other surfactants used in this experiment. These two surfactants also performed the best during the imbibition experiments in terms of recovery factor.

**Zeta Potential Experimental Setup/Procedure**

1. Power up Brookhaven instrument and open the software.
2. Carefully clean the electric probe, cuvette and vial used for testing. Probe calibration may be necessary if prolonged use has occurred, if so, use a 1 M solution of NaCl.
3. If testing with a surfactant solution, allow agitation of 10 minutes.
4. Use a clean 10-20 mL syringe, attach 0.2 μm PTFE filter, and remove plunger, fill with aqueous solution.
5. Slowly insert the plunger, and filter the solution 3 times into a vial.
6. Scoop a small amount of powder, < 0.1 mg in weight and pour into the solution, sonicate for 1 minute then allow the solution to sit for another 5 minutes.
7. Using a pipette, transfer the solution from the vial to a testing cuvette and fill up halfway, place in machine to begin testing.

Figure 22: Zeta potential powder samples used for testing; slight color difference can be seen between the samples. In order from left to right, Core 6, 129H, 227H

| Zeta Potential Results | | |
|---|---|---|
| Core Plug Sample | Synthetic Brine Average | Distilled Water Average |
| Core 6 | -1.35 | -19.18 |
| 129H | -3.20 | -21.14 |
| 227H | 0.68 | -24.90 |

Table 7: Zeta Potential averages using 15 runs for 3 core samples with PALS method. Comparison of zeta potential average for Brine vs. distilled water.

# 3. RESULTS AND DISCUSSION

## 3.1 Results

Contact angle experiments using the Captive Bubble method showed that this area of the Meramec formation is in fact a native neutral/intermediate wet system when multiple measurements were taken in distilled water at 170 °F using the C&F oil. This was also confirmed during imbibition experiments in only distilled water. Wetting angles from over 50 different measurements ranged from 50°-75°, with an average $\Theta_w$ = 63°. These results do not align with previous wettability experiments conducted in the same manner on the Bakken, Eagle Ford, Permian, and Wolfcamp formations. Though the Meramec formation is already in a neutral/intermediate-wet state, the average wetting angle did decrease with the addition of certain surfactants to an even more water-wet state, but the change is not extreme. The average wetting angle of over 50 different measurements including all the surfactants mentioned in Section 2.1.3 at 1 gpt equaled to $\Theta_w$ = 55°, or a 13% reduction compared with distilled water. This decrease in average wetting angle still shows promise in that the slightest shift to a more water-wet system will cause an increase in the capillary pressure according to the Young-Laplace equation stated in Section 2.2.6, but this change is only a major factor if capillary forces are the dominate mechanism of imbibition. It is also important to consider that a 13% change is not relatively large and part of it could be caused by user error during experimentation. According to the Inverse Bond number presented by Schechter (1994) and calculated in Section 2.2.6, gravity forces are the more dominate driving force for imbibition in the Rosemary 1-14H, so this change in capillary pressure may not be useful

after all. This calculation was performed on all the core plugs used for imbibition and only one core plug showed signs of having a gravity/capillary driving force.

Initial contact angle measurements taken in distilled water using the Rosemary 1-14H crude oil showed the formation to be in an intermediate/oil-wet state, but gave discrepancies in results. This was believed to be caused by the produced water and solid particulates in the oil. These contact angles were similar to the contact angles that formed on the outside surface of the core plugs during imbibition experiments in distilled water only, as seen on page 37.

The first round of surfactants used for both contact angle and imbibition produced results that were expected after Core 9 and Core 6 both initially tested as weakly-water wet in distilled water at 170 °F with the Captive Bubble method. Adding different surfactants at 1 gpt loading did not increase the recovery factor significantly but did show signs of increasing the recovery rate when compared to just distilled water. Anionic surfactants performed the best in both imbibition and contact angle for these core plugs. This set of experiments gave somewhat ambiguous answers since the differences in recovery factor between cores using surfactants and cores using distilled water is negligible and no petrophysical information was provided that could have been used as supplementary data.

A second round of imbibition experiments was performed using core plugs that had available petrophysical information such as porosity and permeability. This information can and was used to calculate the $S_{oi}$, which can be compared with the measured $S_{oi}$ after the aging process. It also allowed for the comparison of measured $S_{oi}$

and porosity for the set of plugs, which is presented in the Appendix as Figure 5. The figure shows a strong correlation between the porosity and $S_{oi}$, which means that most of the saturated oil is filling the large pore spaces in the rock matrix. Nine core plugs were chosen for imbibition, three of these plugs were tested in distilled water while the others were tested in surfactants at 1 or 2 gpt. Firstly, recovery is possible during imbibition when testing in only distilled water. The three core plug samples that imbibed in only distilled water yielded an average recovery factor of 19%. Secondly, the results also showed that when the proper surfactant is chosen, the best case being 1 gpt of 2-A tested on sample 38H, the recovery factor does increase compared with imbibition in distilled water alone. 2-A also tested well during contact angle experiments and altered the wetting angle compared with distilled water to a more water-wet state. One important factor to keep in mind is that 38H had the highest porosity value, a 40% difference from the average porosity of all the core plugs, which means it had the highest $S_{oi}$ as well. This could have been the cause for the high recovery factor, but to confirm this theory more testing would be needed. The next set of plugs used surfactant 2-B and were tested at different concentrations on samples 86H and 89H. Both core plugs 86H and 89H were tested at 2 gpt and 1 gpt respectively. 86H had a 40% higher recovery factor compared with 89H, but also had a porosity value that is 2x larger. Again, this higher recovery factor could have been due to the increased surfactant loading or due to the higher porosity value of the core plug. 2-B at 1 gpt performed the best during contact angle experiments, decreasing the average wetting angle by 16% ($\Theta_w = 53°$) across all rock chips tested. The average recovery factor for the three core plugs, 50H, 56H, and 77H,

that tested in distilled water is 19%, with a standard deviation of 3.2 between all three recovery factors. The average porosity for these three plugs is almost identical to the average porosity across all the plugs tested for imbibition, with a difference of less than 0.15%. This confirms the previously mentioned hypothesis that porosity plays a large role in recovery factor. 50H has the highest permeability value of 0.03 mD compared with all the plugs used for imbibition, and 77H has the second highest permeability value of 0.02 mD. 77H had the highest recovery factor compared with 50H and 56H even though the permeability of 50H was higher by 0.01 mD, this can be seen in Figure 26 in the Appendix. Permeability of these core plugs does not correlate with recovery factor in any manner, when plotting the two metrics against each other there is no obvious relation. Porosity however correlates almost impeccably with recovery factor, giving a Pearson Correlation value of 0.77. The graph that displays this observation is in the Appendix labeled Figure 18. The low IFT surfactants had lower initial recovery rates compared with the high IFT surfactants, but the difference was negligible and more testing is needed to confirm this theory. Imbibition experiments performed in distilled water exhibited similar initial recovery rate to imbibition with surfactant 2-A, which had a similar IFT. The difference is that surfactant 2-A recovered oil for a longer period of time compared with distilled water alone, an average of 30-50 hours longer. Recovery factor curves for all the imbibition experiments discussed are provided in the Appendix along with the corresponding CT number curves. CT number provided a good measure to quantify the effectiveness of imbibition, these curves were plotted on the same graph as the recovery factor to show the increase in CT number as the aqueous solution

imbibed into the rock matrix. The change in density from the start of imbibition to the end by looking at the change in CT number is not large, which is expected when gravity forces are dominate and the pore space is on a nanoscale. The average change in CT number from the start of imbibition to the end at 250 hours for all core plugs tested is 5.03 HU with a standard deviation of ~2.5 HU. By using this value along with equation 5 provided in Section 2.2.6, the average change in density for the core plugs can be calculated. This value, when calculated from the start of imbibition to the end at 250 hours, is equal to 1.02 g/cc. This proves that imbibition of the aqueous solution into the rock matrix does take place, regardless of whether surfactants are added. It is also expected that this change in CT number and density would not be large since the volume of oil being produced is not large.

IFT reduction did not seem to play a large role in the imbibition process in terms of recovery factor. This could have been due to the fact that the Meramec is already in a water-wet state and any further IFT reduction without a corresponding change in wetting-angle would just lower the capillary pressure. The best performing imbibition experiment using a surfactant, 2-A at 1 gpt, had an IFT value of 12 mN/m, a 60% reduction in IFT compared with distilled water. The next two best performing imbibition experiments using surfactants 2-B and 6-C at 2 gpt were cores 86H and 95H, which had IFT values of 6.2 mN/m and 6.5 mN/m respectively. Core plug 77H had a final recovery factor of 24.7% but imbibed in only distilled water with an IFT of 30 mN/m.

Zeta potential experiments performed with both distilled water and surfactants gave results similar to what other studies are saying, with a few key differences. The first

difference is that the Meramec formation tested as water-wet, but had an average native zeta potential of -21.5 mV as shown in Table 7. Most other literature is stating that a native oil-wet formation will have a zeta potential of ~-20 mV when testing in only water. This most likely stems from the fact that not many unconventionals test as initially water-wet in the first place, meaning there is not much challenging data in this area of experimentation. The two surfactants that had the largest magnitude of zeta potential, 2-A and 2-B, also performed the best during imbibition experiments. These results align with current literature that states a higher magnitude of zeta potential will lead to higher recoveries during imbibition. More testing should be done to confirm these results. When testing zeta potential in a synthetic brine comparable with the Rosemary 1-14H produced water, the magnitude of zeta potential decreased giving an average of -1.30.

## 3.2 Discussion

Though the Meramec formation is classified as an unconventional formation, it does not behave similar other unconventionals such as the Bakken or Eagle Ford according to wetting experiments conducted in our lab. The two aforementioned formations previously tested as initially oil-wet while the Meramec tested as initially neutral/intermediate-wet by measuring contact angles in distilled water on rock samples using the Captive Bubble method (Alvarez et al, Saputra et al.). This could be due many reasons such as the relatively light oil, nanopore scale, or extreme heterogeneity of the Rosemary 1-14H. Testing contact angle with the crude oil gave erroneous results due to

the large standard deviation within one rock chip. This was thought to be caused by the produced water and solid particulates in the crude oil. To overcome this problem, the oil went through a cleaning and purifying process. Once the oil was separated from the produced water and centrifuged to remove the solids, the standard deviation decreased to less than 8° between contact angle measurements using the same rock chip. Since the Meramec is already in a native neutral/intermediate-wet state, surfactants do not seem as an obvious option for wettability alteration compared with other unconventionals that have proven otherwise. This does not mean that surfactant testing shouldn't be considered, rather more careful testing is needed to choose a suitable surfactant at the correct concentration. Pore geometry also complicates the application of contact angle and wetting principles previously shown in this study. In an ideal experiment, the surface would be a perfectly smooth plane, but pore walls in the subsurface are not smooth or flat and could possibly be comprised of multiple mineral types. Macro-scale contact angle experiments, briefly mentioned in Section 2.2.4, have shown to give a better picture of how surface rugosity can affect contact angle, but were not used in this study. Previous experiments involving IFT investigation (Alvarez et al., Okasha et al., SPE-154178) concluded that a relatively high IFT solution could possibly inhibit the production of oil compared with a low IFT solution, especially if the formation is already water-wet. In the experiments presented in this paper, the solution with the highest IFT, 38H, turned out to be the best performing imbibition experiment in terms of recovery factor, contradicting the earlier statement. As specified early, this is also the core plug with the highest porosity so further testing would be needed to confirm these

results. The lower IFT surfactants did not perform as well during imbibition experiments, with the exception of core plug 86H which was tested at 2 gpt using 2-B and had 10% less recovery than 38H. The IFT of the aqueous solution will slightly decrease with time as it reaches reservoir temperature, experiments conducted in our lab confirm this. The lowering of IFT of the aqueous solution did not seem to be a large influence in terms of recovery factor. The 3 core plugs that tested in distilled water had IFT's that were 2x larger on average and performed better than 3 of the core plugs that tested in a surfactant solution. Imbibition experiments performed by Saputra et al. (2018) and Alvarez et al. (2015) on the Wolfcamp and Permian basin showed the addition of surfactants led to a higher recovery factor compared with using distilled water only. The surfactants increase capillary pressure by shifting the wetting angle to less than 90° and simultaneously lowering the IFT of the aqueous solution. This did not happen at the same scale in the Meramec when conducting imbibition and contact angle experiments with surfactants, but having the porosity values for each core plug provided valuable information that Saputra et al. (2018) and Alvarez et al. (2015) did not have for their experiments. Porosity values correlated extremely well with the final recovery factors in that higher porosity samples were producing more oil. Permeability values were provided and were thought to do the same, but provided no correlation to recovery factor. CT images of the core plug also showed that most of the oil production was coming from low density/high porosity areas such as bedding planes or natural fractures. Pictures taken of the core during imbibition show that the wetting angle of the oil drops on the surface of the core does change to a more water-wet state versus the cores

imbibing in distilled water. Though these wetting angles are not able to be measured, there is a clear difference in wettability. The core plugs that imbibed in distilled water have a variety of contact angles ranging from neutral/water-wet to oil-wet, but most are oil-wet. This aligns with the initial contact angle experiments performed in distilled water using the crude oil. The smaller diameter oil drops look to be in a neutral/water-wet state, just like the contact angle experiments conducted in distilled water while the larger diameter oil drops are in an oil-wet state. All of the oil drops on the surface of the core plugs that tested in surfactants, especially 2-A and 2-B, exhibited a water-wet state. The pictures taken during imbibition, shown in Figure 30 and Figure 31, prove that surfactants such as 2-A tested at 1 gpt will shift the wettability of the displaced oil to a more water-wet state compared with distilled water alone. It is important to consider that the oil drops produced by imbibition should be used qualitatively and differ from CA measurements where a smooth rock surface is used. Taking all this into consideration, surfactants should be considered as a chemical additive to fracturing fluid in all scenarios. Meticulous testing is needed to prove whether or not surfactants are going to be compatible, but from both a scientific and economic standpoint it is impossible to ignore the possibility of higher hydrocarbon production.

# 4. CONCLUSION AND RECOMMENDATIONS

## 4.1 Conclusion

The novelty of the Meramec formation makes for difficult analysis of wettability compared with other unconventionals, in order to overcome this, over 50 different contact angle measurements were taken to establish the native wettability. After thorough contact angle experimentation using multiple rock samples from the Rosemary 1-14H, the Meramec formation shows to be a native neutral/intermediate-wet system, with an average wetting angle of 63°. There were some cases where the sample being tested was in a more neutral/intermediate-wet state, with an average $\Theta_w$ ~ 75-85°, but none of the experiments led to oil-wet results. This is using the Captive Bubble method, in distilled water at 170 °F, with C&F oil taken from the Rosemary 1-14H. These results are unlike other unconventional formations such as the Bakken or Eagle Ford, which test as initially oil-wet when conducting the same contact angle experiments. These differences in native wettability can only be understood through further experimentation or simulation work. Adding surfactants to the contact angle experiments did not alter the wettability to the same extent as the previously mentioned formations that we have tested in the lab, which is expected if it the Meramec is already neutral/intermediate-wet. With that being said, there was still a slight decrease in wetting angle ($\Theta_w$) to a more water-wet state. This was completely dependent on the surfactant and concentration being tested as some surfactants did not alter the wettability at all. In terms of wettability alteration across all the rock samples tested, surfactant 2-A tested the best at a 1 gpt loading, this is an anionic surfactant. This study also tested the possibility of increased

surfactant concentration and its effect on recovery and wettability alteration. Increasing the concentration of the aqueous solution to more than 1 gpt did not clearly affect the contact angle results, but did so when conducting imbibition experiments. This can be seen when looking at the results for cores 86H and 89H which used the same surfactant solution at 2 gpt and 1 gpt respectively. Again, more testing with different surfactants would be needed to confirm these results. Anionic surfactants were shown to test the best for both contact angle and imbibition, giving the largest wettability alteration and largest recovery factor. The type and concentration of surfactant being tested also had an effect on the individual oil drop size being displaced from the core matrix. Surfactant 2-A at 1 gpt made all the oil drops evenly distributed around the entire core and the oil drop sizes were extremely small and looked to be water-wet. This can be seen in Figure 27 in the Appendix. When testing imbibition in distilled water only, the oil drops that covered the surface of the core were larger in volume and more oil-wet, covering more surface area. This can be seen in Figure 30 in the Appendix. Surfactant 2-A at 1 gpt performed the best in terms of wettability alteration and recovery factor in comparison with the other surfactants that were tested. This surfactant also consistently lowered the wetting angle during contact angle experiments to a more water-wet state. 2-A also gave the largest final recovery factor during SI experiments when tested on sample 38H, these results are presented in Table C. It is also important to note that 38H had a porosity value of 7% with a permeability of 0.005 mD, making it the core plug with the highest porosity but not the highest permeability. Zeta potential experiments performed using the PALS technique and Meramec rock samples also confirmed these results. Surfactant

2-A consistently gave the largest magnitude zeta potential compared with the other surfactants tested in all the cases tested except when testing with rock samples taken from 129H where 2-B had a larger magnitude. Surfactant 2-B also gave a consistently large magnitude of zeta potential compared with the other surfactants tested and performed well in both wettability alteration and imbibition experiments. These results agree with the earlier statement that a large magnitude of zeta potential seems to be the most favorable in terms of wettability alteration and recovery. IFT experiments using the Reverse Pendant Drop method were performed in both distilled water and a surfactant solution. The IFT decreased by over 50%, in some cases more, but there was no correlation with a lower IFT and a higher recovery. The aqueous solution that performed the best during imbibition had one of the higher IFT values of 12.0 mN/m. Imbibition experiments using water, which had an IFT of 30 mN/m, and surfactant 2-B at 2 gpt, which had an IFT of 6.3 mN/m, resulted in almost the same final recovery factor. These two core plugs also had identical porosity values at around 5%. Extreme IFT reduction does not seem to be a major factor in the Meramec formation and this could be due to the fact that it is already neutral/intermediate-wet in nature. This means that without any significant change in wetting angle along with the IFT reduction, the capillary pressure would be reduced according to Young-Laplace.

The surfactants chosen for this study, although proven to alter wettability, do not show an obvious improvement regarding recovery factor during imbibition experiments. This again is most likely due to the fact that the Meramec formation is already neutral/intermediate-wet coupled with extreme pore confinement. Imbibition

experiments performed in only distilled water proved that recovery is possible without the addition of surfactants. Three core plugs were allowed to imbibe in distilled water only and gave an average recovery factor of 19%, which is greater than some of the imbibition experiments that used surfactants. Through careful analysis and correlation of experimental results, it is concluded that porosity and the presence of bedding planes/fractures in the core plugs are the largest contributor to recovery factor in the Meramec formation, and the aqueous solution as the second largest contributor. These results should be verified by retesting the same exact core plugs using either distilled water if a surfactant was originally used or vice versa. The porosity values used in this study were provided by Core Lab and were calculated based on well log correlations. There is a strong correlation between the porosity of the core plug and the final recovery factor as can be seen in Figure 18. This same correlation was also seen by comparing the initial oil saturation ($S_{oi}$) after the aging process to the porosity, shown in Figure 5. By utilizing the CT scans taken during the imbibition experiment, it can also be inferred that most of the production takes place from the low density/high porosity regions of the core plug. These CT images are provided in the Appendix and show that most of the change in CT number is taking place in bedding planes/natural fractures in the core plug. This is especially obvious for sample 38H, where the bedding plane along the x-y direction of the core is decreasing in CT number as the experiment continues. This increase in CT number, which means an increase in density, proves that hydrocarbons are being produced from the rock matrix and being replaced with the aqueous solution. These same images also show the imbibition of the aqueous solution into the core matrix

starting from the edges of the plug and moving into the center. This further confirms the fact that spontaneous imbibition of the aqueous solution into the rock matrix takes places and displaces the oil from the matrix. The presence of natural fractures or bedding planes in the core matrix paired with the correct surfactant will lead to the highest recovery during spontaneous imbibition according to the results presented in the study. This is proved by looking at cores 38H and 105H, the best and worst performing experiments. By looking at the planar CT images for 38H, it can be seen that a large bedding plane along the length of the core is present, which increases in CT number as imbibition takes place. This planar bed is thought to account for most of the oil production. This core plug also tested in the best performing surfactant in terms of wettability alteration by contact angle. 105H did not have any obvious bedding planes or natural fractures that can be seen in the CT images, and even though the core imbibed in 1 gpt of Surf X, the recovery was the lowest out of all the experiments performed. These findings confirm that surfactants, although not always applicable, should at least be considered during fracturing operations by analyzing the data and materials being used, performing lab experiments, and conducting simulation when necessary.

## 4.2 Recommendations

The method of contact angle experimentation presented in this paper requires an extremely precise workflow to ensure accurate results and reproducibility. The consistency of results could even be dependent on the operator, in order to mitigate all these outside factors, the same precautions should be taken every step of the procedure.

This starts by cleaning the equipment in the same manner, aging the chips for the same amount of time, and using the same process during the experiment. The measurement process during contact angle experiments starts with wiping the rock chip free of residual oil. Each rock chip that is taken out of the vial after aging should be wiped down in the same manner and the same number of times before being tested. Each chip should only be used for a specific number of measurements, 8-10 being ideal and 15 being the maximum, before moving on to the next chip. If testing with a surfactant solution, the agitation period should be similar for every solution. There is also the problem of the solution evaporating if testing at high temperatures, the only way to avoid this is by reducing the amount of time during measurements. To avoid any external contamination, gloves should be worn at all times while cleaning equipment and wiping rock chips. Making sure the rock chips are properly categorized before testing is also crucial. Rock chips for contact angle should be categorized according to the core block or plug it was taken from, and then subcategorized by each individual chip. This is also a good method of tracking the number of measurements each rock chip has gone through. This categorization can be done by placing a single chip in one vial for the aging process instead of 3-4 chips from the same core plug in one vial. This is especially important in the Meramec formation due to the heterogeneity and variation in contact angle measurements between core plug samples.

The method of measuring IFT between the oil/water interface was done using the Reverse Pendant Drop method at a single point in time. This means that the temperature effect that the aqueous solution has on the oil was not fully captured. The aqueous

solution used for testing was allowed to heat up to 170 °F before measurements were taken, but the full effects that temperature has on the IFT were not taken into account. The IFT between the oil drop and the aqueous solution will slightly decrease with time if allowed to, declining exponentially. This behavior is also akin to how the fracture fluid would react in a reservoir when the well is shut-in and the fluids are allowed to soak. The longer the well is shut-in before production begins, the lower the IFT until a certain point where the IFT cannot decrease any further.

For imbibition, the method of weighing the core plug after aging is critical for calculating $S_{oi}$ and effective porosity, which means that repeatable steps should be taken to ensure maximum accuracy. This means minimizing the amount of time the core plug is exposed to air and using a singular method of wiping the outer surface of the plug free of any oil before it is placed on the scale. Imbibition experiments also require a precise workflow so that CT number and recovery factor can be calculated and applied correctly. Since the CT number is dependent on multiple factors, mainly temperature and OLP % of the tube, the same steps should be used every time scans are taken. CT number is a useful metric for determining the efficiency of imbibition, but the accuracy of the measurement is clouded due to the previously mentioned factors. The OLP tube % should start at the same value every time, 30% is the minimum for this specific machine before scanning can begin. If there are multiple imbibition experiments going on, scan each Amott cell in the exact same order and make sure to scan them as quickly as possible. This ensures that the OLP % of the tube and the temperature of the Amott cell is close to what it was the last time the same Amott cell was scanned. There also should

be a more precise method of measuring the oil that is being produced since the volume is small. The current method of "eye-balling" is acceptable for our purposes, but being as accurate as possible is critical, especially when the results will be upscaled. The more incorporation of technology such as an electronic method of measuring produced oil will lead to less discrepancies and more accurate data. A method of measuring the height of the oil in the graduate column with a laser and converting that to volume is one example that can be considered for future experiments. The consideration of the difference in core dimensions is also important when trying to upscale the results to field size matrix blocks. A scaling method is presented by (Mattax and Kyte 1962) that includes the properties of the core plug and calculates a dimensionless time. This method tries to verify the affect that length, fluid viscosity, and porosity of the core plug have on imbibition recovery.

REFERENCES

1. Adamson, A.W., Gast, A.P., *"Physical Chemistry of Surfaces"*, 6th edition., John Wily & Sons, Inc.: New York, 1997.

2. T. Young, *"An Essay on the Cohesion of Fluids"*, Philosophical Transactions of the Royal Society of London, 1805: 65-87.

3. Mattax, C. C., & Kyte, J. R. (1962, June 1). *Imbibition Oil Recovery from Fractured, Water-Drive Reservoir*. Society of Petroleum Engineers. doi:10.2118/187-PA

4. Chen, H. L., Lucas, L. R., Nogaret, L. A. D., Yang, H. D., & Kenyon, D. E. (2000, January 1). *Laboratory Monitoring of Surfactant Imbibition Using Computerized Tomography*. Society of Petroleum Engineers. doi:10.2118/59006-MS

5. T. Gallegos, B. Varela, *"Trends in hydraulic fracturing distributions and treatment fluids…"*, USGS Investigations Report 2014-5131, 15 p., 2014.

6. Teklu, Alharthy, Kazemi, Yin, Graves, SPE, CSM, *"Phase Behavior and Minimum Miscibility Pressure in Nanopores"*, SPE Reservoir Evaluation & Engineering, August 2014.

7. Bui, Akkutlu, Texas A&M University, *"Hydrocarbon Recovery from Model-Kerogen Nanopores"*, SPE Journal, June 2017.

8. Li, Bui, Akkutlu, Texas A&M University, *"Capillary Pressure in Nanopores: Deviation from Young-Laplace Equation"*, SPE 185801-MS, Europec June 2017.

9. M. Akbaradbadi, S. Saraji, and M. Piri, Chemical and Petroleum Engineering Department, University of Wyoming, *"Spontaneous Imbibition of Fracturing Fluid and Oil in Mudrock"*, SPE-178709-MS, July 2015.

10. S. Ma, N.R. Morrow, X. Zhang, Western Research Institute, University of Wyoming, *"Generalized Scaling of Spontaneous Imbibition Data for Strongly Water-Wet Systems"*, October 1995.

11. Shen, Zhu, Li, Wu, Research Institute of Petroleum Exploration and Development, *"Experimental Study of the Influence of Interfacial Tension on Water-Oil Two-Phase Relative Permeability"*, September 2005.

12. K. Li, SPE, R.N. Horne, SPE, Standford, *"A General Scaling Method for Spontaneous Imbibition"*, SPE-77544, September 2002.

13. O.A. Olafuyi, Y. Cinar, M.A. Knackstedt, SPE, W.V. Pinczewski, University of New South Wales, Australian National University, *"Spontaneous Imbibition in Small Cores"*, SPE 109724, October 2007.

14. M. Shehata, Hisham Nasr-El-Din, Texas A&M University, *"Zeta Potential Measurements: Impact of Salinity on Sandstone Minerals"*, SPE-173763-MS, April 2015.

15. J.O. Alvarez, D.S. Schechter, Texas A&M University, *"Wettability Alteration and Spontaneous Imbibition in Unconventional Liquid Reservoirs by Surfactant Additives"*, SPE-177057, November 2015.

16. A. Neog, D.S. Schechter, Texas A&M University, *"Investigation of Surfactant Induced Wettability Alteration in Wolfcamp Shale for Hydraulic Fracturing and EOR Applications"*, SPE-179600-MS, April 2016.

17. B.B. Hoxha, G. Sullivan, E. van Oort, H. Daigle, The University of Texas, *"Determining Zeta Potential of Intact Shales via Electrophoresis"*, SPE-180097-MS, May 2016.

18. R.W. Parsons, P.R. Chaney, Marathon Oil Co., *"Imbibition Model Studies on Water-Wet- Carbonate Rocks"*, SPE-1091, December 1964.

19. T.L. Foyen, M.A. Ferno, B. Brattekas, Dept. of Physics and Technology, University of Bergen, The National IOR Centre of Norway, *"The Onset of Spontaneous Imbibition: How Irregular Fronts Influence Imbibition Rate and Scaling Groups"*, SPE-190311-MS, 2018.

20. M. Gladkikh, Institute for Computational and Engineering Science; S. Bryant, The University of Texas at Austin, *"Mechanistic Prediction of Capillary Imbibition Curves"*, SPE 90333, 2004.

21. S. Morsy, SPE, Texas Tech University, A. Gomma, SPE, Baker Hughes, J.J. Sheng, SPE, Texas Tech University, *"Imbibition Characteristics of Marcelus Shale Formations"*, SPE-169034-MS, 2014.

22. Yarveicy, H., Habibi, A., Pegov, S., Zolfaghari, A., & Dehghanpour, H. (2018, March 13*). Enhancing Oil Recovery by Adding Surfactants in Fracturing Water: A Montney Case Study*. Society of Petroleum Engineers. doi:10.2118/189829-MS

23. Lan, Q., Zu, M., Dehghanpour, H., & wood, J. (2014, October 27). *"Advances in Understanding Wettability of Tight and Shale Gas Formations"*, SPE. doi: 10.2118/189829-MS

24. Yee, D., Johnston, G., Ahmend, S., & Howard, D. (2017, July 24). *STACKing it Up: An Economic and Geological Analysis of the STACK*. Unconventional Resources Technology Conference. doi:10.15530/URTEC-2017-2690074

25. Yarveicy, H., Habibi, A., Pegov, S., Zolfaghari, A., & Dehghanpour, H. (2018, March 13). *Enhancing Oil Recovery by Adding Surfactants in Fracturing Water: A Montney Case Study*. Society of Petroleum Engineers. doi:10.2118/189829-MS Yarveicy, H., Habibi, A.,

Pegov, S., Zolfaghari, A., & Dehghanpour, H. (2018, March 13*). Enhancing Oil Recovery by Adding Surfactants in Fracturing Water: A Montney Case Study*. Society of Petroleum Engineers. doi:10.2118/189829-MS

26. Dakhlia, H., Wu, W. J., Lim, M. T., Delshad, M., Pope, G. A., & Sepehrnoori, K. (1995, January 1). *Simulation of Surfactant Flooding Using Horizontal Wells*. Petroleum Society of Canada. doi:10.2118/95-82

27. Okasha, T. M., & Al-Shiwaish, A.-J. A. (2010, January 1). *Effect of Temperature and Pressure on Interfacial Tension and Contact Angle of Khuff Gas Reservoir*, Saudi Arabia. Society of Petroleum Engineers. doi:10.2118/136934-MS

28. Mirchi, V., Saraji, S., Goual, L., & Piri, M. (2014, April 12). *Dynamic Interfacial Tensions and Contact Angles of Surfactant-in-Brine/Oil/Shale Systems: Implications to Enhanced Oil Recovery in Shale Oil Reservoirs*. Society of Petroleum Engineers. doi:10.2118/169171-MS

29. Palla, C., Weaver, J. D., Benoit, D., Lu, Z., & Vera, N. (2014, November 10). *Impact of Surfactants on Fracture Fluid Recovery*. Society of Petroleum Engineers. doi:10.2118/171732-MS

30. Adams, W. T., & Schievelbein, V. H. (1987, November 1). *Surfactant Flooding Carbonate Reservoirs*. Society of Petroleum Engineers. doi:10.2118/12686-PA

31. Lohne, A., & Fjelde, I. (2012, January 1). *Surfactant Flooding in Heterogeneous Formations*. Society of Petroleum Engineers. doi:10.2118/154178-MS

32. Saputra, I. W. R., & Schechter, D. S. (2018, August 9). *Comprehensive Workflow for Laboratory to Field-Scale Numerical Simulation to Improve Oil Recovery in the Eagle Ford*

*Shale by Selective Testing and Modelling of Surfactants for Wettability Alteration*. Unconventional Resources Technology Conference. doi:10.15530/URTEC-2018-2884598

33. A. Bhardwaj & S. Hartland, *Applications of Surfactants in Petroleum Industry*, Journal of Dispersion Science and Technology, 14:1, 87-116.

34. Chen, P., & Mohanty, K. K. (2014, April 12). *Wettability Alteration in High Temperature Carbonate Reservoirs*. Society of Petroleum Engineers. doi: 10.2118/169125-MS.

35. Reed, R. L., & Healy, R. N. (1984, June 1). *Contact Angles for Equilibrated Microemulsion Systems.* Society of Petroleum Engineers. doi:10.2118/8262-PA

36. Fischer, H., & Morrow, N. R. (2005, January 1). *Spontaneous Imbibition with Matched Liquid Viscosities*. Society of Petroleum Engineers. doi: 2118/96812-MS

37. Weiss, W. W., & Xie, X. (2007, January 1). *Oilfield Surfactants Improve Recovery via Imbibition*. Society of Petroleum Engineers. doi:10.2118/106402-MS

38. Riddick, T. M. *Control of Stability Through Zeta Potential*; Zeta Meter: New York, 1968.

39. Schramm, L. L. *Emulsions in the Petroleum Industry*; Petroleum Recovery Institute: Calgary, Canada, American Chemical Society, 1992.

40. S. T. Kim, M. E. Boudh-Hir, G. A. Mansoori, "The Role of Asphaltene in Wettability Reversal", 65th ATCE, New Orleans, LA, USA, 1990.

41. Donaldson, E. C., Thomas, R. D., Lorenz, P. B., 1969, Wettability determination and its effect on recovery efficiency: Society of Petroleum Engineers Journal, v. 9, p. 13–20., 10., 2118/2338-PA

APPENDIX

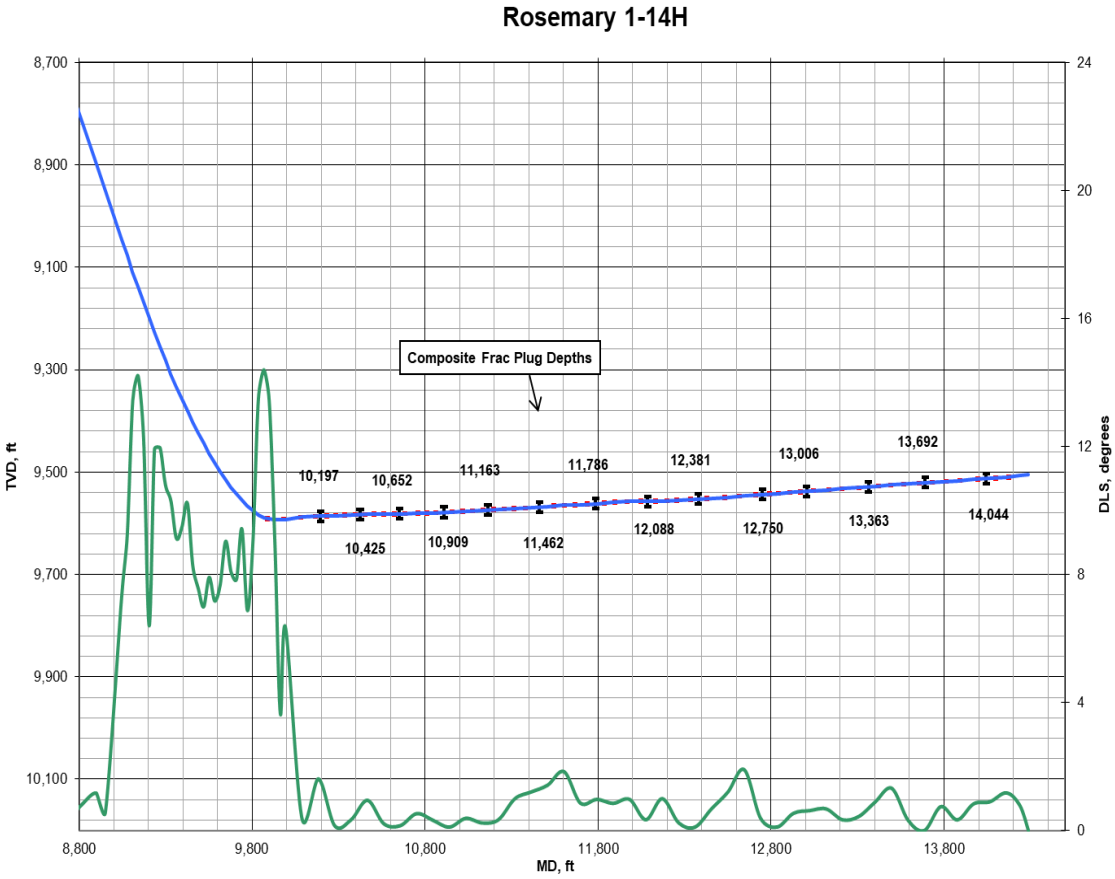


Figure 1: Perforation schedule of Rosemary 1-14H.

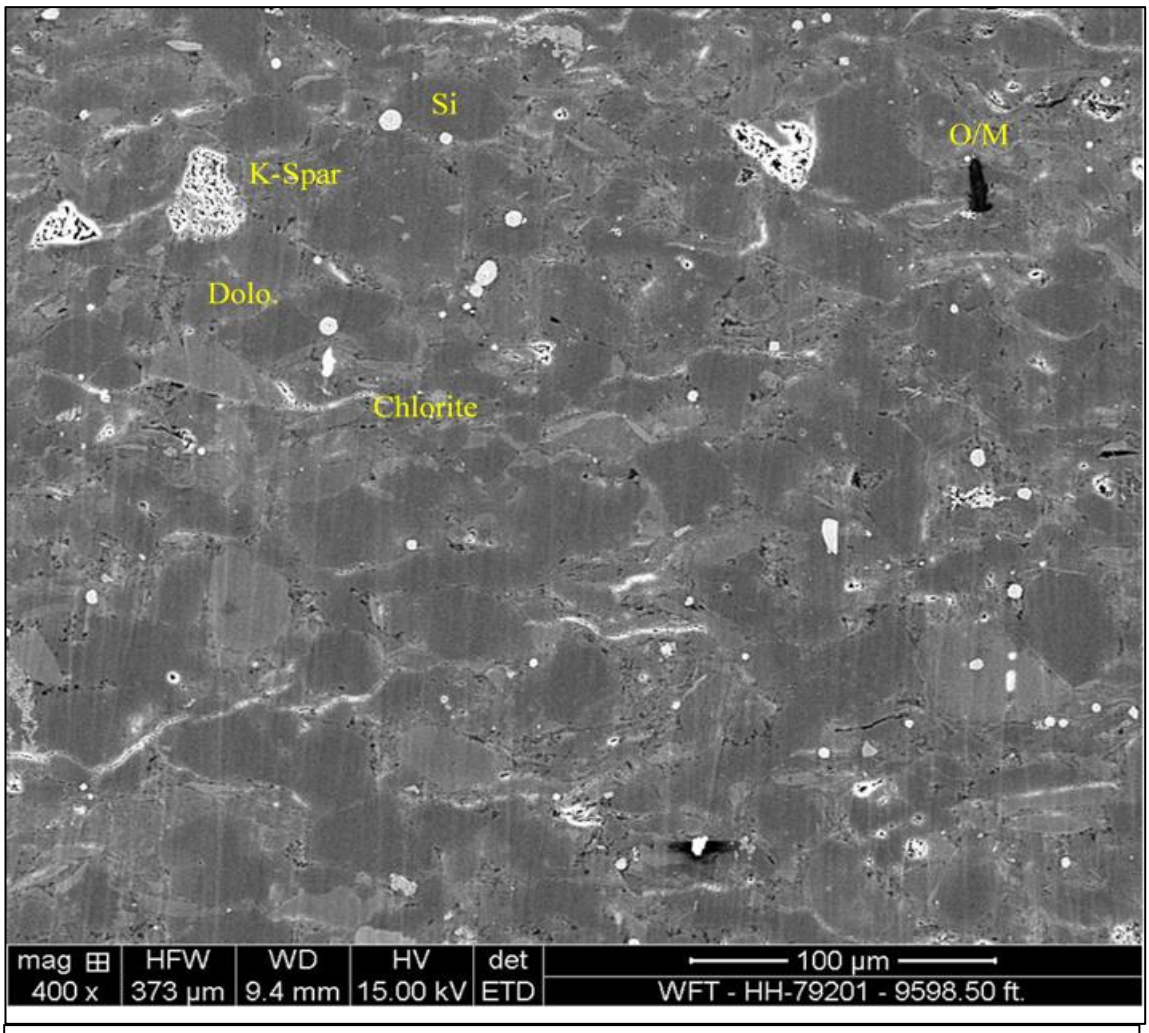


Figure 2: SEM image of the Rosemary 1-14H at 9598'. This shows a relatively high TOC of 0.98% and the intergranular pores are filled with solid organic matter, secondary pores are a dissolution of feldspars with no organic matter.

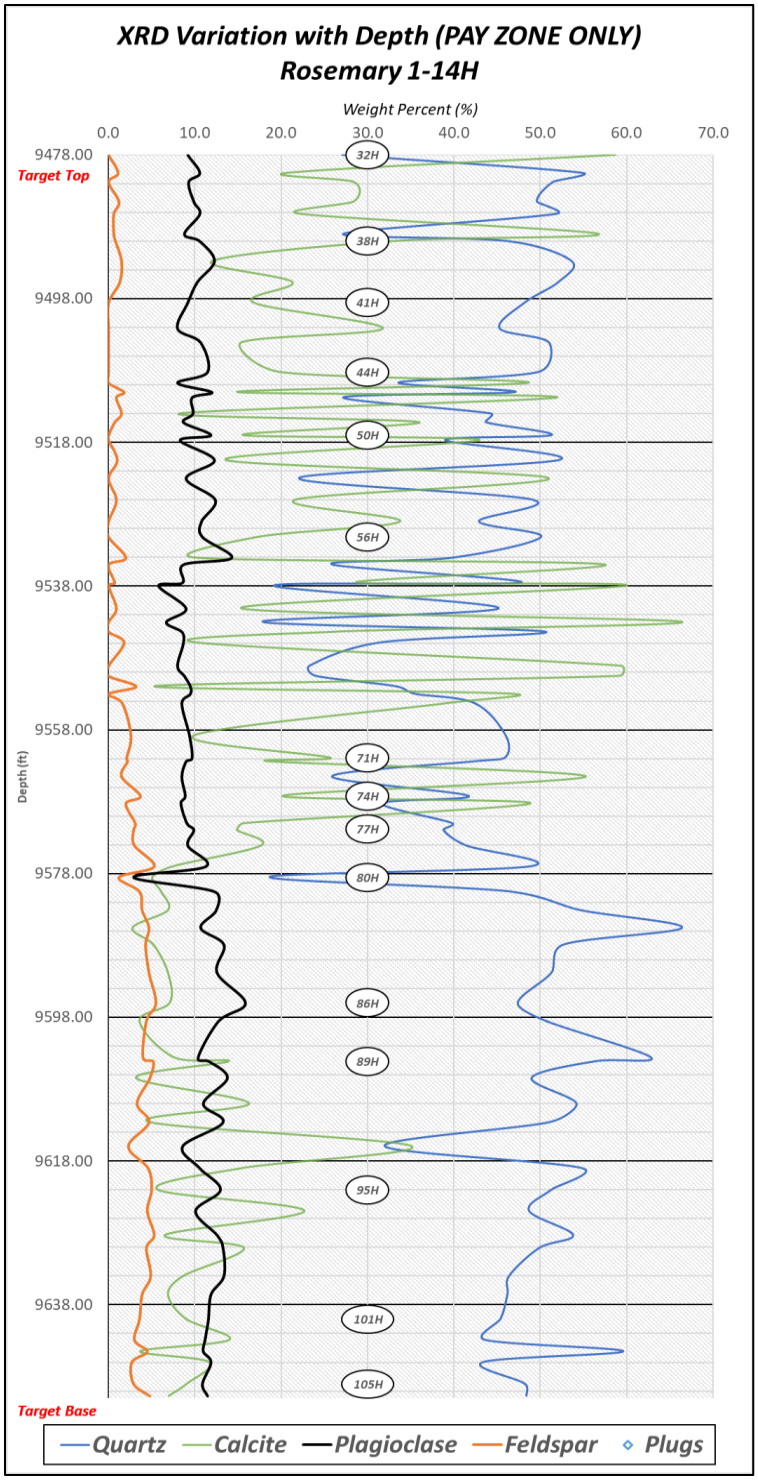


Figure 3: XRD well log showing variation of lithology with depth.

| Core Plug | Quartz | Calcite | Clay | Dolomite | Plagioclase |
|---|---|---|---|---|---|
| 38H | 46% | 33% | 7% | 1.5% | 10.6% |
| 41H | 48% | 17% | 13% | 11% | 9% |
| 44H | 50% | 20% | 14% | 3.5% | 11.5% |
| 50H | 51% | 15.6% | 14% | 6% | 12% |
| 74H | 42% | 20% | 18% | 5% | 9% |
| 77H | 39% | 15% | 25% | 4% | 10% |
| 80H | 19% | 5% | 13% | 58% | 3% |
| 89H | 57% | 14% | 10% | 2% | 12% |

Table A: XRD data for plugs used during imbibition.

| Components | Mole % |
|---|---|
| $N_2$ | 0.50 |
| $CO_2$ | 0.43 |
| $C_1$ | 58.2 |
| $C_2$ | 10.18 |
| $C_3$ | 6.81 |
| $iC_4$ | 0.84 |
| $nC_4$ | 2.93 |
| $C_5+$ | 20.17 |

Table B: Reservoir Fluid Composition summary table for crude oil from Rosemary 1-14H. Reservoir pressure of 5,565 psia and temperature of 194 °F.

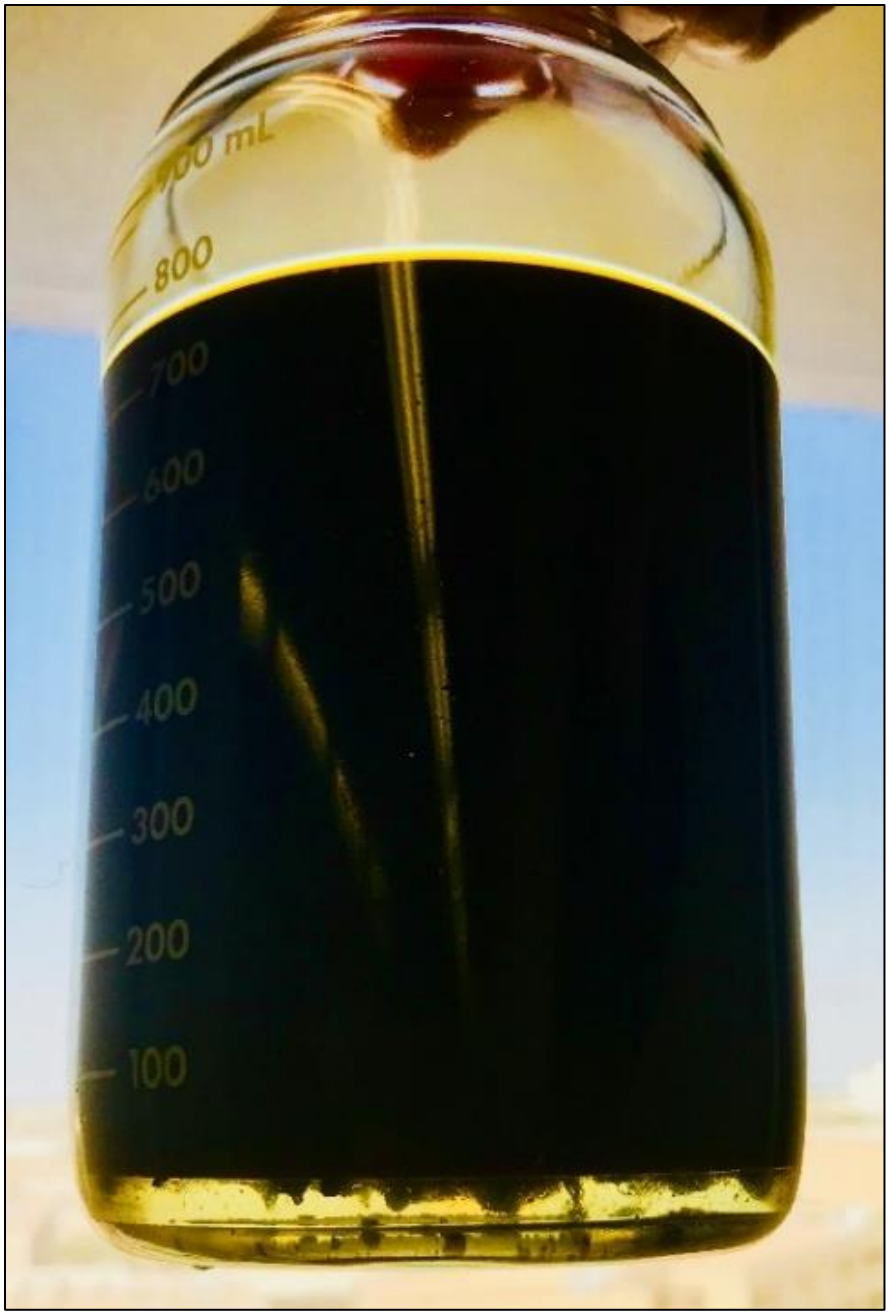


Figure 4: Picture of crude oil showing produced water and other solids.

SDS Information for Surfactants

2-A (Type 3 & 4) Information

| Composition | CAS Number | Percent (wt%) |
|---|---|---|
| Methanol | 67-56-1 | 10-30% |
| Alkylbenzene sulfonate compd. with 2-propanamine | Proprietary | 10-30% |
| Alkylbenzene sulfonate | Proprietary | 5-10% |
| Ethoxylated alcohols | Proprietary | 5-10% |

6-A, 6-C, 6-D Information

| Composition | CAS Number | Percent (wt%) |
|---|---|---|
| Isopropanol | 67-63-0 | 5-20% |
| Proprietary Blend | n/a | n/a |

6-E Information

| Composition | CAS Number | Percent (wt%) |
|---|---|---|
| Fatty Alkyl Sultaine | Proprietary | 5-10% |
| Ethylene Glycol | 107-21-1 | 5-10% |
| 1,2,3-Propanetriol | 56-81-5 | 1-5% |
| Oxyalkylated alcohol | Proprietary | 1-5% |
| Organic sulfonic acid salt | Proprietary | 1-5% |
| Sodium Chloride | 7647-14-5 | 1-5% |

2-B Information

| Composition | CAS Number | Percent (wt%) |
|---|---|---|
| Methyl alcohol | 67-56-1 | 30% |
| Sulfonate | Proprietary | 13% |
| Sulfonate | Proprietary | 7% |
| Ethoxylated alcohols | Proprietary | 7% |

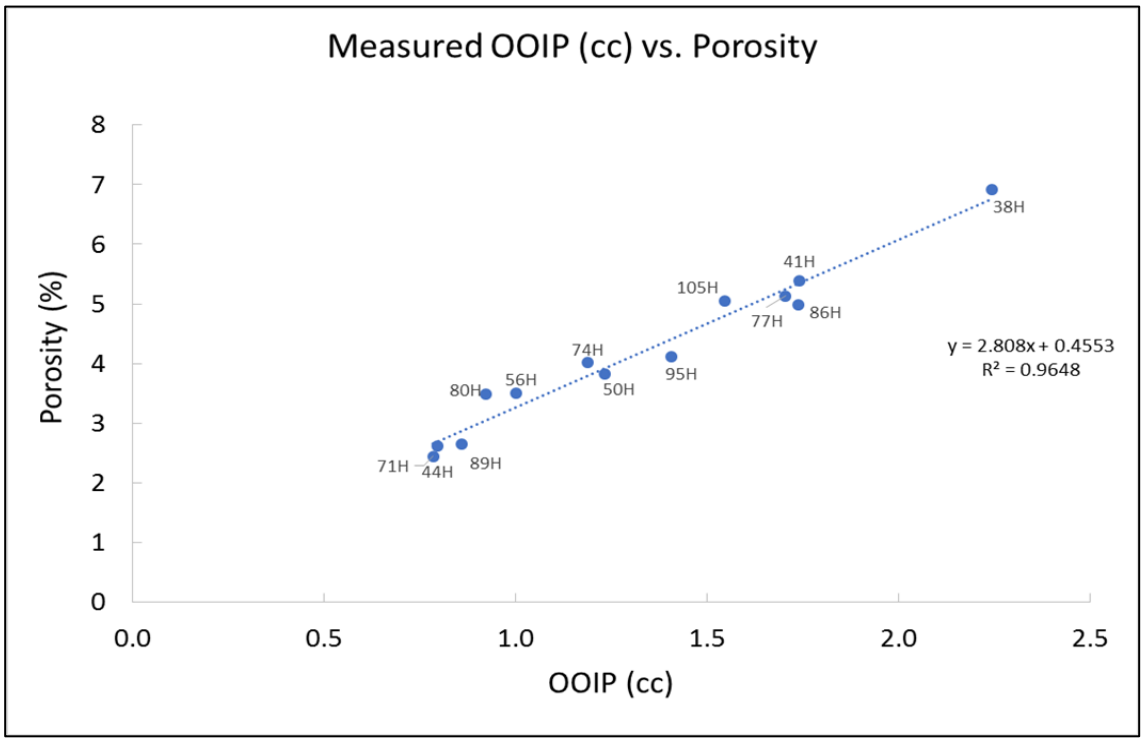


Figure 5: Graph of $S_{oi}$ vs. Porosity for core plugs used in imbibition experiments.


Figure 6: Color-coded chart for facies diagram found in Section 2.1.2 explaining what each color represents.

Figure 7: Example of aging process, rock chip in vial submerged in crude oil.

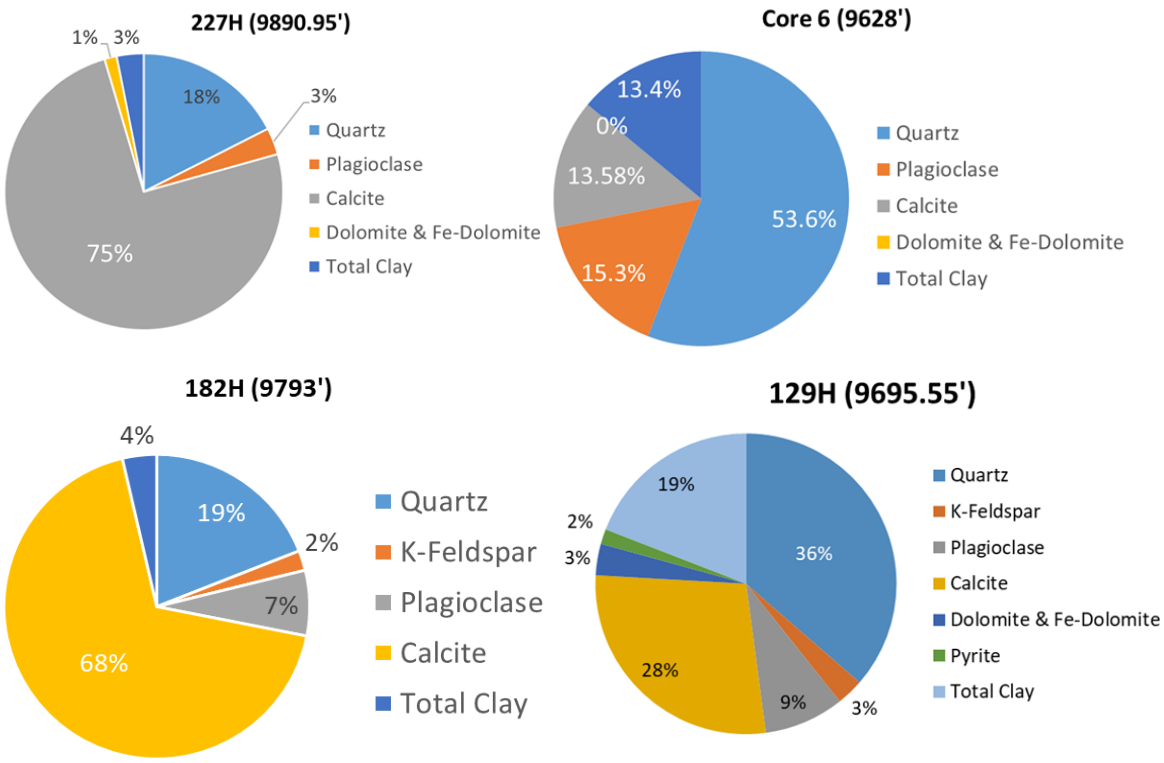


Figure 8: XRD pie charts for samples used in zeta potential and contact angle experiments.

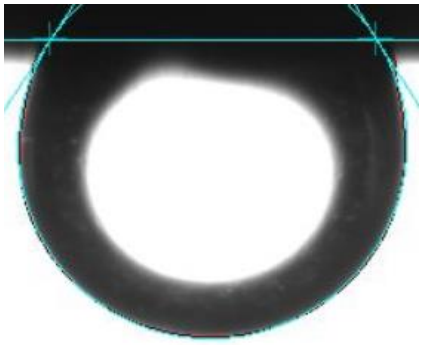

Contact angle of oil drop on Core 6 in distilled water at 170°. Wetting angle of 68°.

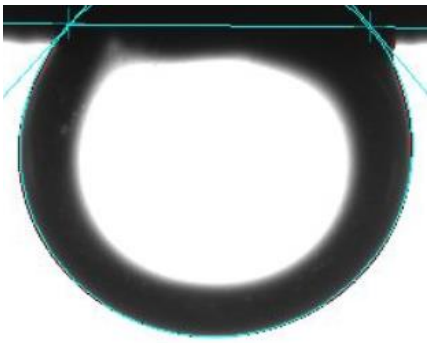

Contact angle of oil drop on Core 6 in a synthetic brine for Rosemary 1-14H at 170°. Wetting angle of 50°.

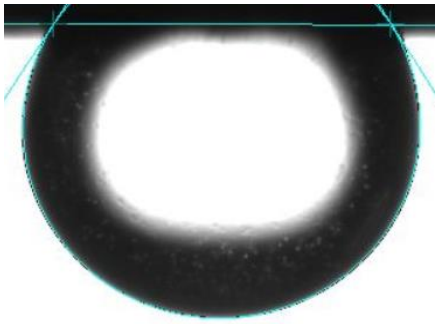

Contact angle of oil drop on 227H in distilled water at 170°. Wetting angle of 70°.

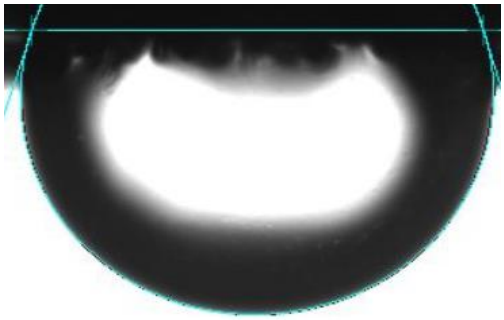

Contact angle of oil drop on 227H in synthetic brine for Rosemary 1-14H at 170°. Wetting angle of 82°.

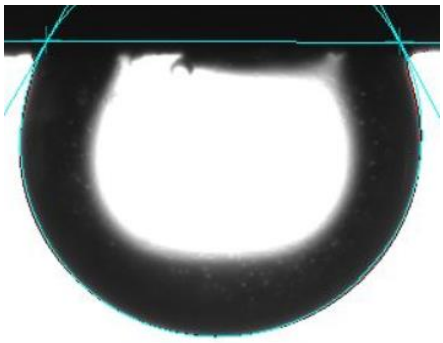

Contact angle of oil drop on 129H in distilled water at 170°. Wetting angle of 72°

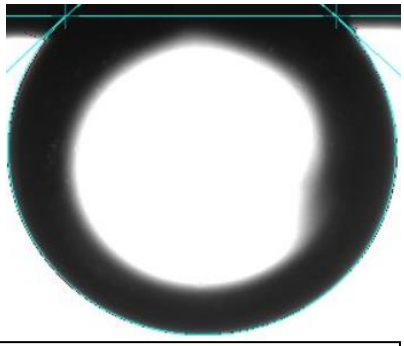

Contact angle of oil drop on 129H in synthetic brine for Rosemary 1-14H at 170°. Wetting angle of 45°.

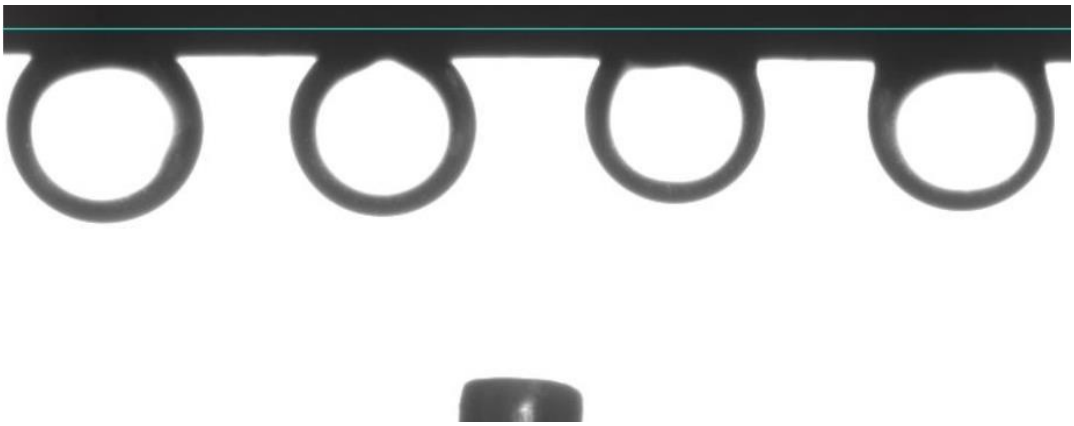

Figure 9: Contact angle measurements taken on Core 6 with Rosemary 1-14H C&F oil in synthetic brine at 170 °F.

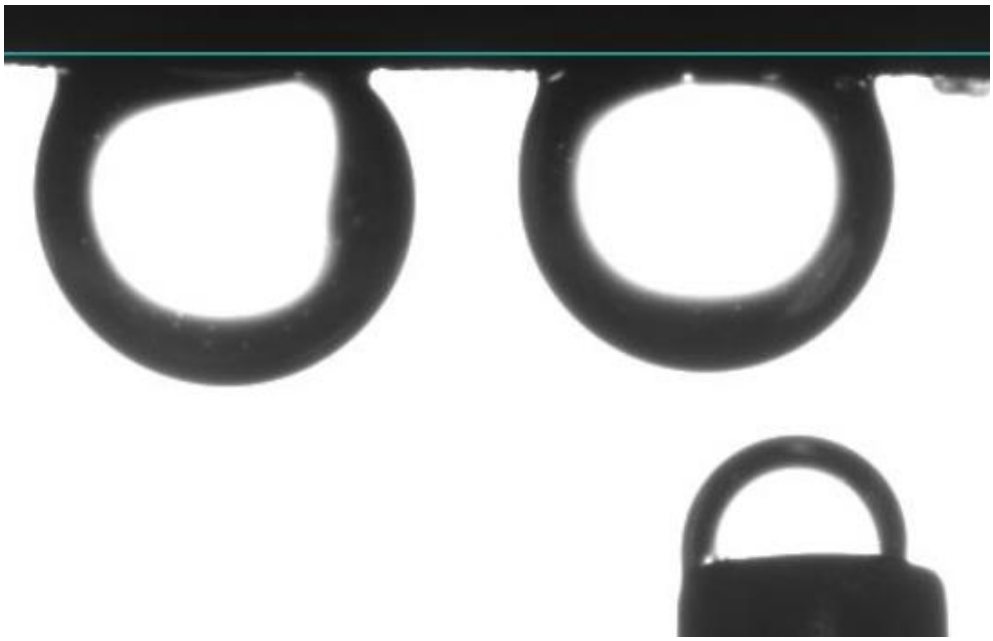

Figure 10: Contact angle measurements taken on 129H with Rosemary 1-14H C&F oil in synthetic brine at 170 °F.

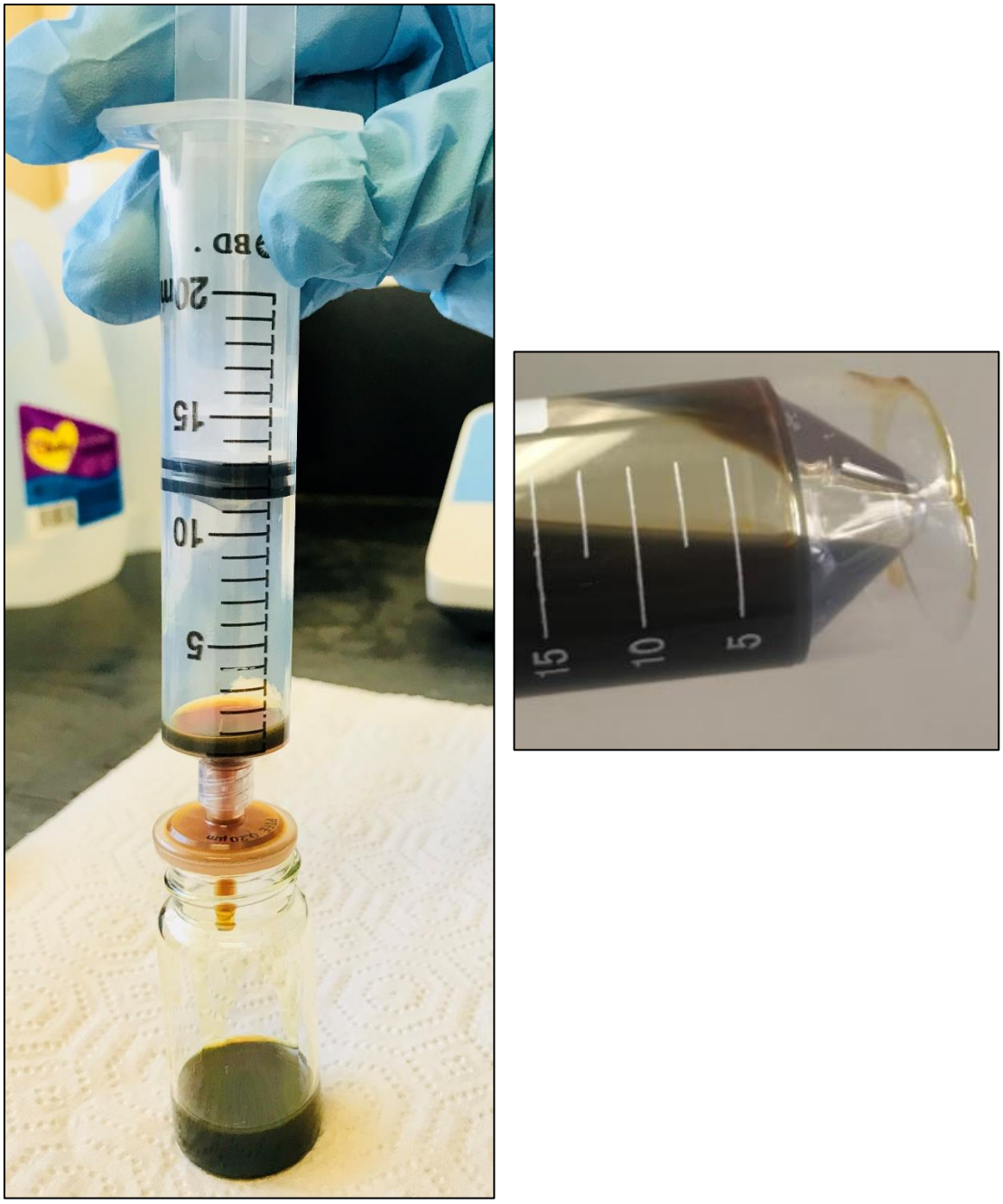


Figure 11: Filtration process showing 0.2 µm PTFE filter in the picture on the left and the centrifuge process showing the solids removed in the picture on the right.

| Core Sample | Depth | Aqueous Solution | TOC | IFT (mN/m) | Volume ($cm^3$) | Density (g/cc) |
|---|---|---|---|---|---|---|
| 38H | 9490’ | 2-A 1 gpt | n/a | 12.0 | 32.4 | 2.69 |
| 50H | 9517’ | DW | n/a | 30.0 | 32.3 | 2.7 |
| 56H | 9531’ | DW | n/a | 30.0 | 28.6 | 2.7 |
| 71H | 9562’ | 6-A 2 gpt | n/a | 10.1 | 32.0 | 2.69 |
| 77H | 9571’ | DW | 1.28 | 30.0 | 33.2 | 2.71 |
| 86H | 9596’ | 2-B 2 gpt | n/a | 6.20 | 34.9 | 2.69 |
| 89H | 9604’ | 2-B 1 gpt | 0.33 | 4.60 | 32.4 | 2.66 |
| 95H | 9622’ | 6-C 2 gpt | n/a | 6.50 | 34.1 | 2.68 |
| 105H | 9649’ | Surf X 1 gpt | n/a | 7.30 | 30.6 | 2.68 |

| Core Sample | $\Delta_{mass}$ (g) | Measured $S_{oi}$ (cc) | Calculated $S_{oi}$ (cc) | K (mD) | Ø (%) | $Ø_e$ (%) | RF (%) |
|---|---|---|---|---|---|---|---|
| 38H | 1.50 | 2.18 | 2.22 | .005 | 7.0 | 6.30 | 35.5 |
| 50H | 0.95 | 1.38 | 1.24 | .0317 | 3.8 | 3.1 | 18.8 |
| 56H | 0.75 | 1.09 | 1.0 | 0.001 | 3.5 | 3.03 | 19.3 |
| 71H | 0.50 | 0.74 | 0.78 | 0.0013 | 2.45 | 2.22 | 15.8 |
| 77H | 0.79 | 1.15 | 1.7 | .02 | 5.13 | 3.34 | 24.7 |
| 86H | 1.06 | 1.47 | 1.54 | 0.0003 | 5.0 | 4.04 | 24.2 |
| 89H | 0.71 | 1.03 | 0.86 | .0002 | 2.7 | 2.24 | 14.7 |
| 95H | 0.90 | 1.31 | 1.41 | 0.00025 | 4.12 | 3.69 | 21.0 |
| 105H | 0.75 | 1.09 | 1.39 | 0.0015 | 5.1 | 3.30 | 10.5 |

Table C: Summary of information of plugs used during imbibition.

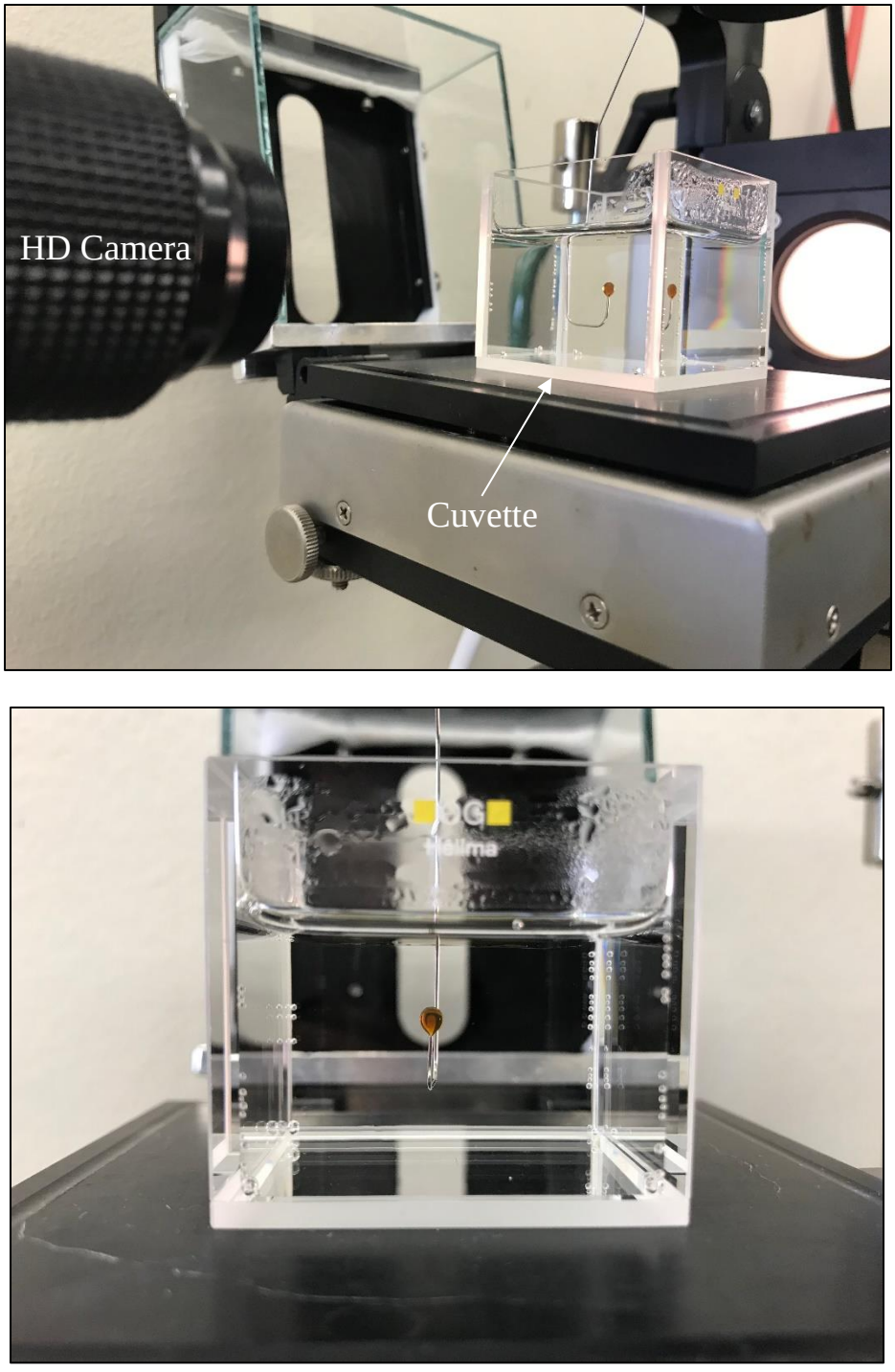


Figure 12: Example of IFT experiment showing reverse pendant drop method.

Figure 13: Picture of oven used for aging process.

| Salts | g/L | 500 mL 1/2 | 250 mL 1/4 | 100 mL 1/10 |
|---|---|---|---|---|
| $CaCl_2$ | 6.09 | 3.045 | 1.5225 | 0.609 |
| NaCl | 74.39 | 37.195 | 18.5975 | 7.439 |
| KCl | 0.63 | 0.315 | 0.1575 | 0.063 |
| $Fe(II)SO_4$ | 0.26 | 0.13 | 0.065 | 0.026 |
| $MgSO_4$ | 0.36 | 0.18 | 0.09 | 0.036 |
| $AlCl_3$ | 0.01 | 0.005 | 0.0025 | 0.001 |
| MgCl2 | 2.47 | 1.235 | 0.6175 | 0.247 |
| $NaHCO_3$ | 0.18 | 0.09 | 0.045 | 0.018 |
| $SrCl_2$ | 0.8 | 0.4 | 0.2 | 0.08 |

Figure 14: TDS report used to create synthetic brine.

| Ion | Conc., mg/L |
|---|---|
| Alkalinity | 2130 |
| pH | 7.32 |
| $H_2S$ | 24.8 |
| Sulfate | 18.1 |
| Total Iron | <1 |
| Calcium | <4 |
| Hardness | 1994 |
| Total Dissolved Solids | 4101 |
| Total Organic Carbon | 976 |

Figure 15: TOC report of produced water taken from Rosemary 1-14H.

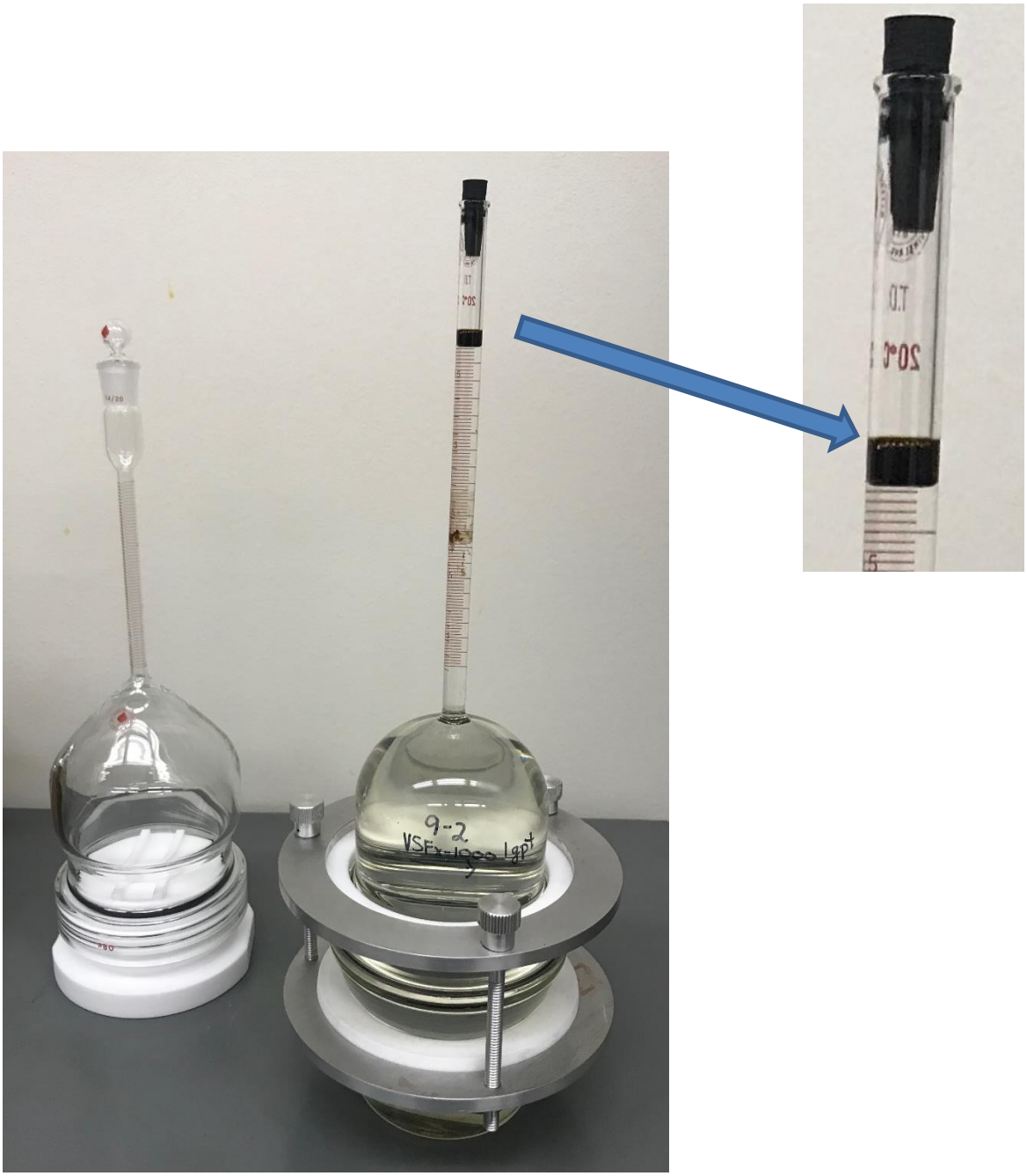


Figure 16: Picture of Amott cells used for imbibition experiments.

| *Sample* | *Test Type* | *Hours in Imbibition* | *IFT (mN/m)* | *PV (cc)* | *RF (%)* |
|---|---|---|---|---|---|
| ***9-1*** | Distilled Water | 500 | 15 | 1.67 | 18% |
| ***9-2*** | 1 gpt 6-D | 500 | 5.6 | 1.43 | 16% |
| ***9-3*** | 1 gpt 6-A | 500 | 9.7 | 1.54 | 15% |
| ***9-4*** | 1 gpt 6-C | 500 | 15.9 | 1.64 | 19% |
| ***9-6*** | 1 gpt 6-E | 500 | <1.0 | 1.46 | 10% |

Table D: Core 9 imbibition summary at 1 gpt loading.

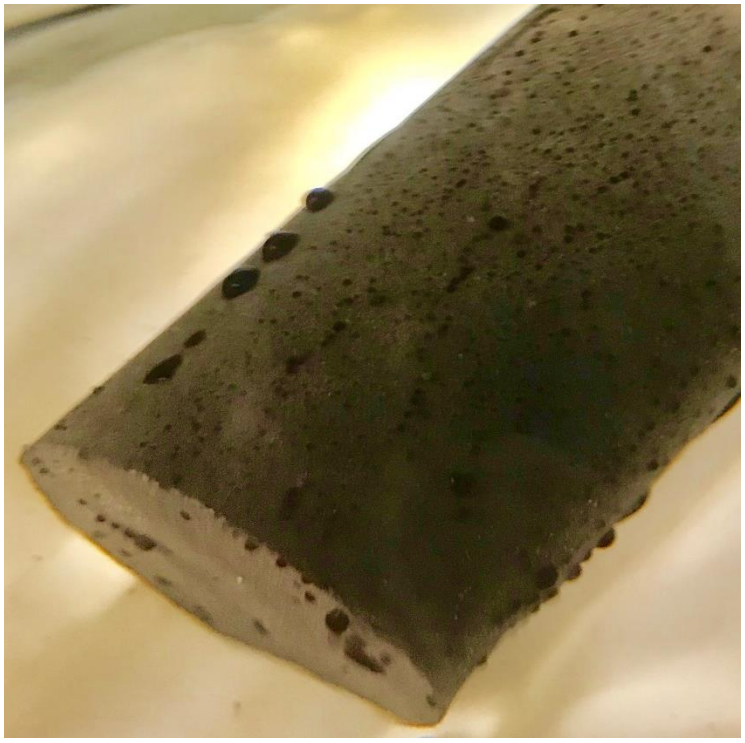

Figure 17: Close-up of core plug 9-1 during imbibition. Distilled water @ 185 °F.

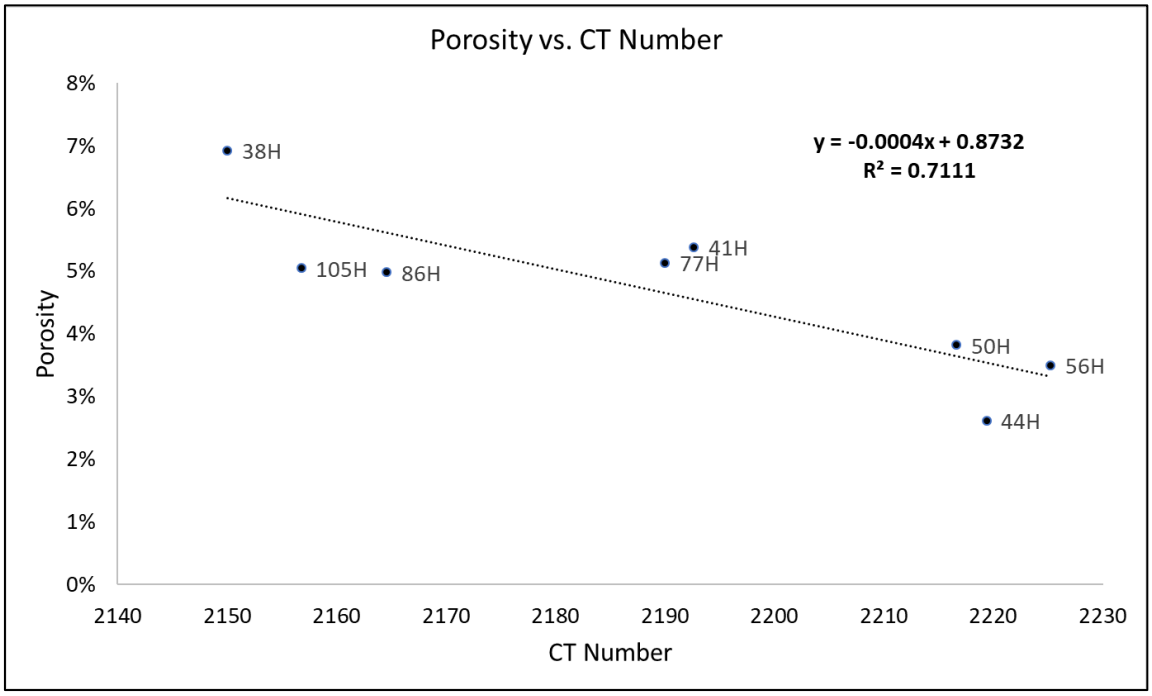


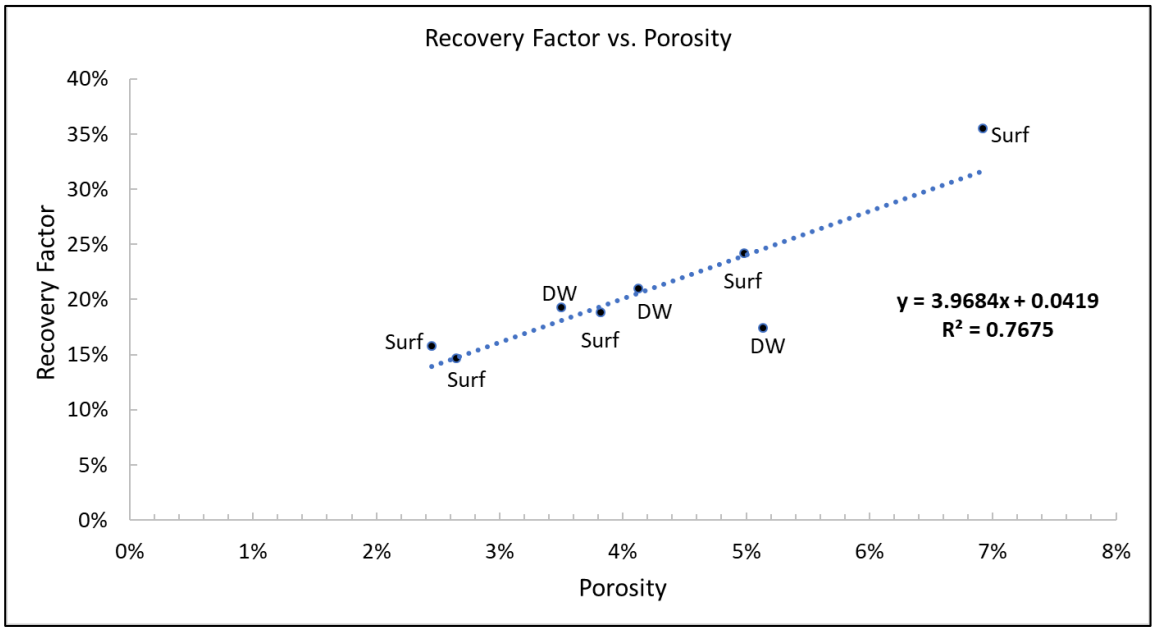


Figure 18: Graphs of Porosity vs. CT number and Recovery Factor vs. Porosity.

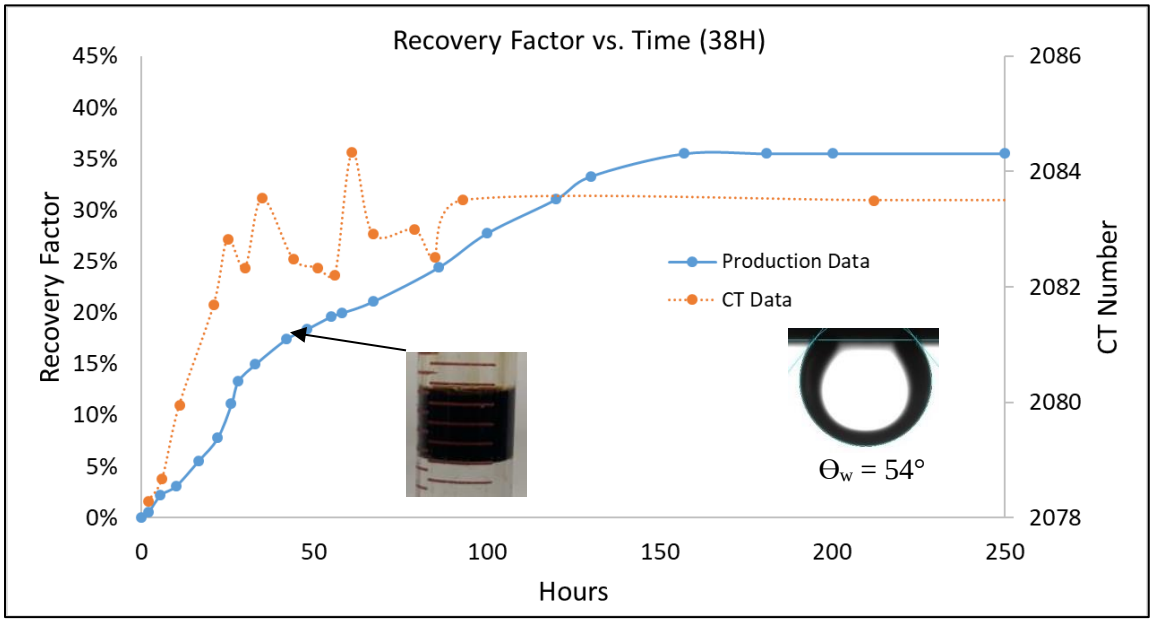


Figure 19: Recovery Factor curve for 38H. CT images provided on next page.

| Category | 38H |
|---|---|
| Fluid Type | 2-A 1 gpt |
| Porosity | 7% |
| Permeability | 0.005 |
| Bulk Vol (cc) | 32.4 |
| Pore Vol (cc) | 2.18 |
| IFT (mN/m) | 12 |

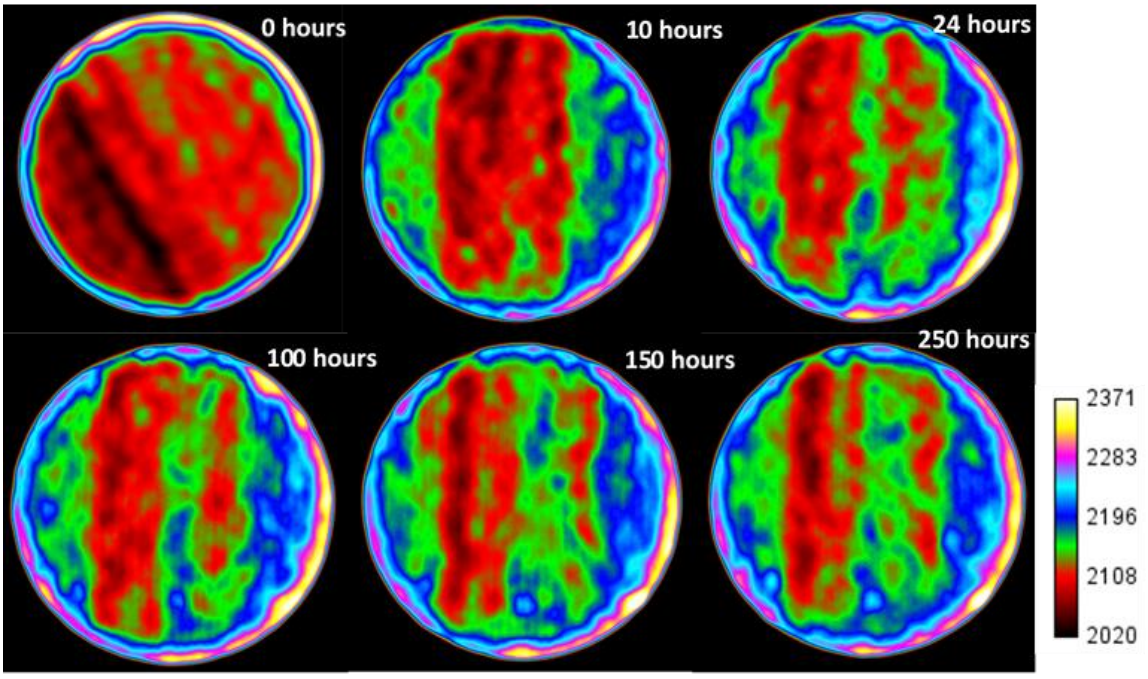
0 hours
10 hours
24 hours
100 hours
150 hours
250 hours
2371
2283
2196
2108
2020

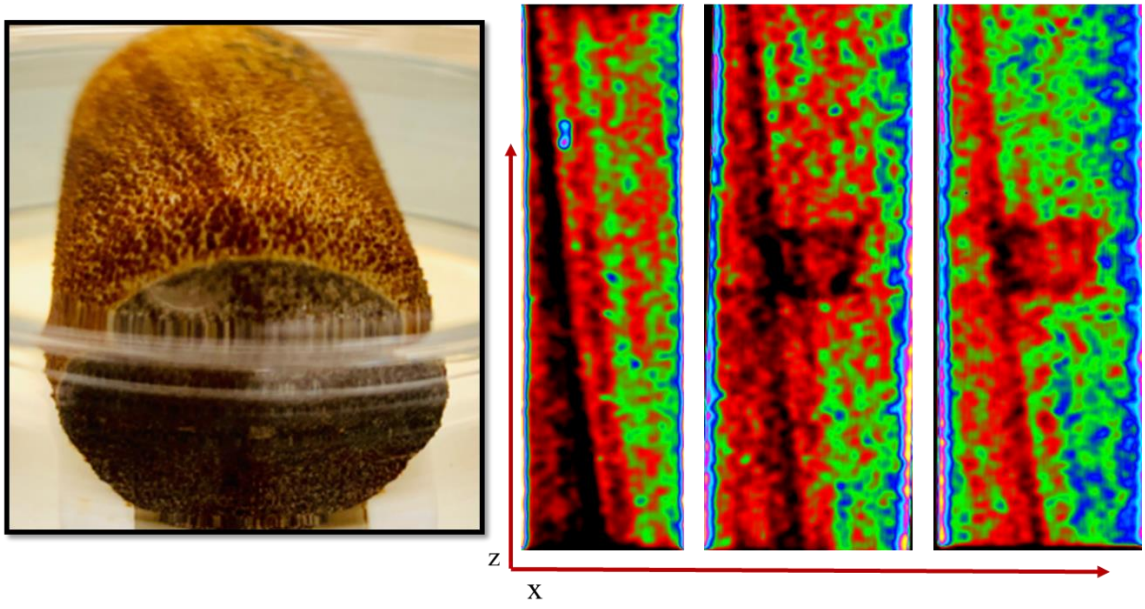
Dry Core
2 hours
90 hours
z
x

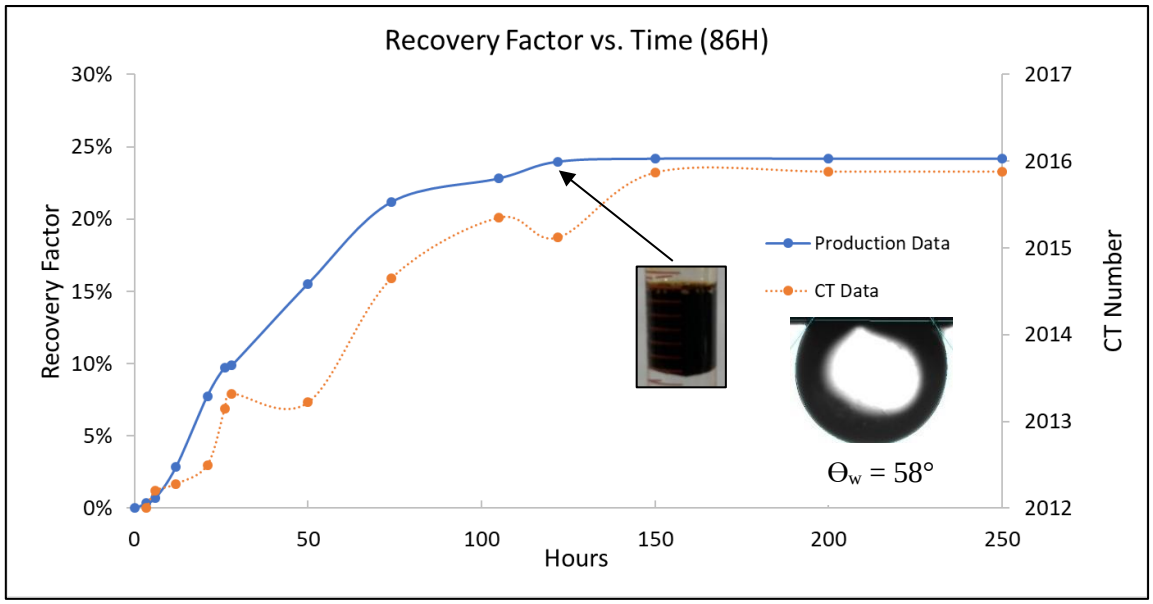


Figure 20: Recovery Factor curve for 86H. CT images for the imbibition of this core plug is given on the next page.

| Category | 86H |
|---|---|
| Fluid Type | 2-B 2 gpt |
| Porosity | 5% |
| Permeability | 0.0003 |
| Bulk Vol (cc) | 34.9 |
| Pore Vol (cc) | 1.47 |
| IFT (mN/m) | 3.21 |

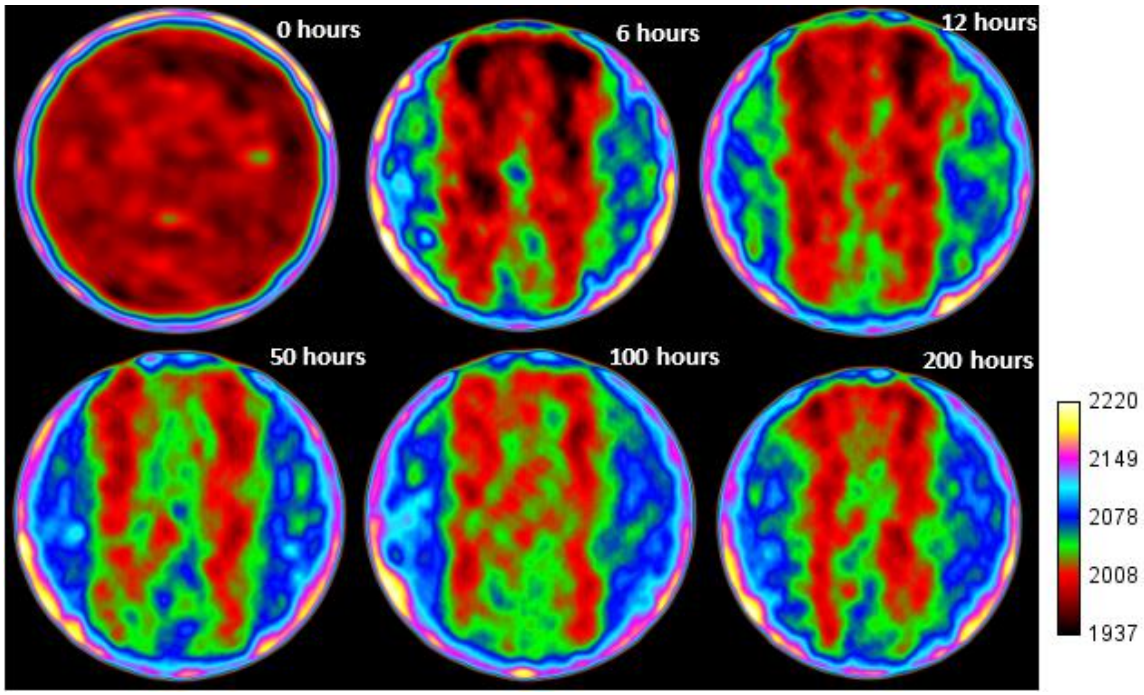
0 hours
6 hours
12 hours
50 hours
100 hours
200 hours
2220
2149
2078
2008
1937

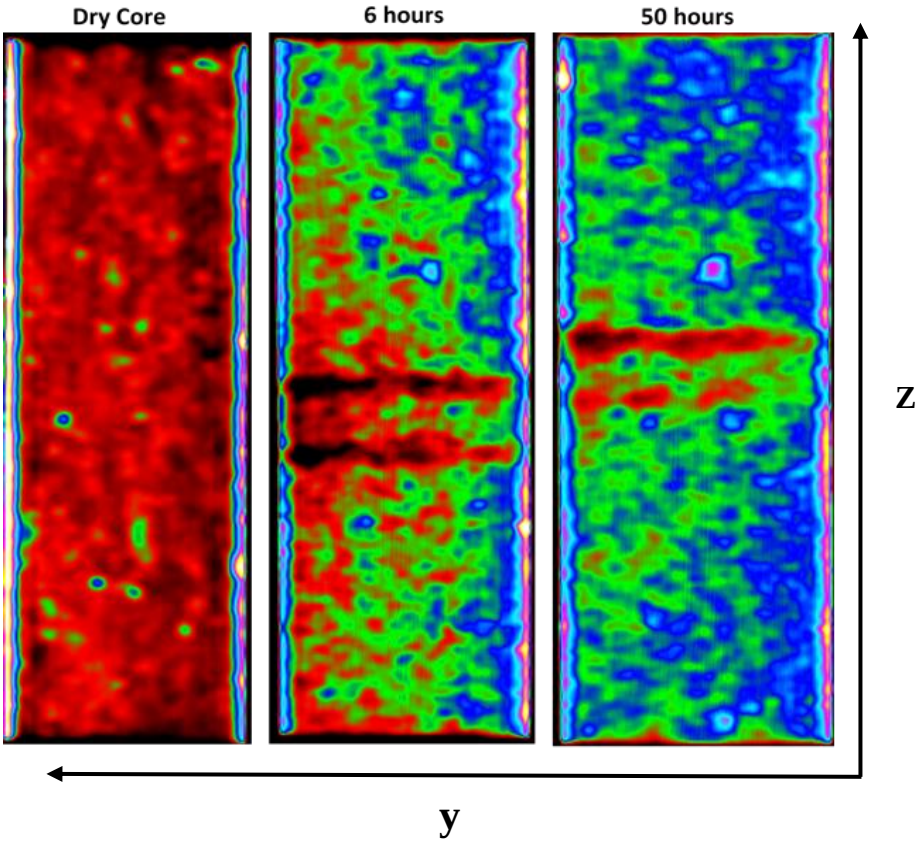
Dry Core
6 hours
50 hours
z
y

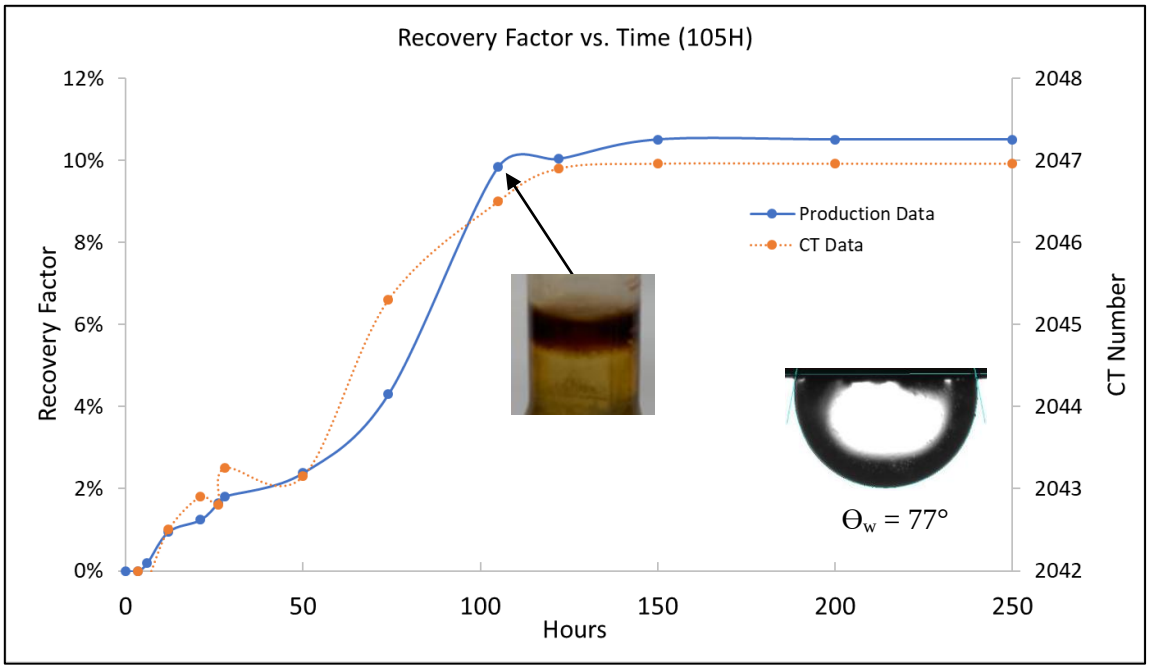


Figure 21: Recovery Factor curve for 105H. CT images for the imbibition of this core plug is given on the next page.

| Category | 105H |
|---|---|
| Fluid Type | Surf X 1 gpt |
| Porosity | 5% |
| Permeability | 0.0015 |
| Bulk Vol (cc) | 30.6 |
| Pore Vol (cc) | 1.09 |
| IFT (mN/m) | 7.3 |

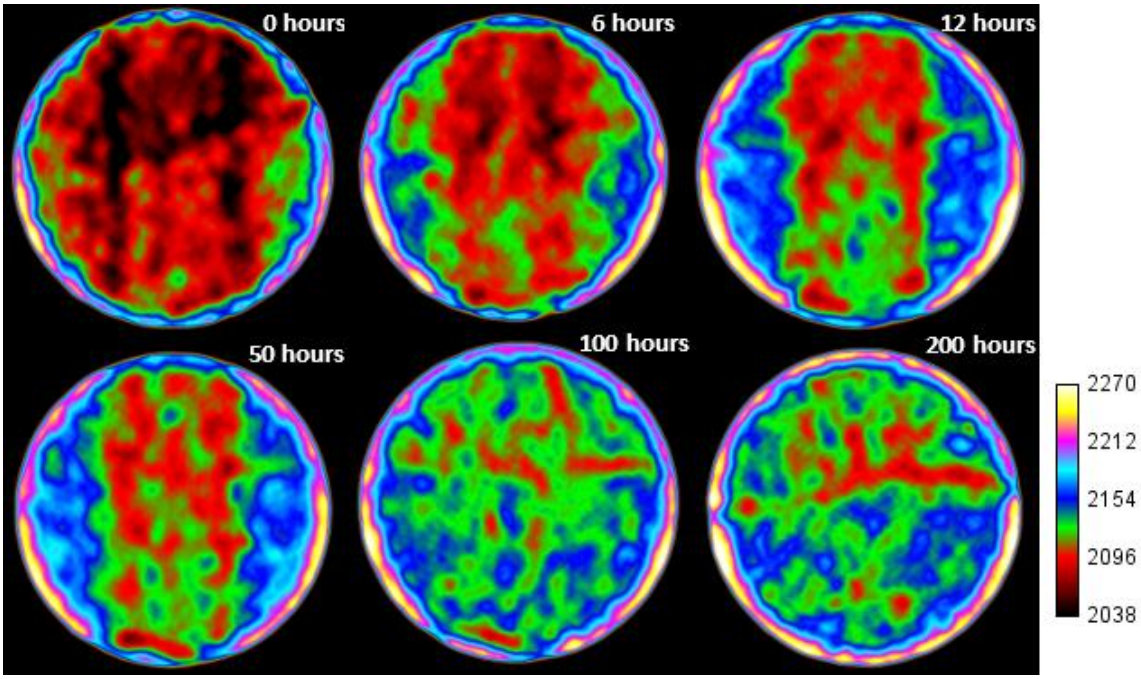
0 hours
6 hours
12 hours
50 hours
100 hours
200 hours
2270
2212
2154
2096
2038

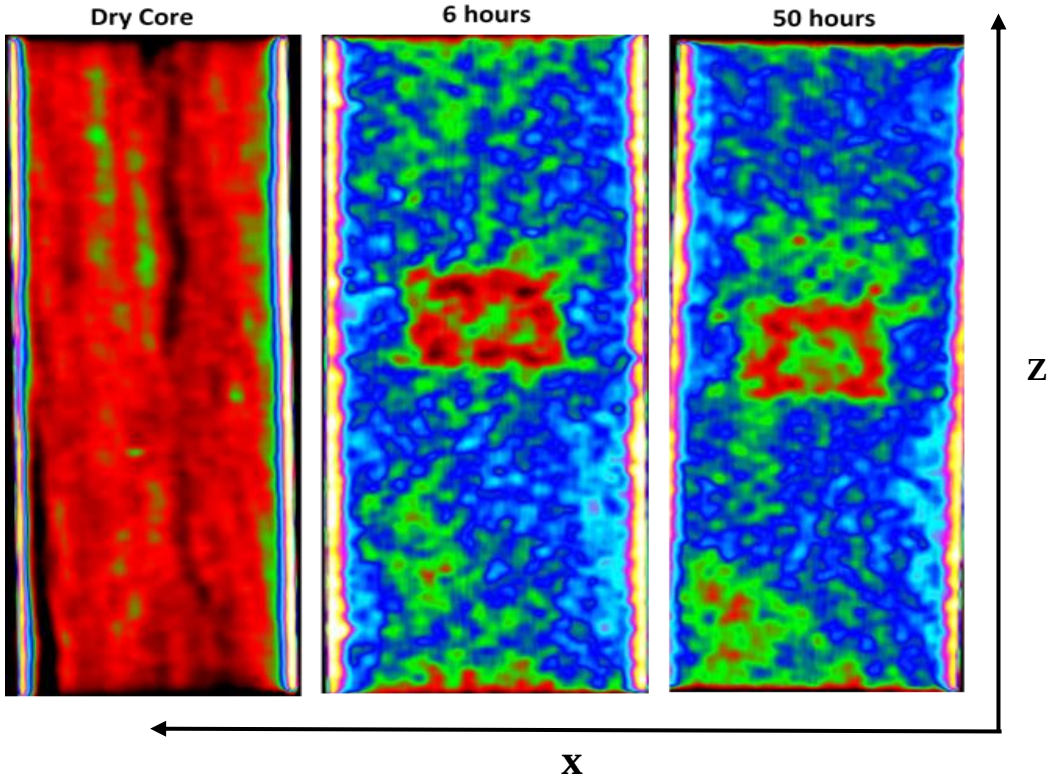
Dry Core
6 hours
50 hours
Z
X

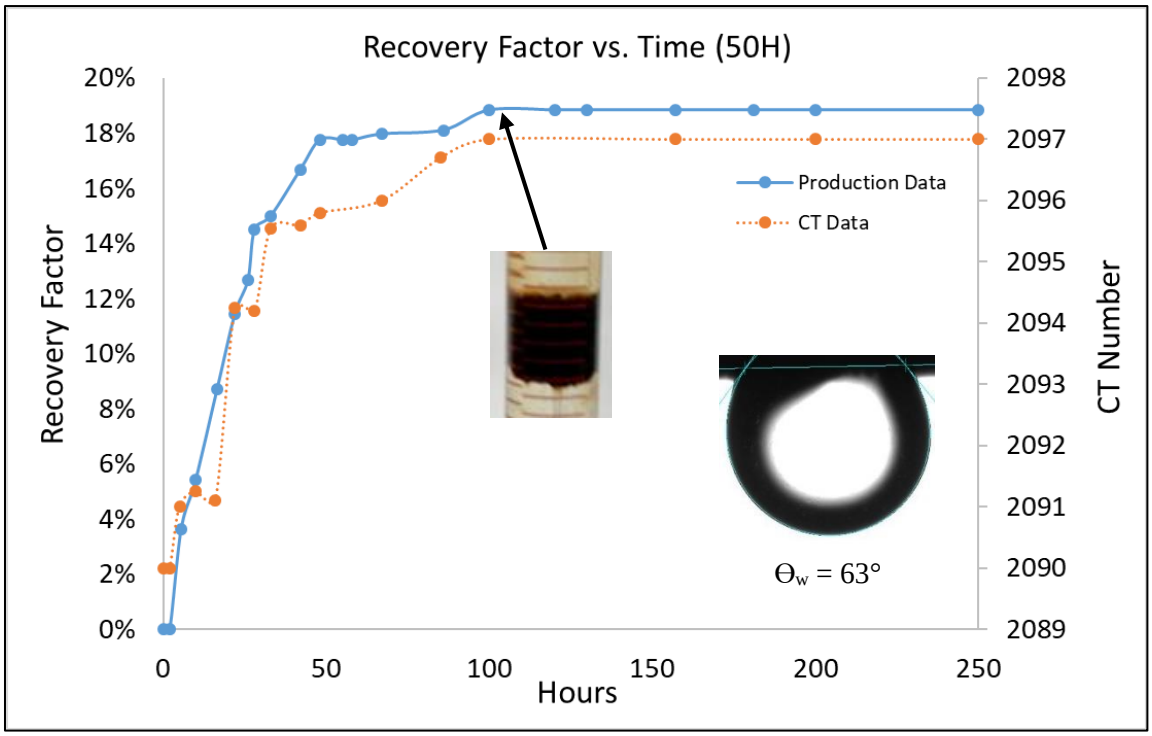


Figure 22: Recovery Factor curve for 50H. CT images for the imbibition of this core plug is given on the next page.

| Category | 50H |
|---|---|
| Fluid Type | DW |
| Porosity | 4% |
| Permeability | 0.032 |
| Bulk Vol (cc) | 32.3 |
| Pore Vol (cc) | 1.38 |
| IFT (mN/m) | 31 |

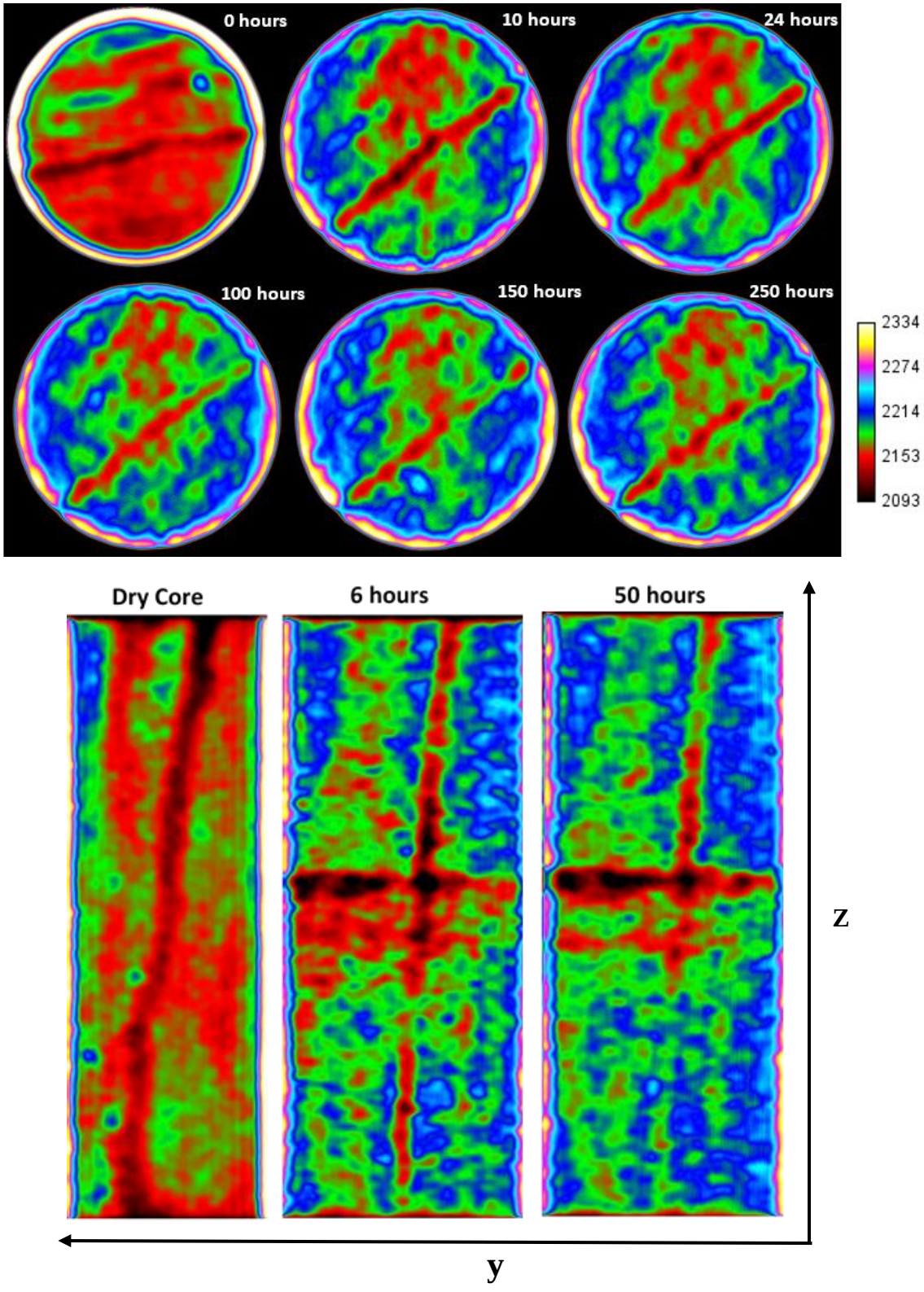
0 hours
10 hours
24 hours
100 hours
150 hours
250 hours
2334
2274
2214
2153
2093
Dry Core
6 hours
50 hours
z
y

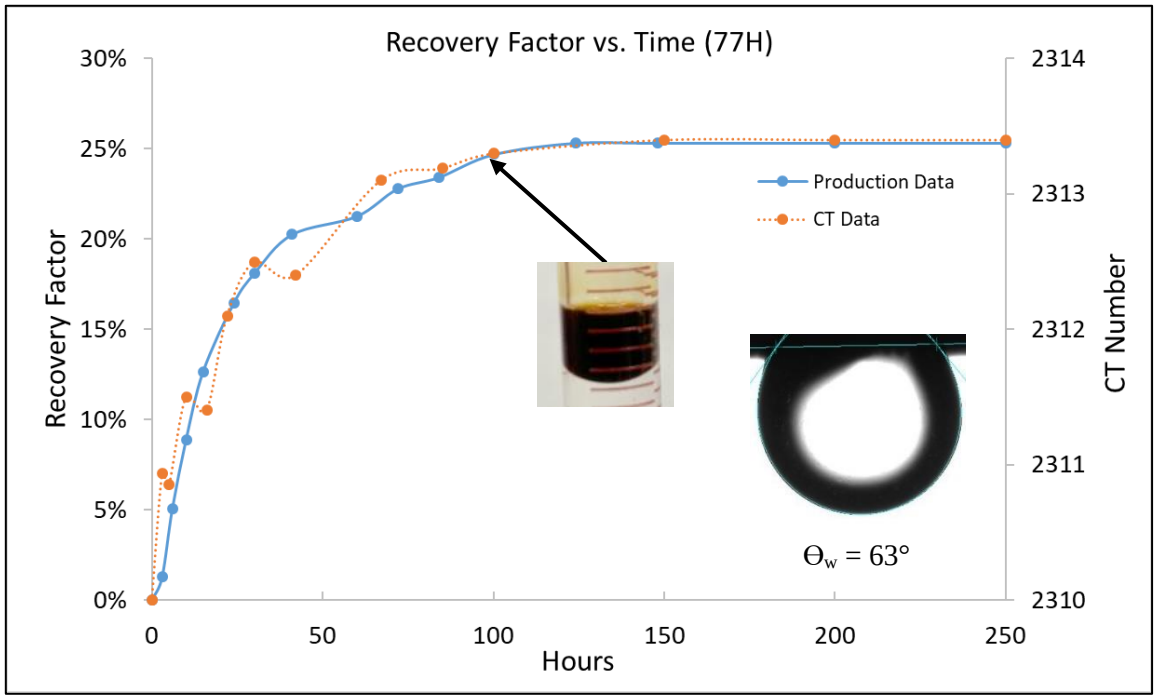


Figure 23: Recovery Factor curve for 77H. CT images for the imbibition of this core plug is given on the next page.

| Category | 77H |
|---|---|
| Fluid Type | DW |
| Porosity | 5% |
| Permeability | 0.02 |
| Bulk Vol (cc) | 33.2 |
| Pore Vol (cc) | 1.25 |
| IFT (mN/m) | 31 |

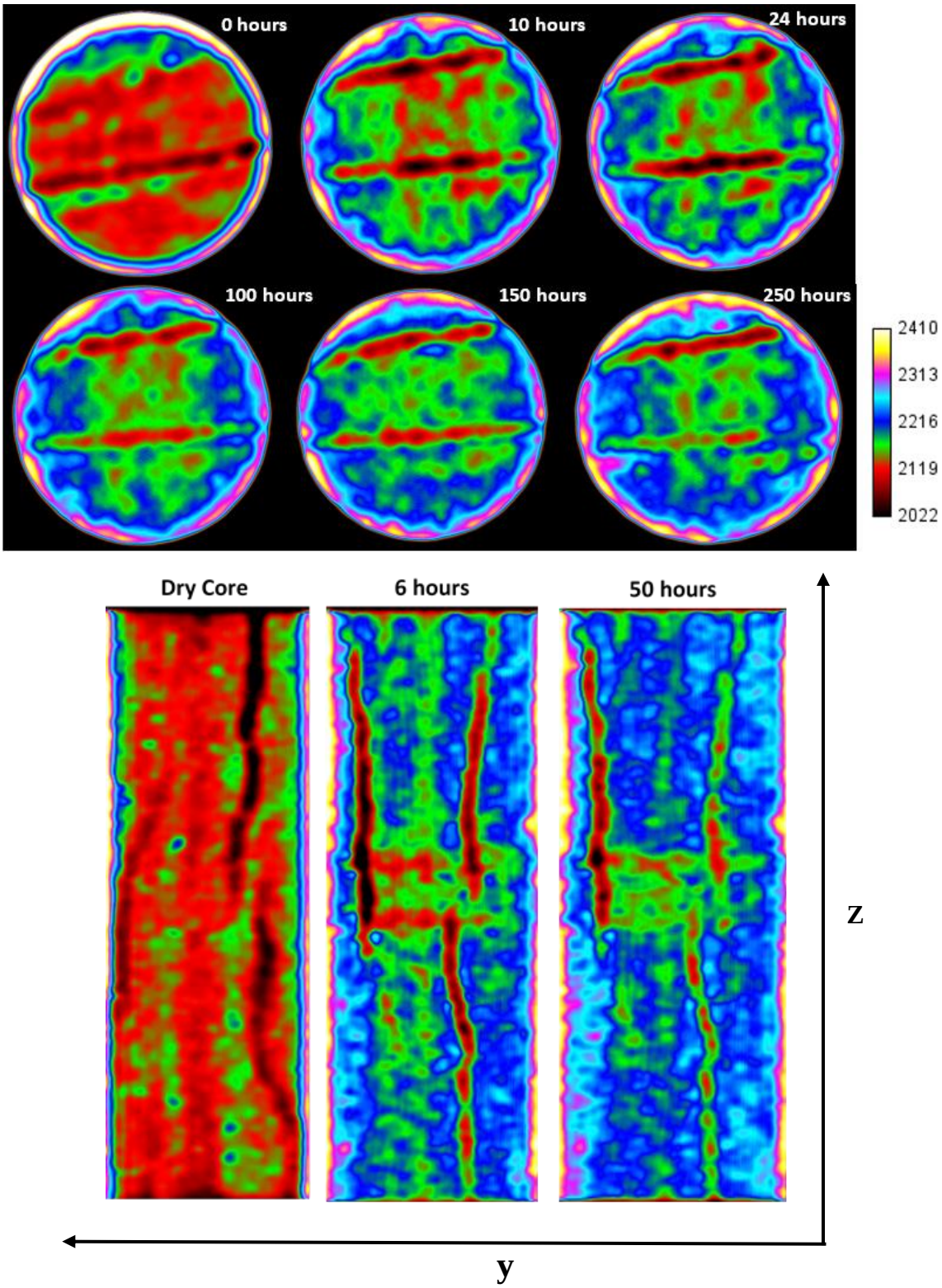
0 hours
10 hours
24 hours
100 hours
150 hours
250 hours
2410
2313
2216
2119
2022
Dry Core
6 hours
50 hours
z
y

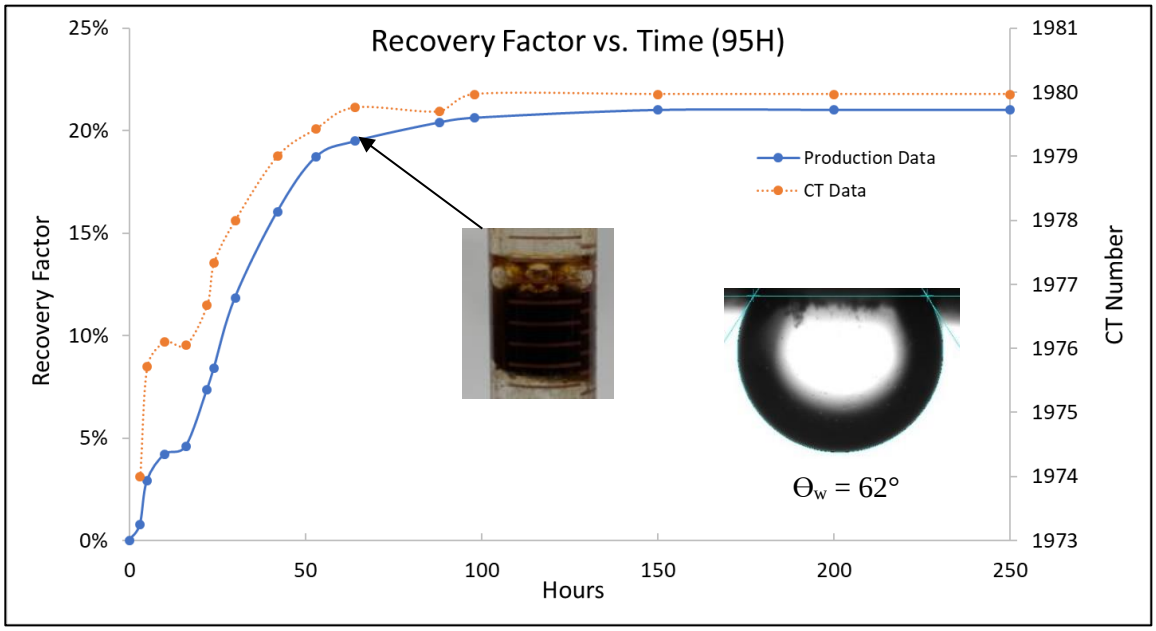


Figure 24: Recovery Factor curve for 95H. This imbibition experiment used 2 gpt of 6-C at 170 °F. Core information is given in a table to the right.

| Category | 95H |
|---|---|
| Fluid Type | 6-C 2 gpt |
| Porosity | 4% |
| Permeability | 0.0002 |
| Bulk Vol (cc) | 34.1 |
| Pore Vol (cc) | 1.31 |
| IFT (mN/m) | 5.16 |

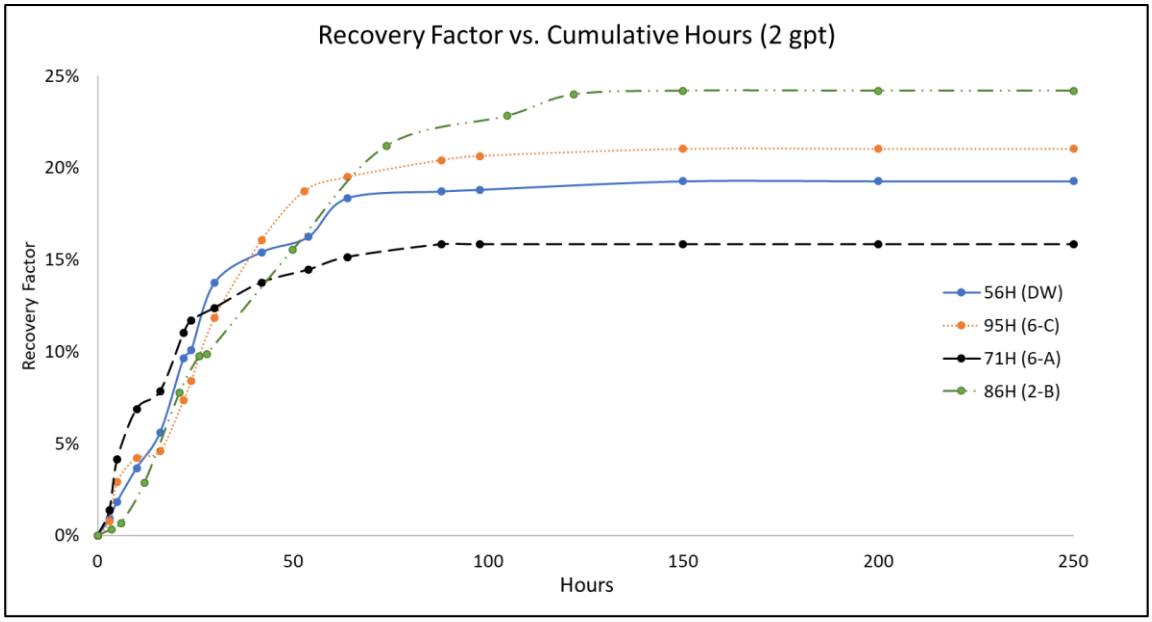


Figure 25: Recovery Factor curves for samples tested at 2 gpt.

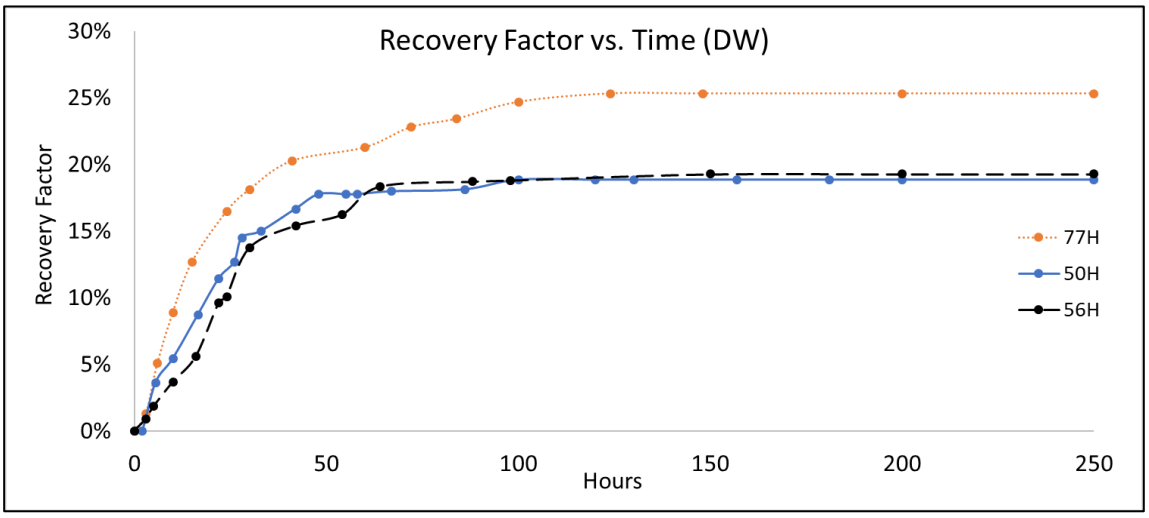


Figure 26: Recovery Factor curve comparing two samples that tested in distilled water.

| Category | 56H | 77H | 50H |
|---|---|---|---|
| Fluid Type | DW | DW | DW |
| Porosity | 3.50% | 5% | 3.80% |
| Permeability (mD) | 0.001 | 0.02 | 0.03 |
| Bulk Vol (cc) | 28.6 | 33.2 | 32.3 |
| Pore Vol (cc) | 1.09 | 1.25 | 1.38 |
| IFT (mN/m) | 31 | 31 | 31 |

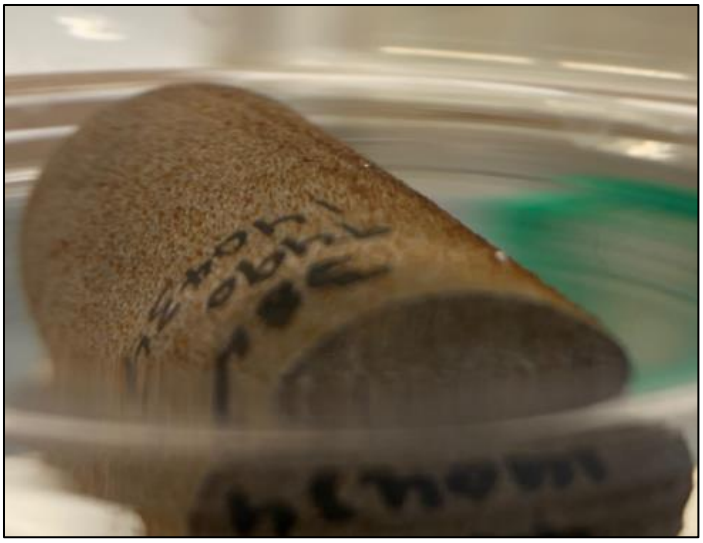

Figure 27: Core 38H 24 hours after imbibition in surfactant 2-A with 1 gpt loading @ 170 °F. Looking closely you can see that the oil droplets are very small and uniform, but in a water-wet state.

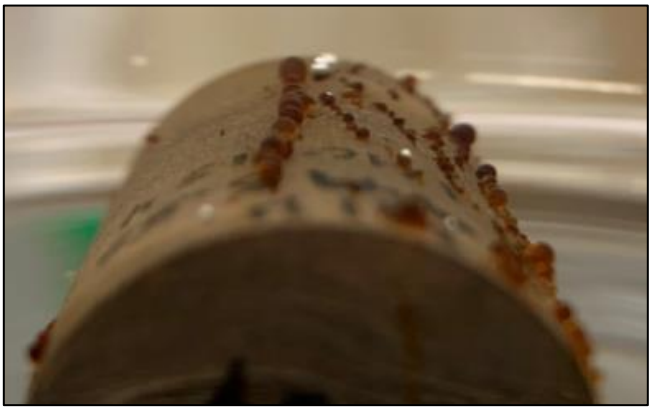

Figure 28: Core 41H 24 hours after imbibition in surfactant 2-A using 1 gpt of 2-A #4 only @ 170 °F. Looking closely you can see that the oil droplets are larger in diameter than core 38H in the figure above.

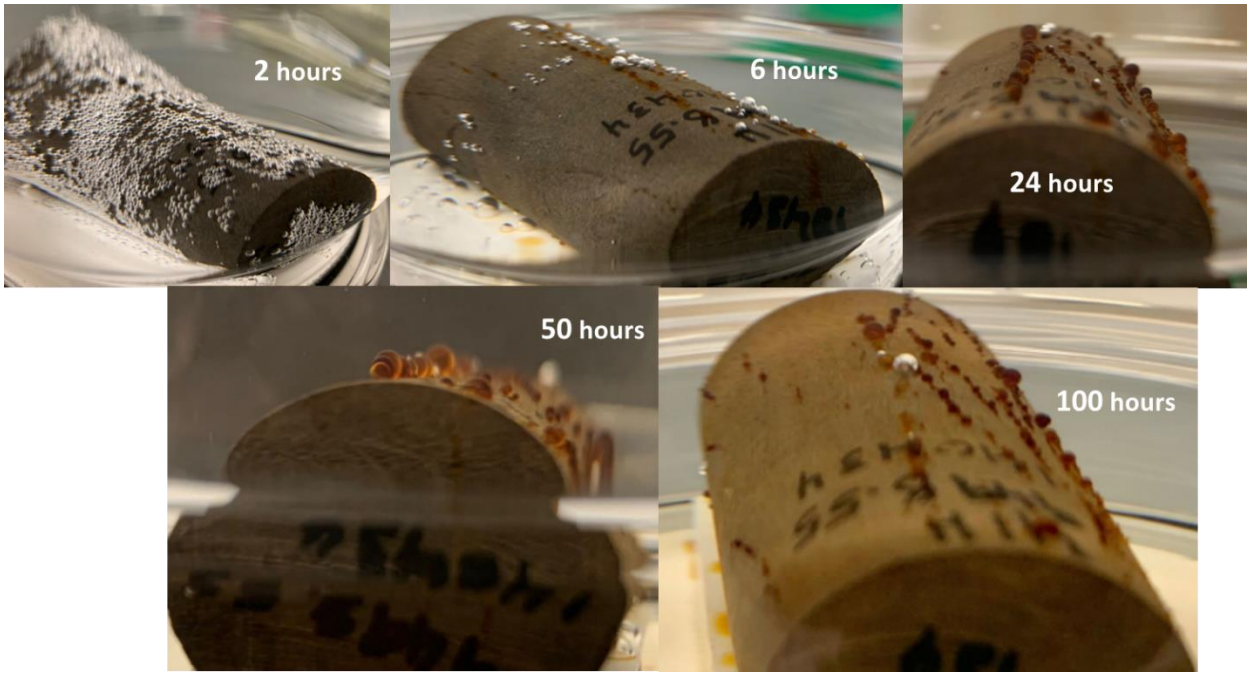


Figure 29: Core 41H during imbibition in surfactant 2-A #4 only at 1 gpt. First picture is 2 hours into imbibition and the core is covered in water droplets. By visual inspection it can be seen that the oil droplets are in a water-wet state. The picture below is a close up of oil drops on the surface at 50 hours of imbibition.

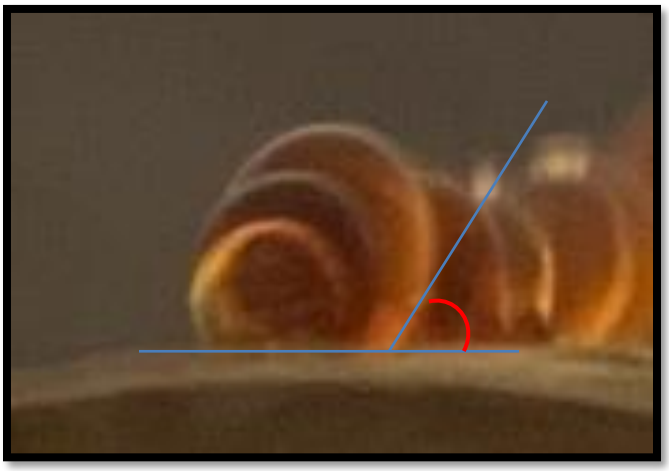

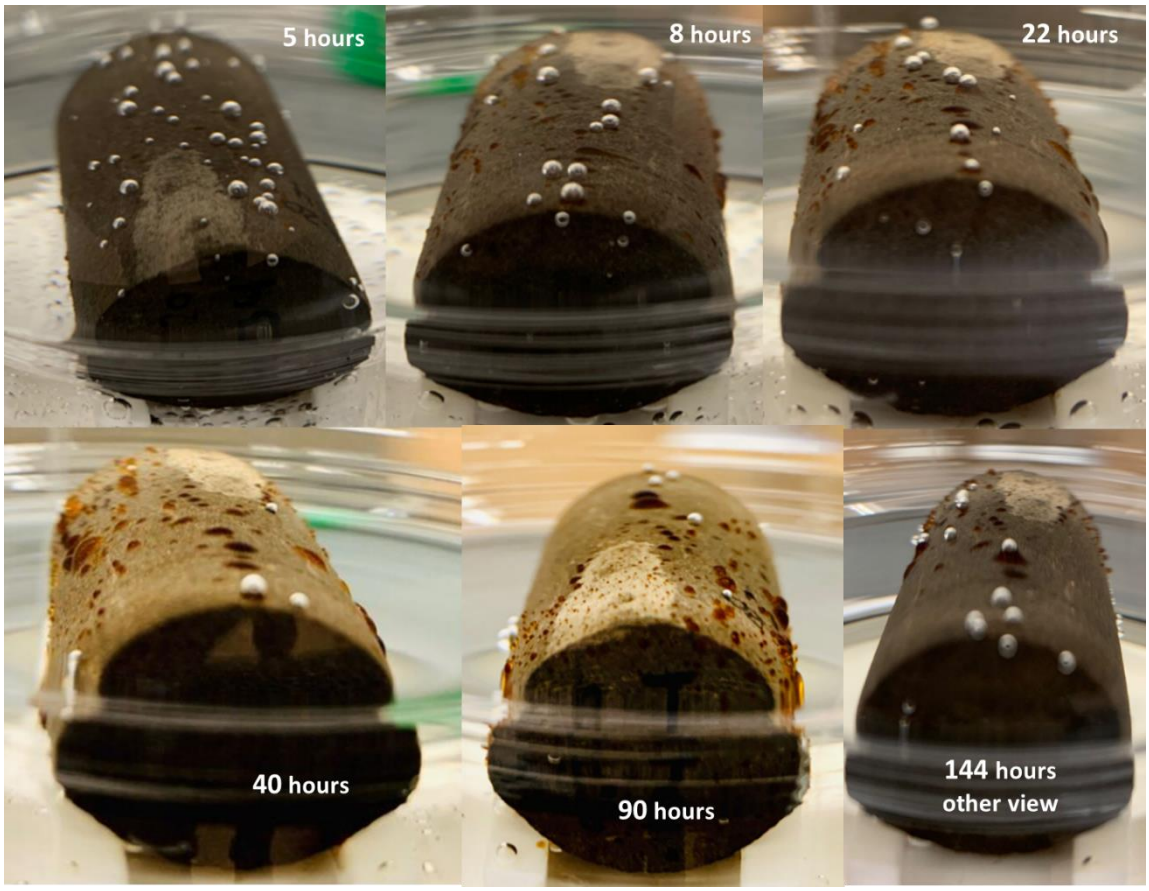


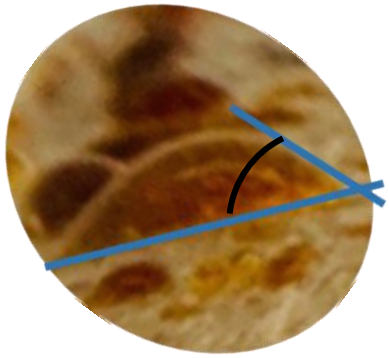

Figure 30: Core 74H during the imbibition experiment in distilled water only at 170 °F. Oil droplets forming on surface are more oil-wet than imbibition with surfactants. Close-up of oil bubble is shown to the left showing an approximate $\Theta_w = 120°$.

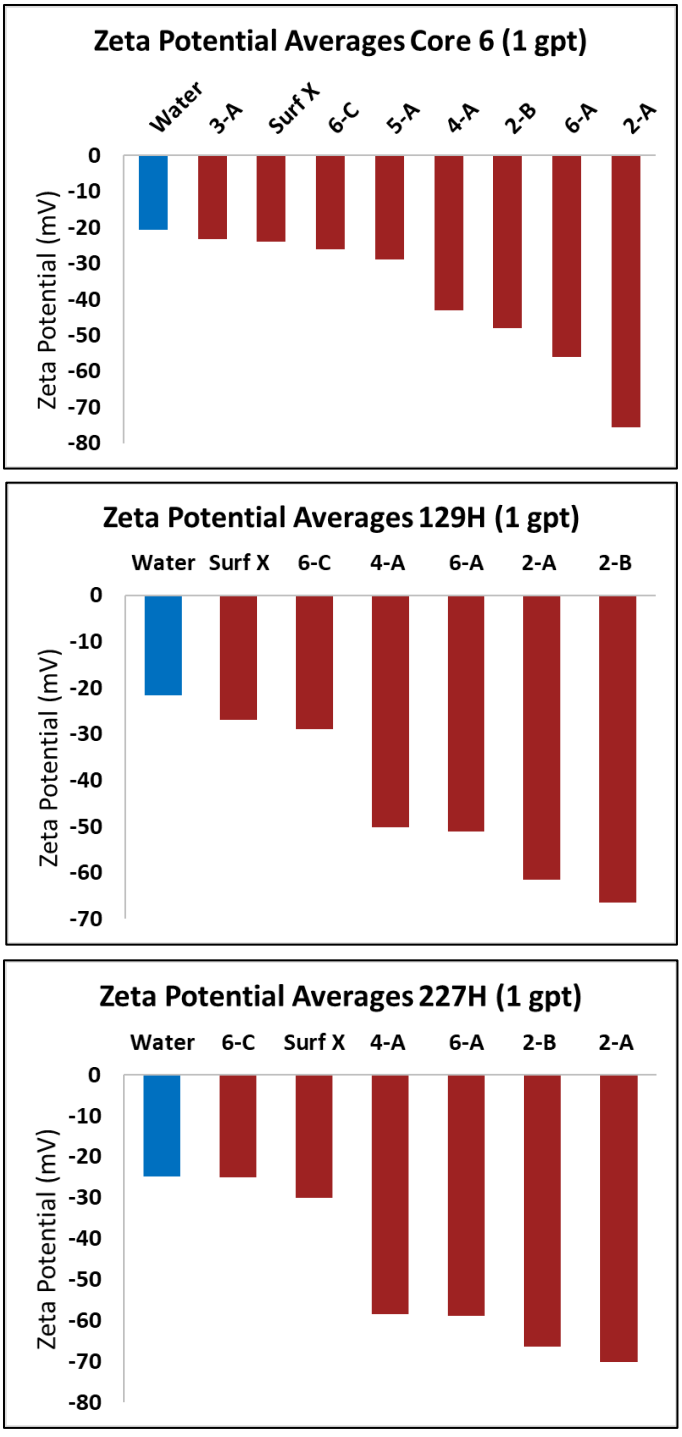


Figure 31: Graphs of zeta potential averages using different surfactants for samples 129H, 227H, and core 6.

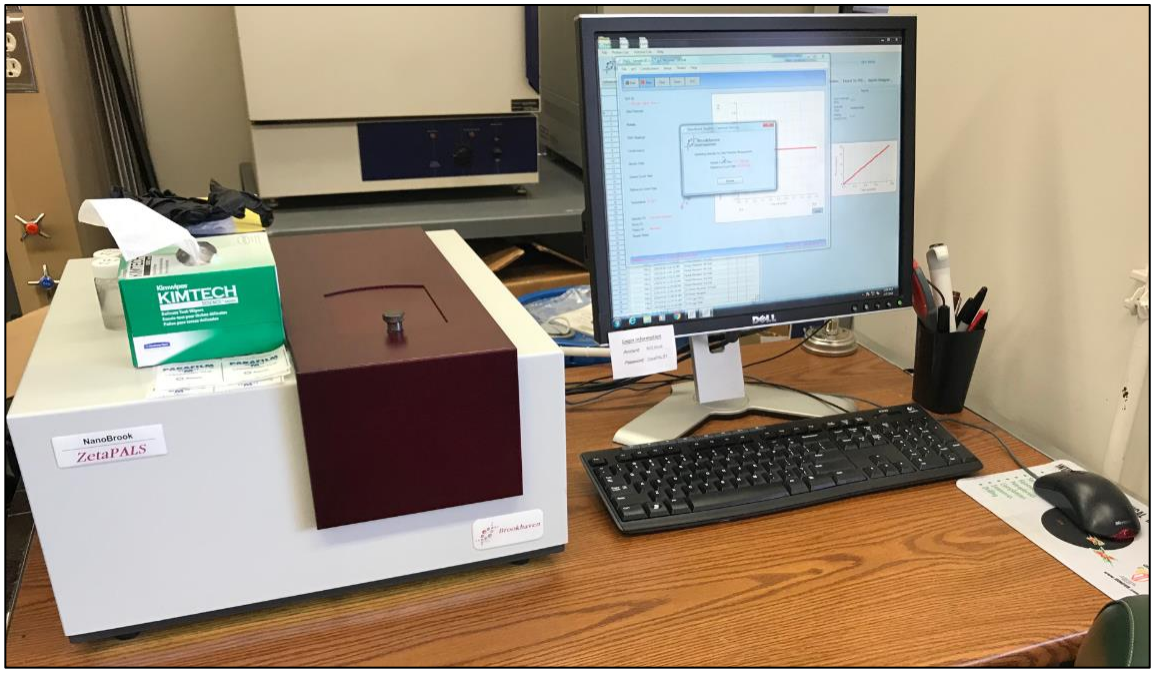


Figure 32: Picture of Brookhaven machine used for zeta potential measurements.

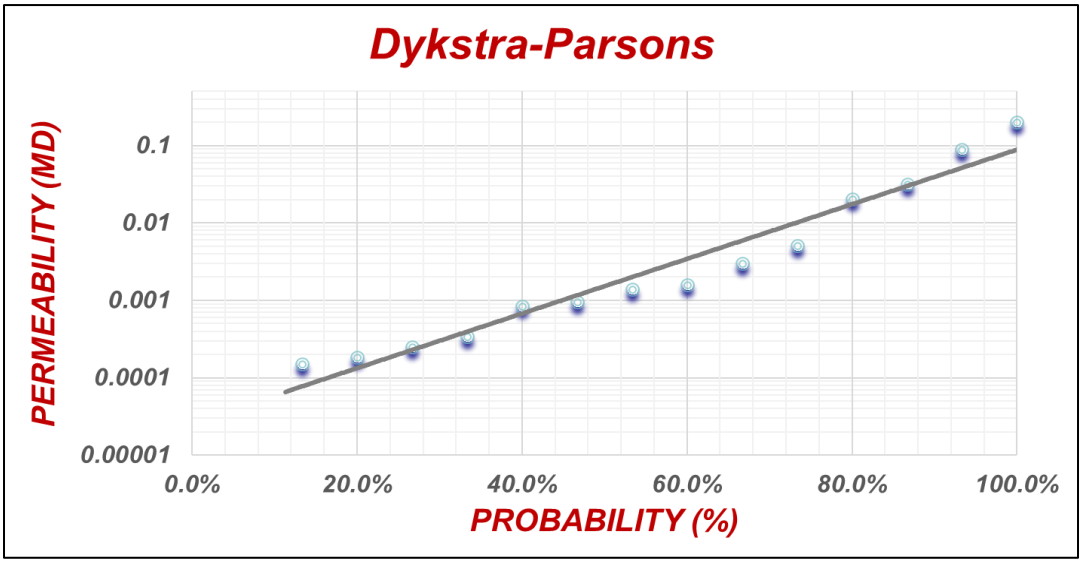


Figure 33: Graph depicting the Dykstra-Parson coefficient, a common measure of permeability variation (Lake et al. 200). $\mathbf{V_{dp}}$ **= 0.56** for this dataset.